Master's thesis

NTNU
Norwegian University of Science and Technology
Faculty of Information Technology and Electrical Engineering
Department of Electric Power Engineering

Sondre Aslaksen Kaldheim

Estimating the dynamic current rating of power cables using the principle of superposition and transient temperature responses

Master's thesis in Energy and Environmental Engineering
Supervisor: Erling Ildstad
August 2022

NTNU
Norwegian University of
Science and Technology

Sondre Aslaksen Kaldheim

Estimating the dynamic current rating of power cables using the principle of superposition and transient temperature responses

Master's thesis in Energy and Environmental Engineering
Supervisor: Erling Ildstad
August 2022

Norwegian University of Science and Technology
Faculty of Information Technology and Electrical Engineering
Department of Electric Power Engineering

NTNU
Norwegian University of
Science and Technology

Preface

With this master's thesis I conclude my M.Sc. degree at the Norwegian University of Science and Technology (NTNU). The thesis has been completed at the Department of Electric Power Engineering.

I would like to express my gratitude towards my supervisor, Prof. Erling Ildstad. Thank you for the guidance and help throughout the thesis period. I appreciate your availability for open discussions regarding scientific topics.

I would also like to thank department engineer Bård Almås for his help with usage and construction of the laboratory setup.

Trondheim, August 2022

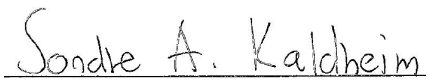

Sondre Aslaksen Kaldheim

Abstract

As electric power consumption increases steadily and more renewable sources are being used to generate power, the available power grid needs to increase its capability and flexibility. Current rating of existing equipment is today determined by static ratings for worst case scenarios, leaving components such as power cables not fully utilized. This thesis proposes an estimation method that facilitates advancing the current rating of power cables from static to dynamic rating.

The method uses two different procedures as basis, that has established transient and steady-state conductor temperature for given load and laying conditions. By using an applied scaling principle that corresponds to the change in load current, thus considering the thermal changes in the cable. As well as applying the principle of superposition. The total transient temperature response of the cable conductor during dynamic loading can be estimated. The estimate can then be utilized to enhance the current rating of the power cable.

The first basis used in the estimation method is calculated conductor temperature according to international standards. The second basis uses a long-term established temperature measurement of the cable conductor with known conditions. The estimates are compared to a dynamic loading case, experimentally executed in a practical laboratory setup. The setup uses a Nexans TSLF 24kV 1x50 A power cable, that has an aluminium conductor with a cross-sectional area of 50 mm^2, and cross-linked polyethylene (XLPE) insulation.

Results show that the estimates are able to give a realistic imitation of the experimentally measured conductor temperature response. The estimate based on measured temperature has the least average temperature deviation compared to measurement, which is 5.2°C. This estimate also has an additional scaling for the temperature dependency of the conductor resistance. Estimation based on analytical calculations only gives an adequate estimate when the change in conductor resistance is included, with an average temperature deviation of 8.3°C.

The simplicity and precision level of the developed method suggest that its applicability has potential to facilitate the current rating of power cables from static calculations to more dynamic considerations. Improving the utilization of the potential grid reserve not fully exploited in power cables.

Sammendrag

Ettersom strømforbruket øker jevnt og mer fornybare kilder brukes til å generere elektrisk energi, må det tilgjengelige strømnettet øke sin kapasitet og fleksibilitet. Gjeldende strømføringsevne bestemmes i dag av statiske vurderinger for verst mulig tilfelle, slik at eksisterende komponenter ikke blir fullt utnyttet. Denne masteroppgaven foreslår en estimeringsmetode som vil bidra til å øke gjeldende vurdering av strømkabler fra statisk til dynamisk betraktning.

Metoden bruker to ulike prosedyrer som har etablert transient og stabil ledertemperatur for en gitt belastning og forlegning. Ved å anvende et skaleringsprinsipp som tilsvarer endringen i laststrømmen, og dermed også inkluderer de termiske endringene i kabelen. Samt å anvende superposisjonsprinsippet. Vil den totale transiente temperatur responsen til kabelens leder under dynamisk belastning bli estimert. Estimatet kan deretter brukes til å forbedre strømføringsevnen til kabelen.

Den første prosedyren som brukes i estimeringsmetoden er beregnet ledertemperatur i henhold til internasjonale standarder. Den andre prosedyren bruker en langtids etablert temperaturmåling av kabelens leder under kjente forhold. Estimatene sammenlignes med et dynamisk belastnings tilfelle, eksperimentelt utført i et praktisk laboratorieoppsett. Oppsettet bruker en Nexans TSLF 24kV 1x50 A kabel, som har en aluminiumsleder med et tverrsnitts areal på 50 mm^2, og tverrbundet polyetylen (XLPE) isolasjon.

Resultater viser at estimatene er i stand til å gi en realistisk imitasjon av den eksperimentelt målte ledertemperatur responsen. Estimatet basert på målt temperatur har minst gjennomsnittlig temperatur avvik sammenlignet med måling, som er 5,2°C. Dette estimatet har også en ekstra skalering for temperaturavhengigheten til ledermotstanden. Estimering basert på analytiske beregninger gir kun et tilstrekkelig estimat når endringen i ledermotstand er inkludert, med et gjennomsnittlig temperatur avvik på 8,3°C.

Enkelheten og presisjonsnivået til den utviklede metoden antyder at anvendeligheten har potensialet til å forbedre gjeldende vurdering av kabler fra statiske beregninger til mer dynamiske betraktninger. Dette vil føre til forbedring av utnyttelsen til den potensielle overførings reserven som ikke utnyttes fullt ut i kraftkabler i dag.

Table of contents

List of tables

List of figures

List of abbreviations and symbols

Abbreviations

AC	Alternating current
DC	Direct current
DR	Dynamic rating
DTS	Distributed temperature sensing
IEC	International Electrotechnical Commission
RTTR	Real-time temperature rating
SCADA	Supervisory control and data acquisition
TWh	Terawatt-hour
XLPE	Cross-linked polyethylene

Symbols

Symbol	Description	Unit
A	Cross-sectional area of conductor	[m^2]
$a_{(n-1)i}$	Transfer function, numerator equation coefficient	
b_n	Transfer function, denominator equation coefficient	
c	Volumetric specific heat of the material	$\left[\frac{J}{^\circ C m^3}\right]$
c_{con}	Volumetric specific heat capacity conductor	$\left[\frac{J}{^\circ C m^3}\right]$
c_i	Volumetric specific heat capacity XLPE insulation	$\left[\frac{J}{^\circ C m^3}\right]$
c_{sheath}	Volumetric specific heat capacity sheath	$\left[\frac{J}{^\circ C m^3}\right]$
c_{screen}	Volumetric specific heat capacity screen	$\left[\frac{J}{^\circ C m^3}\right]$
D_{con}	Internal diameter of insulation	[m]
D_e	External diameter of cable	[m]
D_{es}	External diameter of sheath	[m]
D_{ex}	External diameter of layer	[m]
D_i	Diameter beneath layer i	[m]

D_{in}	Internal diameter of layer	[m]
D_{ins}	External diameter of insulation	[m]
D_s	Internal diameter of sheath	[m]
E	Tabulated constant for cables in air with black surface placed on ground	
g	Tabulated constant for cables in air with black surface placed on ground	
H_1	Transfer function of the first node of a two loop network	
H_2	Transfer function of the second node of a two loop network	
h	Heat dissipation coefficient that includes heat transfer mechanisms	
I	Load current	[A]
K_A	Iteration variable when finding T_4	
l	Length	[m]
P_j, P_k	Poles of transfer function	
P_1, P_2	Poles of transfer functions for both H_1 and H_2	
p	Van Wormer coefficient insulation layer	
p'	Van Wormer coefficient sheath layer	
Q	Thermal capacitance per unit length	$\left[\frac{J}{Km}\right]$
Q_A	Thermal capacitance first loop of simplified model	$\left[\frac{J}{Km}\right]$
Q_B	Thermal capacitance second loop of simplified model	$\left[\frac{J}{Km}\right]$
Q_{con}	Thermal capacitance conductor	$\left[\frac{J}{Km}\right]$
Q_i	Thermal capacitance insulation	$\left[\frac{J}{Km}\right]$
Q_{screen}	Thermal capacitance screen	$\left[\frac{J}{Km}\right]$
Q_{sheath}	Thermal capacitance sheath	$\left[\frac{J}{Km}\right]$
R_{AC}	Alternating current resistance of the conductor at operating temperature	[Ω]
R_θ	Direct current resistance of the conductor at operating temperature	[Ω]
R_{20}	Conductor resistance at 20°C	[Ω]
T_A	Thermal resistance first loop of simplified model	$\left[\frac{Km}{W}\right]$
T_B	Thermal resistance second loop of simplified model	$\left[\frac{Km}{W}\right]$

T_i	Thermal resistance of layer i	$\left[\frac{Km}{W}\right]$
T_{ij}	Coefficient	$[\frac{^\circ Cm}{W}]$
T_1	Thermal resistance of cable insulation	$\left[\frac{Km}{W}\right]$
T_3	Thermal resistance of cable sheath	$\left[\frac{Km}{W}\right]$
T_4	External thermal resistance of cable surroundings	$\left[\frac{Km}{W}\right]$
t	Time	[h]
t_i	Thickness of layer i	[m]
V	Voltage	[V]
V_o	Volume of the object	[m^3]
W_c	Ohmic losses in the conductor per unit length	$\left[\frac{W}{m}\right]$
Z	Tabulated constant for cables in air with black surface placed on ground	
Z_b	Subsequent impedance seen from node two of a two loop network	[Ω]
Z_{ki}	Zeros of transfer function	
Z_{tot}	Total network impedance of a two loop network	[Ω]
Z_{11}	Zeros of transfer function H_1	
α	Temperature coefficient for the conductor material	[$^\circ C^{-1}$]
$\Delta\theta_s$	Iterated temperature of cable surface above ambient temperature	
θ	Operating temperature at the conductor	[°C]
θ_1	Temperature response function of cable conductor	[°C]
θ_2	Temperature response function of cable sheath	[°C]
$\rho_{con,20}$	Thermal resistivity conductor at 20°C	$\left[\frac{Km}{W}\right]$
ρ_i	Thermal resistivity of layer i	$\left[\frac{Km}{W}\right]$
ρ_{ins}	Thermal resistivity of XLPE insulation at 20°C	$\left[\frac{Km}{W}\right]$
ρ_{sheath}	Thermal resistivity sheath resistivity at 20°C	$\left[\frac{Km}{W}\right]$
ρ_{20}	Conductor resistivity at 20°C	[Ωm]

Chapter 1

Introduction

The objective of this master's thesis has been to develop an estimation method that can be used to determine the expected transient temperature response of a power cable conductor, to improve the dynamic current rating of the cable. First, this chapter presents an introductory to the background and motivation for developing and testing the presented method. Further it gives the problem definition and report structure.

1.1 Background and motivation

A report from the Nordic grid operators predicts a growth in electric power consumption from 400 TWh, which is present-day consumption, to 655 TWh by the year of 2040. This means the Nordic countries will consume 65 % more electric power by 2040. The power generation will also increase, as more renewable sources are implemented into the grid. The report anticipates a 122 % increase in renewable capacity by 2040, mostly due to on- and offshore wind and solar energy. [1].

As the electric power consumption steadily increases not only in the Nordics, but on a global basis as well, there is a growth in research regarding more efficient use of already existing components in the grid. Mainly, how the grid could be better utilized and operated at higher loading levels [2]. Also, as more renewable sources are implemented, the grid is required to be more flexible, due to renewable sources such as wind and solar causing unpredictable energy generation.

Existing equipment is mainly operated according to conservative methods, using static ratings based on limited parameter information, and worst-case scenario presumption. To further facilitate the increase in consumption and generation, state of the art methods are necessary for grid operators to make advanced use of already existing grid equipment [3]. This thesis focuses on increasing the power transmission capacity of power cables, by developing a method for estimating the conductor temperature during dynamic loading.

A substantial restriction when utilizing power cables are thermal limitations due to risk of overheating, which in worst case could cause damage to the cable. The extent of the damage varies, depending on the quantity of overheating the cable is exposed to. To avoid any possibility of overheating, current limits are imposed [4]. These limits govern the current-carrying capacity of a power cable, often referred to as the ampacity of the cable. The ampacity is the maximum current the conductor of the cable can be loaded with continuously to not exceed allowed operating temperature of the cable insulation.

The current capacity of a cable is generally based on conservative analytical calculations performed according to International Electrotechnical Commission (IEC) standards. These standards consider steady-state temperature after being subject of a long-term continuous static load current in worst case scenario conditions. For cables, this could be the hottest temperature measured at one spot. However, the temperature will rarely exceed steady-state rating and the cable is rather operated at conditions that leads to less thermal stress than it initially is designed for. Therefore, the actual power transfer ability of a practical power cable is seldom utilized [5].

This represents an unused grid reserve in implemented power cables. To utilize this reserve, the ampacity considerations need to evolve from a static perspective to dynamic considerations. By using real-time data of varying load current, transient temperature response in the cable layers and impact from laying conditions such as surrounding medium and ambient temperature, more realistic capacities of power cables could be estimated.

Modern methods that make use of a numerical approach, such as finite element method, boundary element and finite difference are widely applied to cable systems for better and more realistic computations of the cable temperature. However, these methods are considered complex and requires advanced knowledge and computers. Which makes them poorly suitable for real-time operations, and faster methods should be considered [6].

As new methods are required for a more uncomplicated current rating capacity estimation, this thesis presents a method for estimating current rating of power cables. The method is a further enhancement of a similar estimation method developed for a specialization project preceding this thesis. In the project, the method showed great tendencies of estimating the conductor temperature of a low voltage electrical installation during dynamic loading. Having an average temperature deviation between estimated and measured temperature of 0.8°C [7].

1.2 Problem definition and thesis structure

As mentioned, the objective of this thesis has been to develop a method to estimate the dynamic current rating of power cables. The method uses measured transient temperature response of a laboratory setup with an XLPE power cable, to estimate the conductor temperature during dynamic loading. As well as analytical calculations of transient temperature response according to IEC standards, for the same purpose. Both measured and calculated temperature responses are used for comparison. The total dynamic temperature response estimation is tested and verified experimentally on a laboratory setup for a case of dynamic loading.

By using an experimental laboratory setup to compare the simulated estimates with real-time temperature measurements, the thesis aims to determine the precision, possible limitations and applicability of the method. A goal is to also show that temperature measurements of cable sections exposed to hotspots, could facilitate dynamic current rating of power cables. Meaning, sections of the cable where highest temperature occurs.

Further, this thesis is structured as follows. Chapter 2 presents the dynamic rating principle for power cables. This chapter covers the definition, application and advantages of going from static to dynamic current ratings for power cables. Chapter 3 gives the theoretical background for heat generation in a cable, along with a description of how to model a cable system as a thermal circuit. This chapter also includes analytical equations for transient temperature response in cable layers, as well as a thorough explanation of the developed estimation method with an example.

Chapter 4 displays the analytical calculations and laboratory setup, along with a description of how the estimation method is simulated using the computer software MATLAB. The results are then displayed and discussed in chapter 5 and 6 respectively. The conclusion is found in chapter 7 and suggestions for further work in chapter 8. Following the last chapter is the bibliography and appendices.

Chapter 2

Dynamic rating - power cables

The following chapter gives a brief literature review on the dynamic rating for power cables. It covers the principle of dynamic rating and how it could be used to reduce the effect of thermal bottlenecks. Moreover, it presents a common modern temperature measurement of power cables which is distributed temperature sensing (DTS). Lastly it covers methodology and application of dynamic rating of power cable systems today.

2.1 Dynamic rating principle

To exploit this potential grid reserve in established power cables, the term dynamic rating (DR) has been a focus area for both scientific researchers and grid operators. The principle of DR is based on live measurements of load current, temperature in different cable layers and external parameters depending on laying conditions. The measurements are used to determine a real-time dynamic current rating capacity for a power cable [3].

According to [8], the dynamic current ratings are generally greater than the static ratings. As there is a higher transmission potential in already existing grid equipment, research on DR has been conducted for other power components as well, such as power lines and transformers. For power cables, DR requires that the operators have sufficient information about operating temperature in the cable [9]. However, grid operators often lack information about the conductor temperature during operation as it is complex to measure [10].

It is vital to operate cables within safe measures, and advanced dynamic methods uses an estimation of the conductor temperature based on real-time measurable parameters. These methods operate with live data from advanced temperature measuring systems such as DTS. Combined with a real-time temperature rating (RTTR) system to give operators an adequate estimate of conductor temperature. Number of time varying parameters contained in the RTTR algorithm differs between methods, but commonly load variation and DTS data are used [11].

A primary issue when using an estimate of the conductor temperature is the reliability of the estimate. If the cable is operated at overload conditions for longer time periods, it could cause harm to the cable system and result in unnecessary costs for grid operators. This enhances the demand for more scientific research on the DR topic. Creating reliable verification of different RTTR algorithms is essential to ensure a stable power grid.

Available literature has mainly focused on DR of power lines, which shows great potential for transmission increase. However, the thermal limits of power cables could make a thermal bottleneck, that also impacts the DR of power lines. As the grid sometimes combine lines and cables in the distribution network [12]. Cherukupalli and Anders suggests in [11] that implementation of DR systems could potentially rise the transmission capacity by 5-25 %, compared to static ratings.

2.2 Power cables as thermal bottlenecks in the grid

Ampacity rating of power cables are associated with laying conditions and heat dissipation to the surroundings. Commonly, power cables are placed throughout varying laying conditions that impacts the rate of heat dissipation differently. Sections with modest dissipation often tends to experience the highest temperature levels, often described as thermal bottlenecks of the cable. These sections are often where the cable is laid in ducts, together with other cables and air as surrounding medium [13].

As the thermal properties of the surroundings are not persistent throughout the whole cable length, the conductor temperature will be higher in the areas with the least heat dissipation. In some cases where the thermal conditions are least favourable, it might surpass 20°C compared to the conductor temperature in other sections. For these worst-case areas, grid operators lack sufficient formulas or tabulated values easily accessible to determine the ampacity rating, such that a percentage reduction is used instead [14]. These reductions often contain large safety margins which could lead to not utilizing the full potential of the cable.

For operators to reduce the effect of thermal bottlenecks or hotspots, these areas need to be detected and analyzed using proper temperature measurement and detection technology. Once these spots are mitigated and handled, the full potential of the ampacity can be exploited [15]. One technique is to increase the thermal conductance at these areas by using a medium with low thermal resistivity in the cable surroundings. With then a proper thermal bottleneck detection method that uses precise temperature measurement along with a DR system for better current-carrying capacity, grid operators will then be able to ensure safe operation of power cables.

2.3 Temperature measurement of power cables

To ensure temperature data along the total cable length, one of the most prominent technologies used today is DTS. It is fibre optics placed along the cable, in different layers such as the sheath or at the surface. This gives the opportunity to monitor several points and sections of the cable and real-time temperature readings are made available. Operators could then access different thermal profiles for the varying laying conditions [16]. Figure 2.1 shows how the optical fibre could be placed in the metal screen layer of a power cable.

Figure 2.1: *"Optical fibres integrated in the power cable between the metal wire screen"*, from [17, p. 65].

A report constructed by a working group from Cigre showed that 66 % of the involved grid operators in the survey uses DTS systems combined with RTTR. Of these, only 3 % uses the data for actual transmission purposes. This implies that the data is not being utilized completely. The report also stated that 96 % of the operators preferred DTS as temperature measuring system, but more than 70 % of these said that the data gathered was mostly used for learning purposes. Furthermore, 50 % of the operators replied blank on what their main purpose of installing DTS was for [17].

Even with modern technology for more dynamic considerations of power cables, the potential is still not being exploited. Advanced temperature systems and algorithms for live capacity computation is being installed, but not used for its purpose. Static ratings might still be the governing method for cable operations. However, as the majority of data is used for learning and training, future operations could improve the transmission capacity.

2.4 Modern application of dynamic rating on power cable systems

To operate power cables according to dynamic ratings a temperature measurement system combined with a RTTR system is often used by operators. Temperature and load current data are provided by the use of supervisory control and data acquisition (SCADA). The algorithm calculates the temperature of the conductor, other cable layers and surroundings if necessary. The communication between SCADA and RTTR usually handles different zones of the cable, depending on laying conditions. The system generates a thermal model for each zone, which makes detection of bottlenecks possible [18].

Figure 2.2 shows a common RTTR system where the algorithm is either based on rating calculations according to IEC standards 60287 and 60853 or numerical finite element method (FEM). This gives the operators access to data for the entire cable route. Although according to the Cigre report, the data is still not being used even though it is accessible. From [11], by deploying such a system, grid operators want to consider the following:

- Live transmission limitations of the system
- What is the overload capacity of the system at certain operating conditions
- At what point does the cable exceeds operating limits during applied overloading of current rating

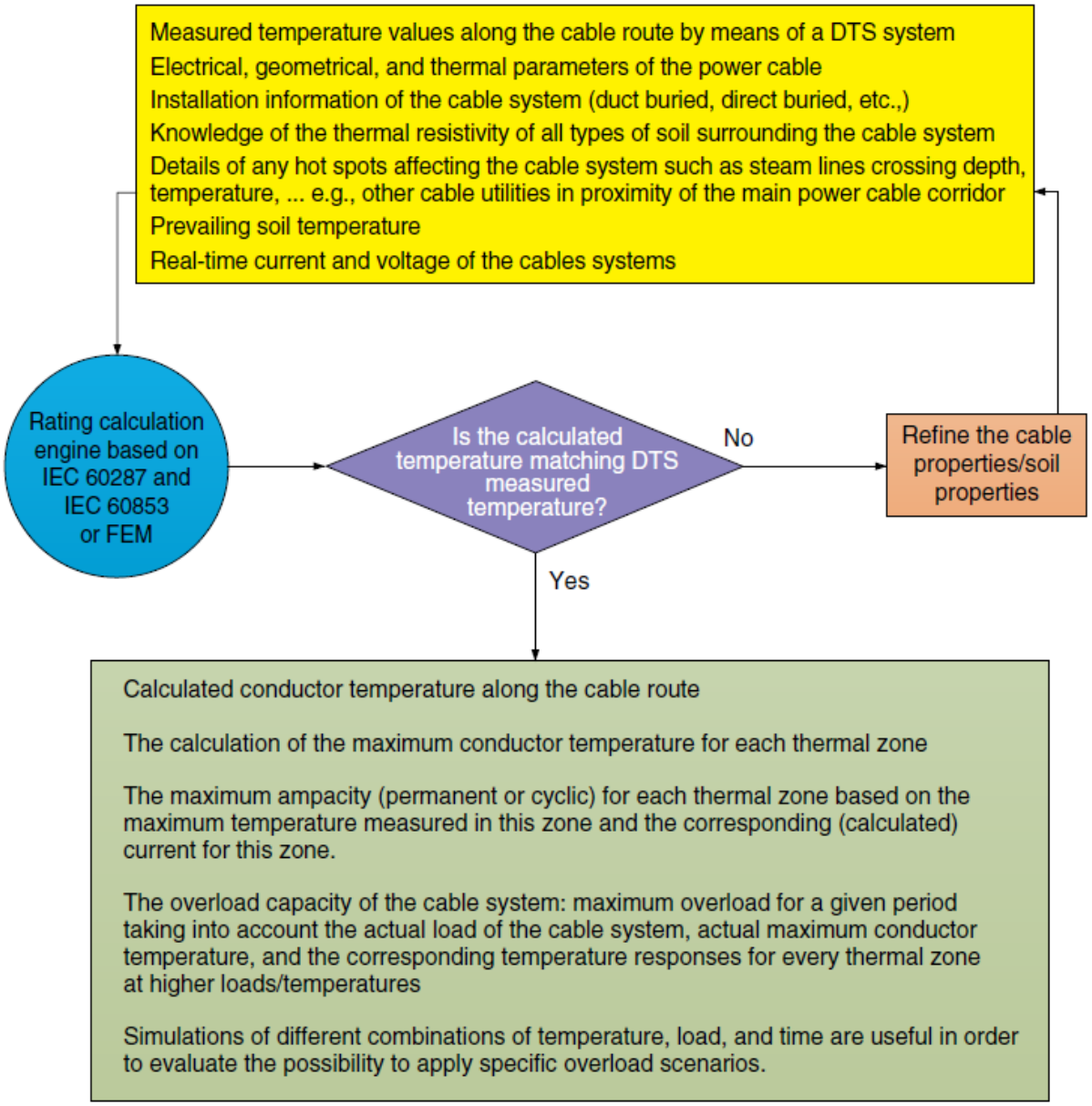

Figure 2.2: Common RTTR system analysis from [11].

Chapter 3

Theory

The theoretical basis for the thesis is presented in four different sections. First section gives a description of how heat is generated in power cables. Section two describes how power cables are modelled as thermal circuits, using electrical to thermal analogies. The third section depicts how transient temperature response functions of different cable layers are calculated analytically according to the IEC standards. Lastly, the fourth section covers how the transient temperature response can be calculated during dynamic loading of a power cable. Also, it presents the developed estimation method for conductor temperature response during dynamic loading.

3.1 Heat development in power cables

Heat is generated internally in power cables from voltage- and current dependent losses occurring in various layers of the cable. Depending on the construction of the cable, layers such as the conductor, sheath, metallic screens and armour could be considered as heat sources [19]. Heat generated in these layers dissipates through the surrounding medium, making the laying conditions a vital parameter that affect the ampacity of the cable [20].

External heat sources such as solar radiation from the sun, ambient temperature in the cable environment, type of surrounding medium, air or soil and other factors are considered as laying conditions. The cable installation studied in this thesis is a single-core XLPE insulated cable with an aluminium conductor. The only losses considered are the current-dependent losses in the conductor, called ohmic losses. No other internal losses are included further. The cable installation is placed on the floor inside, with air as the surrounding medium. External heat sources are neglected, as the cable is not exposed to any solar radiation.

3.1.1 Ohmic losses

Ohmic losses, denoted as W_c, are current dependent losses that generate heat in the conductor. The losses occur as a load current is applied to the cable and the conductor having a resistance. The following equation from [19], equation (3.1), can be used to calculate the ohmic losses.

$$W_c = I^2 \cdot R_{AC} \tag{3.1}$$

- I: Load current [A]
- R_{AC}: Alternating current resistance (AC) of the conductor at operating temperature [Ω]

Conductor resistance changes linearly with operating temperature, as the temperature at the conductor increases the resistance also increases. The conductor resistance is either a direct current (DC) resistance, denoted as R_θ. or AC resistance, denoted as R_{AC}. Depending on if the conductor is carrying DC or AC. From [21], the DC resistance can be calculated as shown in equation (3.2).

$$R_\theta = R_{20}[1 + \alpha(\theta - 20)] = \frac{\rho_{20} \cdot l}{A}[1 + \alpha(\theta - 20)] \tag{3.2}$$

- R_{20}: Conductor resistance at 20°C [Ω]
- α: Temperature coefficient, for aluminium $\alpha = 0.0043$ [$°C^{-1}$]
- θ: Operating temperature at the conductor [°C]
- ρ_{20}: Conductor resistivity at 20 °C, for aluminium $\rho_{20} = 2.8264 \cdot 10^{-8}$ [Ωm]
- l: Length [m]
- A: Cross-sectional area of conductor [m^2]

The AC resistance is not only impacted by varying temperature, effects such as proximity- and skin effect will also affect the conductor resistance. Cables close or parallel, will impact the current density of each other when carrying an AC. The density is reduced on the closer sides and increased on the remote sides due to the induced currents. This effect is called the proximity effect, denoted by y_p [19].

Carrying an AC also result in the current distribution being unequally spread in the conductor. This effect is called the skin effect, denoted by y_s [19]. Including these effects, the AC resistance is always greater than the DC resistance of a conductor. How these effects are included in R_{AC} is show in equation (3.3) from [19].

$$R_{AC} = R_\theta(1 + y_p + y_s) \tag{3.3}$$

As the proximity effect is dependent on other cables close or parallel to each other and the skin effects dependency of large cross-sectional area of the conductor and high system frequency. Both effects have been neglected when calculating the conductor resistance, as the cable used in this thesis does not have any neighbouring cables, a cross-sectional area of 50 mm^2 and a system frequency of 50 Hz. Such that R_{AC} is only considered to be temperature dependent. In [21], the relationship between R_θ and R_{AC} equals 1.0267 for a conductor with a 100 mm^2 cross-section and 50 Hz system frequency, when proximity- and skin effects are considered.

3.2 Thermal modelling - power cable

Modelling a thermal circuit of a power cable requires the use of fundamental similarities between current flowing due to an electric potential and heat flow caused by temperature difference between the loaded conductor and surrounding medium. Analogies between electrical- and thermal terminology are presented in table 3.1 from [22]. For thermal circuits, Ohm's law correlate to Fourier's law of heat conduction, due to charge being the electrical analogy to heat. Temperature and heat transfer rate is the equivalents of voltage and current respectively. Resistance and capacitance are similar properties for both terminologies. The thermal resistance of a material is the ability to limit heat flow and heat capacity describes heat stored in a material [23].

Table 3.1: Electrical and thermal analogies for thermal circuits [22].

Electrical terminology			**Thermal terminology**		
Property	Symbol	Unit	Property	Symbol	Unit
Voltage	V	[V]	Temperature	θ	$[^{\circ}C]$
Current	I	[A]	Heat transfer rate	q	[W]
Resistance	R	[Ω]	Thermal resistance	R	$[\frac{Km}{W}]$
Capacitance	C	[F]	Heat capacity	C	$[\frac{J}{^{\circ}C}]$

To represent the thermal model of a cable system as a circuit, it can be sectioned into several loops. Where each loop is characterised by a thermal resistance and a thermal capacitance. This is considered as a lumped parameter method, used for solving complex cable systems. The thermal circuit is considered linear as long as the thermal characteristics does not vary with temperature, which makes the use of superposition principle possible when solving heat flow difficulties [23].

Prior to newer technology that made solving cable systems consisting of several loops possible, simplified networks with only two loops were developed, called a two-loop circuit. Solving a system with numerous loops was considered a tedious task and a two-loop representation proved to be valid for the majority of applications [23]. Further sections cover calculations of parameters used in a two-loop model and how a thermal circuit with multiple loops are reduced to a two-loop circuit.

3.2.1 Thermal resistance

Different sections of the cable system such as metallic armour and screen, cable sheath and the surroundings will limit heat dissipation from the conductor. Meaning all nonconductive parts will restrict heat flow and needs to be considered as a thermal resistance, denoted by T. For cylindrical power cables, the circular geometry of different layers can be used as an advantage. The thermal resistance of the metallic layers such as the screen can be neglected, due to having a high thermal conductivity [23].

Equation (3.4) from the international standard IEC 60287-2-1 [24], calculates the thermal resistance, T, of a given cylindrical layer i in the cable. Index i is a denotation of cable insulation and sheath, using numbers 1 or 3 respectively. 2 is used for metallic parts, which is neglected. The thermal resistivity, ρ, can be found as a tabulated value in [24] for both insulation and sheath, depending on what material the respective layer is constructed of.

$$T_i = \frac{\rho_i}{2\pi} ln \left(1 + \frac{2t_i}{D_i}\right) \tag{3.4}$$

- ρ_i: Thermal resistivity of layer i $[\frac{Km}{W}]$
- t_i: Thickness layer i [m]
- D_i: Diameter beneath layer i [m]

Thermal response of a cable in air depends on heat transfer mechanisms, neighbouring cable configuration that could cause induced heating and solar radiation [25]. The external thermal resistance for the cable, T_4, is highly dependent on what medium the surroundings consist of. For cables located in air, T_4 has a smaller impact on the rating compared to cables located underground, however the calculation is considered more complex [23].

IEC 60287-2-1 gives a thorough description of a method to calculate the external thermal resistance for cables laid in air. It includes a simple iterative method to acquire the cable surface temperature above ambient temperature, $\Delta\theta_S$. The external thermal resistance, T_4 can be calculated from equation (3.5) [24].

$$T_4 = \frac{1}{\pi D_e h (\Delta\theta_S)^{\frac{1}{4}}} \tag{3.5}$$

- De: External diameter of cable [m]
- h: Heat dissipation coefficient that includes heat transfer mechanisms
- $\Delta\theta_S$: Temperature of cable surface above ambient temperature

The heat dissipation coefficient, h, can be calculated as shown in equation (3.6).

$$h = \frac{Z}{(D_e)^g} + E \tag{3.6}$$

- Z, g and E: Tabulated constants for black surfaced cables in air placed on ground

Values used in this thesis for these constants are Z = 1.69, g = 0.20 and E = 0.79 from [23]. Due to the practical power cable used in the laboratory setup having a black surface and being placed directly on the floor with air surrounding it.

To initiate the iterative process, variable K_A used during the iteration is defined, and calculated from equation (3.7).

$$K_A = \frac{\pi D_e h}{(1 + \lambda_1 + \lambda_2)} \left[T_1 + T_2(1 + \lambda_1) + T_3(1 + \lambda_1 + \lambda_2)\right] \tag{3.7}$$

- λ_1: Sheath loss ratio factor, neglected in further calculations
- λ_2: Armour loss ratio factor, neglected in further calculations
- T_1: Thermal resistance of insulation $\left[\frac{Km}{W}\right]$
- T_2: Thermal resistance of metallic parts, neglected in further calculations $\left[\frac{Km}{W}\right]$
- T_3: Thermal resistance of sheath $\left[\frac{Km}{W}\right]$

$\Delta\theta_S$ can then be calculated using equation (3.8), where the initial value is set as $(\Delta\theta_S)^{\frac{1}{4}}$ = 2. The iteration is repeated until $(\Delta\theta_S)^{\frac{1}{4}}_{n+1}$ - $(\Delta\theta_S)^{\frac{1}{4}}_{n} \leq 0.001$.

$$(\Delta\theta_S)^{\frac{1}{4}}_{n+1} = \left[\frac{\Delta\theta + \Delta\theta_d}{1 + K_A(\Delta\theta_S)^{\frac{1}{4}}_{n}}\right]^{0.25} \tag{3.8}$$

- n: Iteration index
- $\Delta\theta$: Maximum operating conductor temperature above ambient temperature [$^\circ C$]
- $\Delta\theta_d$: Dielectric loss factor, 0 if dielectric losses are neglected

3.2.2 Thermal capacitance

Calculating the transient temperature response includes the thermal capacitance of different cable sections. The thermal capacitance per unit length, Q, is considered as heat stored in each layer of the cable, and can be calculated as shown in equation (3.9) [23].

$$Q = V_o \cdot c \tag{3.9}$$

- V_o: Volume of the object [m^3]
- c: Specific heat of the material, volumetric $\left[\frac{J}{^\circ C m^3}\right]$

Layers such as cable insulation and sheath have a coaxial configuration, to calculate the thermal capacitance of these layers equation (3.10) can be used.

$$Q = \frac{\pi}{4}\left(D_{ex}^2 - D_{in}^2\right) \cdot c \tag{3.10}$$

- D_{ex}: External diameter of layer [m]
- D_{in}: Internal diameter of layer [m]

The thermal capacity is not a linear function of the layer thickness. This makes the modelling of transient temperature response complex and involves prolonged calculations. Van Wormer developed a method where an equivalent π circuit is used. The method uses lumped parameters to distribute the thermal capacitance of the cable insulation between the thermal capacitance of the conductor and the sheath [26]. The ratio of portioned thermal capacitance is called the Van Wormer coefficient, denoted as p. Distributed thermal capacitance in the insulation is shown in figure 3.1, where pQ_i is placed at the conductor and $(1-p)Q_i$ is placed at the screen.

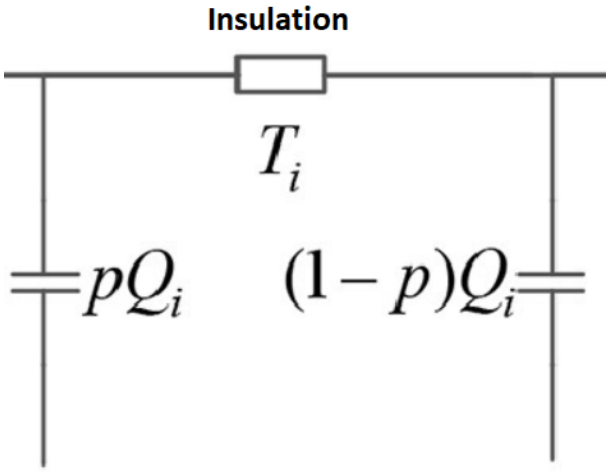

Figure 3.1: Lumped parameter thermal model of cable insulation using Van Wormer coefficient p from [27].

Calculation of p for the insulation can be carried out as shown in equation (3.12) [23].

$$p = \frac{1}{2ln\left(\frac{D_{ins}}{D_{con}}\right)} - \frac{1}{\left(\frac{D_{ins}}{D_{con}}\right)^2 - 1} \tag{3.11}$$

- D_{ins}: External diameter of insulation [m]
- D_{con}: Internal diameter of insulation [m]

Similar approach can also be used for thermal capacitance of the sheath, where the Van Wormer coefficient is denoted as p', and can be calculated using the following equation [23]:

$$p' = \frac{1}{2ln\left(\frac{D_{es}}{D_s}\right)} - \frac{1}{\left(\frac{D_{es}}{D_s}\right)^2 - 1} \tag{3.12}$$

- D_{es}: External diameter of sheath [m]
- D_s: Internal diameter of sheath [m]

3.2.3 Thermal model of a cable system

Figure 3.2 shows a thermal model of a single-core cable where the only losses considered are the ohmic losses, W_c, covered in section 3.1.1. The thermal resistance of the screen is neglected as it has a low thermal resistance [19]. The thermal resistance T_1, T_3 and T_4 represents the thermal resistance of the insulation, cable sheath and the surroundings respectively. Q_{con}, Q_i, Q_{sceen} and Q_{sheath} represents the thermal capacitance of the different layers respectively, conductor, insulation, screen and sheath.

In steady-state the thermal resistances are governing the circuit, thus thermal capacitances can be neglected. However, when considering the transient thermal response of a cable the thermal capacitance has a great influence. To be able to consider the total temperature response of a cable, both steady-state and transient parameters are included in the model. Further this model can be reduced to a two-loop circuit.

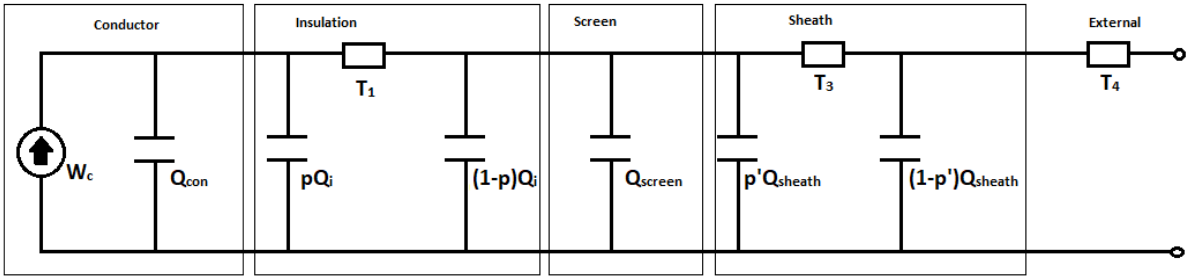

Figure 3.2: Thermal circuit of a cable system.

IEC standard 60853 [28] uses a thermal model containing only two loops when calculating the cable ampacity. This is a standardized simplification for basic cable types to reduce complexity of transient response calculations [29]. The circuit contains two thermal resistances, T_A and T_B that represents the thermal resistances of the full model. Also, two thermal capacitances, Q_A and Q_B, that represents the thermal capacitances. The two-loop circuit is shown in figure 3.3. The following equations (3.13-16) shows the calculation of each parameter in the two-loop circuit for a cable with air as surrounding medium. As mentioned earlier λ_1 is neglected [19].

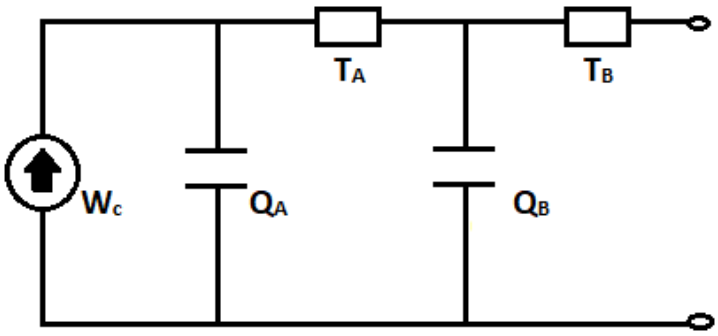

Figure 3.3: Thermal circuit of a cable system, reduced to two loops.

$$T_A = T_1 \tag{3.13}$$

$$T_B = \frac{1}{2}T_1 + (1 + \lambda_1)(T_3 + T_4) \tag{3.14}$$

$$Q_A = Q_{con} + pQ_i \tag{3.15}$$

$$Q_B = (1 - p)Q_i + \frac{Q_{screen} + p'Q_{sheath}}{1 + \lambda_1} \tag{3.16}$$

3.3 Transient temperature response in cable layers

To calculate the transient temperature response in different layers, the linear network displayed in figure 3.2 is analysed and reduced to two loops. It is required to determine the response function for the temperature rise, produced by a forcing function, which is the ohmic losses in the conductor. To determine this, a transfer function for the circuit can be used. The transfer function is the Fourier transform for the unit impulse response in the circuit. Laplace transformation of the transfer function as a ratio is given in equation (3.17) from [23].

$$H(s) = \frac{P(s)}{Q(s)} \tag{3.17}$$

- $P(s)$ and $Q(s)$: Polynomials, dependent on number of loops in the network. Zeros and poles can be found by setting these polynomials as zero

The response function, temperature rise at node i in the thermal circuit, is shown in equation (3.18) from [23]. The response function in this thesis is calculated for node $i = 1$, which corresponds to the conductor temperature rise, θ_1. As well as for node $i = 2$, the response function of the sheath temperature rise, θ_2.

$$\theta_i(t) = W_c \sum_{j=1}^{n} T_{ij} \left(1 - e^{P_j t}\right) \tag{3.18}$$

- W_c: Conductor losses $[\frac{W}{m}]$
- T_{ij}: Coefficient $[\frac{^\circ Cm}{W}]$
- P_j: Time constant $[\text{sec}^{-1}]$
- t: Step starting time [sec]
- n: Number of loops
- i: Node index
- j: Index from 1 to n

Coefficients T_{ij} and time constants P_j can be obtained by the zeros and poles for the network transfer function. Calculation of the coefficients, T_{ij}, are shown in the following equation (3.19) [23].

$$T_{ij} = -\frac{a_{(n-1)i}}{b_n} \frac{\prod_{k=1}^{n-i} (Z_{ki} - P_j)}{P_j \prod_{k=1, k\neq j}^{n} (P_k - P_j)} \tag{3.19}$$

- $a_{(n-1)i}$: Transfer function, numerator equation coefficient
- b_n: Transfer function, denominator equation coefficient
- Z_{ki}: Zeros of transfer function
- P_j and P_k: Poles of transfer function
- k: Index from 1 to n $\neq j$

3.4 Estimating transient temperature response in power cables

The following sections covers the theoretical background for calculating the temperature response during dynamic loading and a presentation of the developed method for estimating the temperature at the conductor. The first section, 3.4.1, was initially presented in the preceding specialization project and is a draft directly from that report [7, pp. 6-7].

3.4.1 Transient temperature response during dynamic loading

"When calculating the transient temperature response during variable loading of a power cable, the load curve can be split up into a sequence of steps with constant magnitude. For each different consecutive step, the calculation is repeated. The total transient response can then be calculated using the superposition principle, that sums up each step going towards a hypothetical steady-state temperature. The result will be a final transient temperature response, as a function of time [23].

When studying a thermal equivalent system of an electric equipment such as a cable, the analogies used such as thermal resistance and capacitance can be considered linear components. This makes the principle of linear superposition valid for a thermal system analogy of the electrical equipment. The superposition principle assumes that if one component of the system is switched on individually, and the effect it has on the system is measured. It is possible to sum up the contribution from each invidual component to get the total effect. Just as if the components were turned on at the same time [30].

Figure 3.4 shows an example from [19] of how resulting temperature is calculated using the superposition principle when there is a single step current, I, lasting for one hour. This single step current can be compared with an equivalent series of positive and negative step currents with respectively the value I and -I. Positive steps represent when the current is on, the negative when the current is off. The positive steps starting at time t = 0 and the negative steps starting at t = 1 hour The third plot in the figure represents the transient temperature response for each of the positive and negative steps, going towards a hypothetical steady-state temperature. The resulting temperature rise at time τ, above ambient temperature can be calculated as shown in (3.20) from [23] and is displayed in the fourth and last plot of figure 3.4.

$$\theta(\tau) - \theta(\tau - 1) \tag{3.20}$$

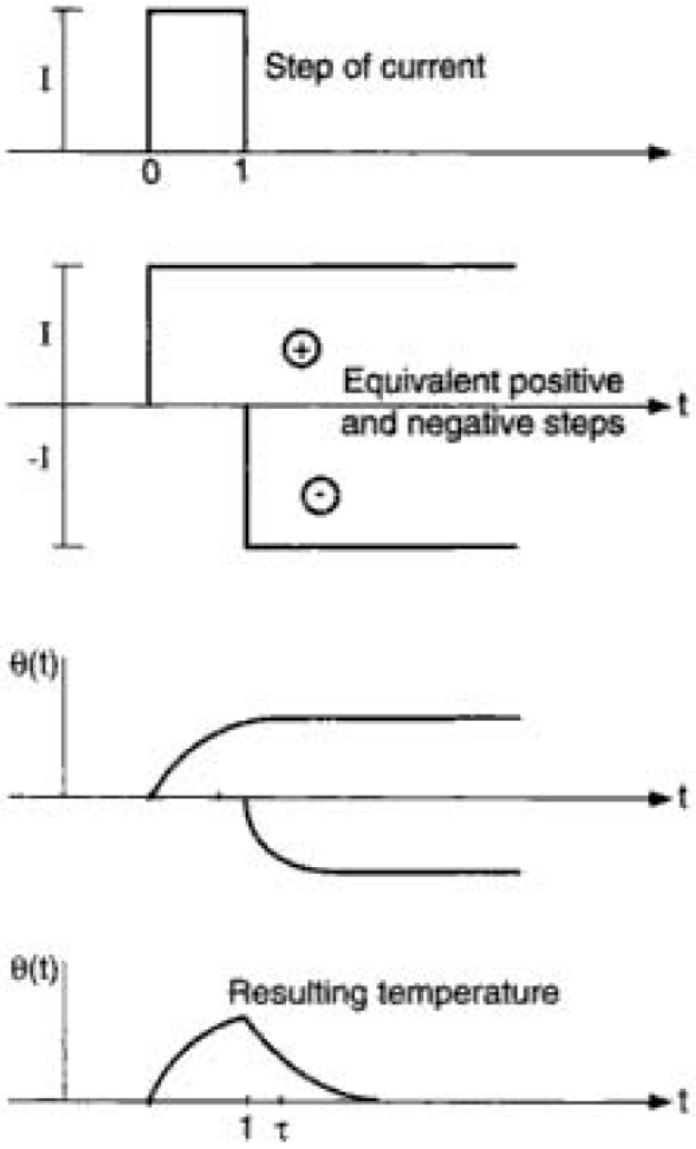

Figure 3.4: Transient temperature rise of single step current [19]."

3.4.2 Developed estimation method for conductor temperature

Following method make use of established temperature responses at the conductor for a given load situation with known laying condition parameters, to estimate the conductor temperature during dynamic loading. The established responses are considered to be a basis for the developed method. The estimation could then further facilitate the dynamic current rating of a power cable. The established responses used is a long-term measurement that has both transient and steady-state temperature information for the conductor. Another procedure used is analytical calculations of the conductor temperature response according to IEC standards, as previous sections of this chapter cover.

In this thesis, both procedures are used as basis for comparison. The aim is to be able to produce realistic estimates of the conductor temperature during changes in load current, also known as dynamic loading. The experimental laboratory measurements are described later in section 4.2. During research for theoretical material, no other relevant scientific theses covering similar methods of temperature estimation in power cables were discovered.

The estimation is based on having available long-term temperature data of the cable conductor. Temperature response needs to be simulated or measured for a period that ensures temperature data for both the transient temperature rise and steady-state. This can be considered as measuring or calculating the response function of the conductor, $\theta_1(\mathrm{t})$. The idea is that the established conductor temperature response, for a given load situation and same laying conditions is split up into sequences of individual contributions depending on the change in load current. Each contribution is scaled to fit the present load current. The scaling uses equation (3.1) from section 3.1.1 as background principle.

Each individual temperature contribution is scaled by the squared value of change in load current. The change in current is relative to the load current applied when establishing the long-term temperature responses. Load current, I, applied during establishing of the basis can be denoted as 100 %. If an increase of 50 % in load current is applied, it can be considered an increase of $(1.5)^2$ for W_c. As temperature is considered to be linear with the losses, the new temperature response will then resemble the established long-term temperature. As if the initial load current used was 50 % larger than the initial current (100 %) and laying conditions remain unchanged.

The AC resistance, R_{AC}, of the conductor varies linearly with change in temperature. Equation (3.1) includes this variation in resistance. However, the scaling principle of this estimation method was not initially developed to include change in R_{AC}, as the preceding project [7] showed great potential when neglecting this parameter. Introductory testing showed that for larger power cables, R_{AC} would have a larger impact. This impact has then later been implemented in the scaling principle used in the method and is covered in section 4.3.1.

The superposition principle, described in the previous section, can then be applied to estimate the total temperature response at the conductor during dynamic loading. Each individual contribution is added together, equal quantity of both positive (current on) and negative (current off) contributions, to make up the temperature response. To demonstrate this method a following example resembling figure 3.4 follows. The example contains a larger number of individual contributions.

Figure 3.5 shows a experimental measurement of the conductor response function, total temperature above ambient temperature, $\theta_1(t)$. As well as measured ambient temperature of the cable surroundings. A load current of 225 A was applied for a period of 12 hours, the laboratory setup used to obtain these measurements are described in section 4.2.

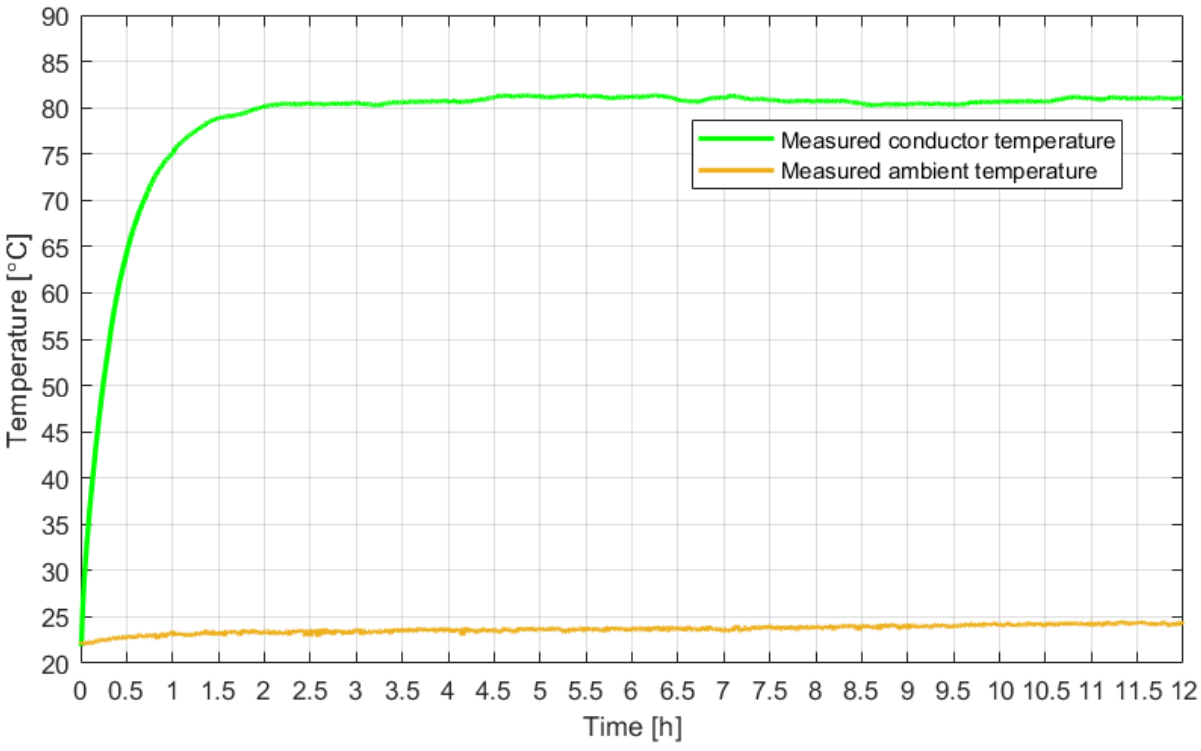

Figure 3.5: Long-term temperature measurement of conductor (light green line) and ambient temperature (brown line), with a load current of 225 A applied for 12 hours.

$\theta_1(t)$ is then split up into equal number of positive and negative contributions that is scaled for a dynamic load current. Individual contributions are denoted by $\theta_1(t)$ and the percentage value in parenthesis is relative to load current that was applied during establishment of the basis. The changes in load current for this case is as follows, where t is the time correlated to when the change in load current occurs.

- $0 \leq t < 1$ hour, $I = 225$A (100%), no scaling applied to individual contribution
- $1 \leq t < 2$ hours, $I = 337.5$A (150%), temperature response scaled by a factor of $(1.5)^2 = 2.25$
- $2 \leq t < 3$ hours, $I = 112.5$A (50%), temperature response scaled by a factor of $(0.5)^2 = 0.25$
- $3 \leq t < 8$ hours, $I = 0$, current turned off

The individual contributions for this case of dynamic loading are shown in figure 3.6. Solid lines represent current on, dashed lines represent current off. To give each contribution the same initial starting temperature, each step is corrected for the starting temperature, initial temperature at the cable conductor which also is the ambient temperature. This difference is added to the total transient temperature response to include the impact of ambient temperature.

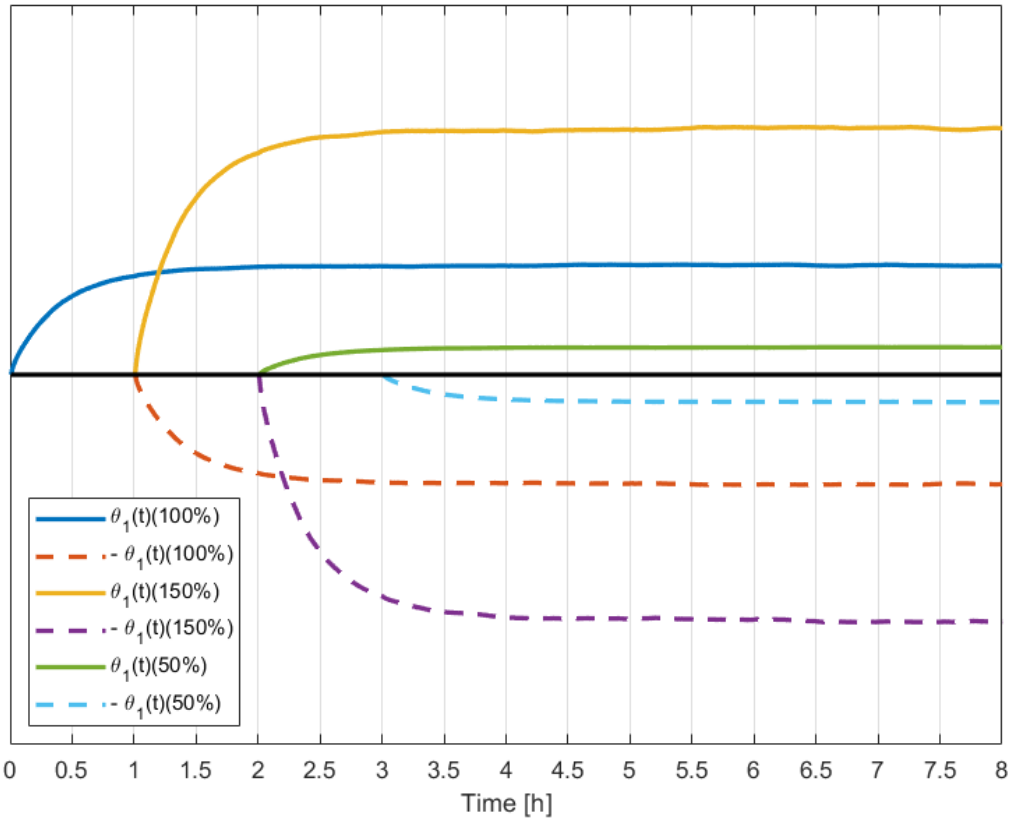

Figure 3.6: $\theta_1(t)$ split up into individual contributions that are scaled according to the changes in current, I.

Each of the contributions can then be added together using the superposition principle for linear circuits. The total temperature response of the contributions will be an estimation of the transient temperature response at the cable conductor. The sum of the contributions can be completed as follows and the total estimated transient temperature response of the conductor are show in figure 3.7:

- $0 \leq t < 1$ hour, total transient temperature response = $\theta_1(t)(100\%)$
- $1 \leq t < 2$ hours, total transient temperature response = $\theta_1(t)(100\%)$ + (-1) $\theta_1(t-1)(100\%)$ + $\theta_1(t-1)(150\%)$
- $2 \leq t < 3$ hours, total transient temperature response = $\theta_1(t)(100\%)$ + (-1) $\theta_1(t-1)(100\%)$ + $\theta_1(t-1)(150\%)$ + (-1) $\theta_1(t-2)(150\%)$ + $\theta_1(t-2)(50\%)$
- $3 \leq t < 8$ hours, total transient temperature response = $\theta_1(t)(100\%)$ + (-1) $\theta_1(t-1)(100\%)$ + $\theta_1(t-1)(150\%)$ + (-1) $\theta_1(t-2)(150\%)$ + $\theta_1(t-2)(50\%)$ + (-1) $\theta_1(t-3)(50\%)$

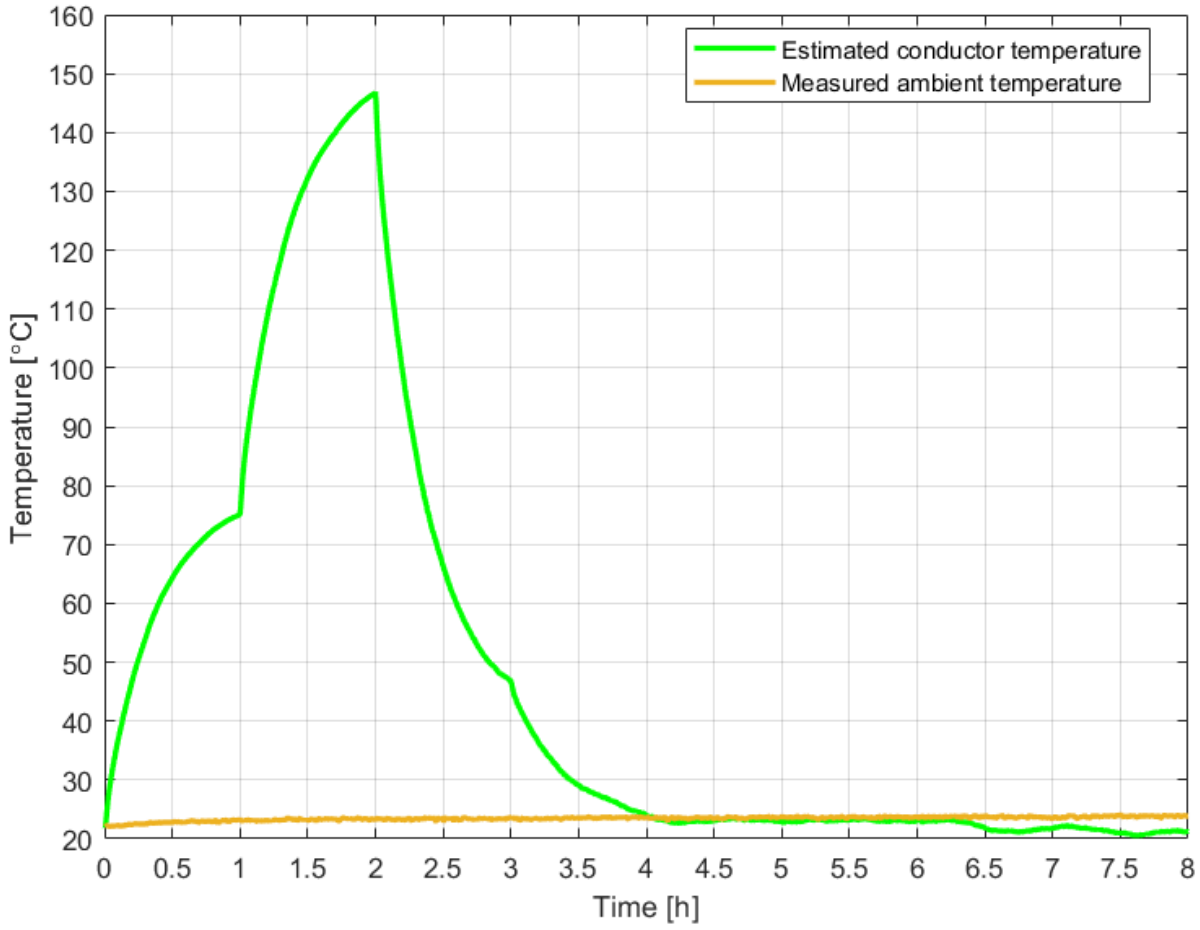

Figure 3.7: Estimate of the total transient temperature response of the conductor (light green line) and measured ambient temperature during the long-term temperature measurement (brown line).

Chapter 4

Method

This chapter covers the two different procedures used to establish a temperature basis for the estimation method. Firstly, it gives a step-by-step description of how the temperature responses for both the conductor and cable sheath are analytically calculated. Further, the experimental laboratory setup used for temperature measurement of the XLPE cable are presented. Lastly, it explains the methodology of how each of the two bases are used for estimation of conductor temperature.

4.1 Analytical calculation of temperature response functions

The following calculations are based on equations presented in sections 3.2 and 3.3. As well as methodology from Anders in [19], based on IEC standards 60287 and 60853. Firstly, the full thermal network shown in figure 3.2 are reduced to a two-loop network, displayed in figure 4.1. Where θ_1 and θ_2 are the temperature response functions of the conductor (node one) and the sheath (node two) respectively. The physical parameters of the cable system used in the laboratory, are displayed in tables 4.1 and 4.2.

The long-term transient and steady-state analytical calculation applies a load current of 225 A to the cable for a period of 12 hours. The load current was simulated to be applied continuously on a cable with identical characteristics and laying conditions as the one used in the laboratory setup. 225 A was chosen due to being the maximum allowed load current of the practical XLPE cable.

The calculated values for the cable system are shown in tables 4.3 - 4.5. These values are for the two-loop thermal network that is further used in calculation of the temperature response functions, displayed in the following sections. The calculations were carried out in MATLAB software [31] and the code is presented in appendix B. The cable characteristic are presented in table 4.8.

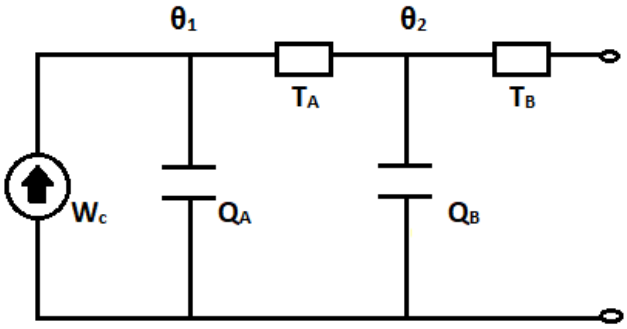

Figure 4.1: Thermal circuit of a cable, reduced to two loops. θ_1 and θ_2 temperature response functions of node 1 and 2 respectively.

Table 4.1: Thermal resistivity of the cable system used in the laboratory setup.

Thermal resistivity of the cable system $\left[\frac{Km}{W}\right]$	
Thermal resistivity conductor, at 20 °C: $\rho_{con,20}$	$2.83{\cdot}10^{-8}$
Thermal resistivity XLPE insulation, at 20°C: ρ_{ins}	3.5
Thermal resistivity sheath, at 20°C: ρ_{sheath}	3.5

Table 4.2: Specific heat capacities of the cable system used in the laboratory setup.

Specific heat capacity, volumetric, of the cable system $\left[\frac{J}{m^3K}\right]$	
Specific heat capacity conductor: c_{con}	$2.4{\cdot}10^6$
Specific heat capacity XLPE insulation: c_i	$2.4{\cdot}10^6$
Specific heat capacity sheath: c_{sheath}	$2.4{\cdot}10^6$
Specific heat capacity screen: c_{screen}	$3.45{\cdot}10^6$

Table 4.3: Calculated thermal resistances.

Calculated thermal resistance $\left[\frac{Km}{W}\right]$	
T_1	0.48
T_3	0.09
T_4	0.95
T_A	0.48
T_B	1.28

Table 4.4: Calculated Van Wormer coefficients.

Calculated Van Wormer coefficients	
p	0.36
p'	0.45

Table 4.5: Calculated thermal capacitances.

Calculated thermal capacitance $\left[\frac{J}{Km}\right]$	
Q_{con}	121.1
Q_i	581.5
Q_{screen}	399.3
Q_{Sheath}	394.3
Q_A	330.6
Q_B	946.5

4.1.1 Conductor temperature response function, θ_1

Conductor response function, θ_1, in node one can be expressed by finding the transfer function for the first node, H_1(s), as shown in equation (3.17).

$$H_1(s) = \frac{\theta_1}{W_c} = Z_{tot} \tag{4.1}$$

- Z_{tot}: Total network impedance, fracture can be solved as follows:

$$Z_{tot} = \frac{1}{sQ_A + \frac{1}{T_A + \frac{1}{sQ_B + \frac{1}{T_B}}}}$$

$$Z_{tot} = \frac{1}{sQ_A + \frac{1+sQ_BT_B}{sQ_BT_AT_B + T_A + T_B}}$$

$$Z_{tot} = \frac{sQ_BT_AT_B + T_A + T_B}{s^2Q_AQ_BT_AT_B + s(Q_AT_A + Q_AT_B + Q_BT_B) + 1}$$

The transfer function in equation (4.1) can then be written as:

$$H_1(s) = \frac{sQ_BT_AT_B + T_A + T_B}{s^2Q_AQ_BT_AT_B + s(Q_AT_A + Q_AT_B + Q_BT_B) + 1}$$

Further, the coefficients T_{ij} for node one is determined, using equation (3.19). For node one, or the conductor temperature rise, index $i = 1$ and $j = 1$ and 2. Firstly, the zeros, Z_{11}, and poles, P_1, P_2, of the transfer function, H_1, are calculated.

$$M_0 = \frac{1}{2}(Q_AT_A + Q_AT_B + Q_BT_B), \qquad N_0 = Q_AQ_BT_AT_B$$

$$a = \frac{M_0 + \sqrt{M_0^2 - N_0}}{N_0}, \qquad b = \frac{M_0 - \sqrt{M_0^2 - N_0}}{N_0}$$

Zeros of H_1:

$$Z_{11} = -\frac{T_A + T_B}{Q_BT_AT_B}$$

Poles of H_1:

$$P_1 = -a, \qquad P_2 = -b$$

Furthermore, T_{ij} are found:

$$T_{11} = -\frac{a_{11}}{b_2}\frac{Z_{11} - P_1}{P_1(P_2 - P_1)}$$

Where the numerator and denominator coefficient of the transfer function, a_{11} and b_2:

$$a_{11} = Q_B T_A T_B, \qquad b_2 = Q_A Q_B T_A T_B \tag{4.2}$$

Inputting values in T_{11}:

$$T_{11} = -\frac{Q_B T_A T_B}{Q_A Q_B T_A T_B}\frac{-\frac{T_A+T_B}{Q_B T_A T_B} - (-a)}{-a(-b-(-a))}$$

Solving the fraction gives:

$$T_{11} = \frac{1}{a-b}\left[\frac{1}{Q_A} - b(T_A + T_B)\right] \tag{4.3}$$

Applying same procedure for T_{12}:

$$T_{12} = T_A + T_B - T_{11} \tag{4.4}$$

Finally, the conductor temperature response function can be found, using the coefficients, T_{11} and T_{12}.

$$\theta_1(t) = W_c\left[T_{11}\left(1 - e^{-at}\right) + T_{12}\left(1 - e^{-bt}\right)\right] \tag{4.5}$$

4.1.2 Sheath temperature response function, θ_2

Sheath response function, θ_2, in node two can be expressed by finding the transfer function for the second node, H_2(s), as shown in equation (3.17).

$$H_2(s) = \frac{\theta_2}{W_c} = \frac{Z_b}{1 + sQ_A(T_A + Z_b)} \tag{4.6}$$

- Z_b: Subsequent impedance seen from node two:

$$Z_b = \frac{1}{sQ_B + \frac{1}{T_B}}$$

The transfer function in equation (4.6), with the fracture solved as follows:

$$H_2(s) = \frac{\frac{1}{sQ_B + \frac{1}{T_B}}}{1 + sQ_A\left(T_A + \frac{1}{sQ_B + \frac{1}{T_B}}\right)}$$

$$H_2(s) = \frac{\frac{T_B}{sQ_BT_B + 1}}{1 + \frac{sQ_A(T_A + T_B + sQ_BT_AT_B)}{sQ_BT_B + 1}}$$

Transfer function for node two:

$$H_2(s) = \frac{T_B}{s^2Q_AQ_BT_AT_B + s(Q_AT_A + Q_AT_B + Q_BT_B) + 1} \tag{4.7}$$

Further, the coefficients T_{ij} for node two is determined, using equation (3.19). For node two, or the sheath temperature rise, index $i = 2$ and $j = 1$ and 2. The poles, P_1, P_2, of the transfer function, H_2, are the same as for H_1. H_2 does not have any zeros.

Furthermore, T_{ij} are found:

$$T_{21} = -\frac{a_2}{b_2}\frac{-P_1}{P_1(P_2 - P_1)}$$

Where the numerator and denominator coefficient of the transfer function, a_2 and b_2:

$$a_2 = T_B, \qquad b_2 = Q_AQ_BT_AT_B \tag{4.8}$$

Inputting values in T_{11}:

$$T_{21} = -\frac{T_B}{Q_AQ_BT_AT_B}\frac{-(-a)}{-a(-b - (-a))}$$

Solving the fraction gives:

$$T_{21} = \frac{1}{Q_A Q_B T_A} \frac{1}{(a-b)} \tag{4.9}$$

Applying the same procedure to T_{22}:

$$T_{22} = \frac{1}{Q_A Q_B T_A} \frac{1}{(ab-b^2)} \tag{4.10}$$

Finally, the sheath temperature response function can be found, using the coefficients, T_{21} and T_{22}:

$$\theta_2(t) = W_c \left[T_{12} \left(1 - e^{-at}\right) + T_{22} \left(1 - e^{-bt}\right) \right] \tag{4.11}$$

4.1.3 Calculated parameters for the response functions

The calculated parameters for θ_1 and θ_2 are displayed in table 4.6.

Table 4.6: Parameters used in calculations of conductor and sheath temperature response functions, θ_1 and θ_2, respectively.

Parameters used in computation of temperature response functions	
a	0.0087
b	0.0006
M_0	895.12
N_0	192 550
T_{11}	0.24
T_{12}	1.52
T_{21}	$8.2 \cdot 10^{-4}$
T_{22}	1.37

4.2 Experimental setup for temperature response measurement

4.2.1 Laboratory setup

To measure the temperature response of a practical power cable, an experimental laboratory setup was constructed. The setup uses a Nexans TSLF 24kV 1x50 A power cable connected to a combined VARIAC and transformer. The cable is equipped with two thermocouples placed at two different positions. The temperature is measured at the conductor and beneath the cable sheath. A single-line diagram of the setup is shown in figure 4.2.

The cable is placed in a flat formation directly on the floor, with neither neighbouring cables or potential external heat sources. The cable is not directly attached to the floor, but is assumed to not be elevated at any points except at the terminations. Both cable ends are terminated using cable lugs, that are connected directly to the transformer as a short-circuit, making a loop. Using this form of connection, the voltage drop across the cable is small, justifying the neglect of voltage dependent losses. The load current is measured using a plier ammeter.

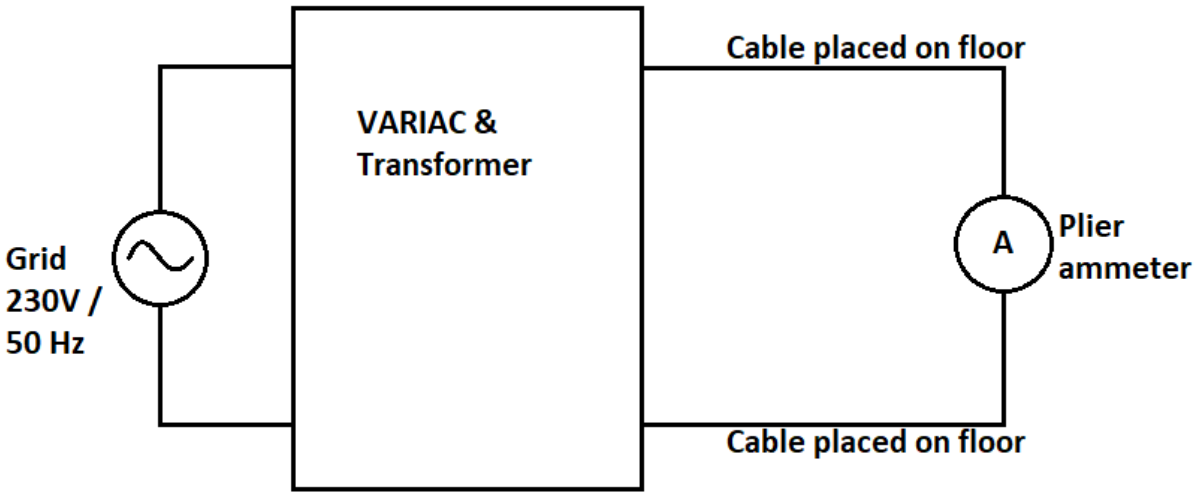

Figure 4.2: Single line diagram of laboratory setup.

Each of the total four thermocouples and the plier ammeter are connected to a data logger, further connected to a computer which uses the program Agilent Test - BenchLink Data Logger 3 to log the current and temperature data from the measurements. The data logger logs both current and temperature every 20 seconds. The data is then exported to Microsoft Office Excel and graphed using MATLAB software. A list of the laboratory equipment used are described in table 4.7.

Table 4.7: Equipment list for the laboratory setup.

Equipment list
Ruhstrat transformer, 400/0-400 V, 250 kVA
Nexans TSLF 24kV 1x50 A power cable [32]
FLUKE plier ammeter
KEYSIGHT data logger
KEYSIGHT Channel Multiplexer Module, circuit card
DELL PC
Thermocouples (Type T)
Various laboratory materials and equipment, such as cable lugs

4.2.2 Nexans TSLF 24kV power cable

The cable used in the laboratory setup is a single-core Nexans TSLF 24kV power cable, that has an aluminium conductor with a cross-sectional area of 50 mm^2 [32]. Total cable length of 12 m. The conductor is stranded and round and the surrounding insulation is XLPE. The cable screen contains stranded round copper wires and aluminium foil for waterproofing, the screen cross-section is in total 16 mm^2. The cable characteristics are displayed in table 4.8.

Table 4.8: Cable characteristics for Nexans TSLF 24kV [32].

Cable characteristics
Conductor diameter: 8.0 mm
Diameter across insulated conductor: 19.3 mm
Nominal insulation thickness: 5.5 mm
Average sheath thickness: 2.1 mm
Nominal outer diameter of cable: 27.0 mm
Allowed current load in air at 25 °C - flat formation: 225 A
Maximum allowed continuous conductor temperature: 90°C

An XLPE insulated cable have a maximum allowed operational temperature at the conductor of 90°C, considering thermal limitations of the surrounding insulation. The emergency temperature of XLPE cables are 125°C, that the cable can hold for the maximum time of one hour [21]. This temperature occurs in the events of short overloads or other situations where the cable temperature is increased.

4.2.3 Temperature measurement

As mentioned, two thermocouples that are copper-constantan type T, were placed at two different positions of the cable. The two positions are three meters from each end to avoid elevation from the ground, as the connection between cable ends and transformer are raised. The cause for measuring temperature at two different positions of the cable is to be able to compare and verify temperature measurement in the cable and possible fault detection.

On both positions two thermocouples are placed beneath the cable jacket for sheath temperature and directly on the cable conductor. The two thermocouples are placed with a gap of 5 cm of each other. To place them beneath the jacket and at the conductor, a small hole was drilled at a tilted angle. The holes impact on the measurements have been neglected. Figure 4.3 illustrates the placement in the cable composition. The ambient temperature of the surroundings was also measured using a thermocouple connected to the same data logger.

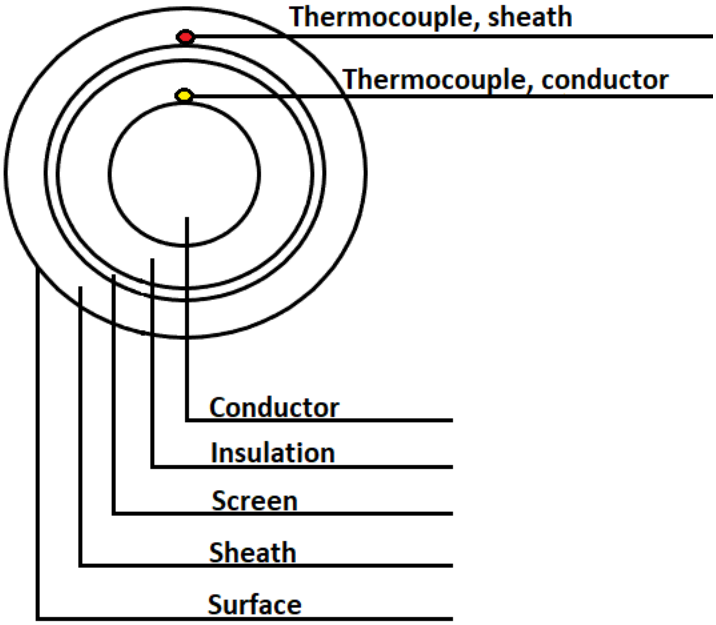

Figure 4.3: Cable composition and placement of thermocouples for temperature measurement.

During testing of the setup, one position showed a 3.8°C higher steady-state temperature at the conductor. As this was the worst-case scenario of conductor temperature, temperature measurement data from this position are used for both the long-term steady-state temperature measurement and the dynamic variable loading case. The measured conductor temperature for both positions during a 12 hour test with a load current of 225 A, are shown in figure A.1 displayed in appendix A.

4.3 Simulation of temperature estimates during dynamic variable loading

The estimates are simulated using a constructed code in the computer software MATLAB [31], that reads data from either the analytical calculations or the long-term experimental measurement of temperature responses in the cable layers. The motivation for using both calculations based on IEC standards and experimental measured temperature is to compare the applicability of both bases when using the estimation method to determine the dynamic current rating of a power cable.

The precision of the conductor temperature estimates are examined using the practical laboratory setup of the cable. The load case used when simulating the estimates has been replicated experimentally, to be able to compare the simulated estimates with a real time temperature measurement with the same changes in load current.

The analytical calculations shown in previous section, see 4.1, was performed using MATLAB. Both temperature response functions for the cable conductor and sheath, $\theta_1(t)$ and $\theta_2(t)$, was calculated and displayed graphically. Sheath response function is calculated for comparison to experimental measured sheath temperature. The constructed code for the calculations is found in appendix B.

The calculated temperature response for the conductor is the first basis used for estimating the temperature during dynamic loading. The MATLAB code is constructed to read the temperature calculations contained in a column vector and apply the developed estimation method on that vector. The scaling principle coefficients are manually set to predetermined values for a given dynamic load case.

The second basis used for estimation is the long-term measurement of conductor temperature. This can as previously mentioned, be compared to a measurement of the temperature response function, $\theta_1(t)$. The measured data gathered from the laboratory setup is then put into a column vector which is then applied a constructed MATLAB code that simulates the estimation and displays the total temperature response graphically, just as for the calculations. The code that simulates the conductor temperature estimation using measurement as basis can be found in appendix C.

4.3.1 Impact of temperature dependent conductor resistance R_{AC}

During analyzation of the simulated and experimental results, more precisely the comparison of estimated conductor temperature response to measured response, there was discovered a large deviation. To investigate this, the period containing this deviation was applied a simplified additional scaling to its individual contribution. This additional scaling included the temperature dependency of the conductor resistance R_{AC}.

The additional scaling was applied together with the scaling for change in load current. This was a fracture containing the relation between conductor resistance at initial starting point and resistance at end point for the given load current during this interval. Meaning, conductor resistance when the contribution is turned on and when it is turned off. For the dynamic case studied, this is at the elapsed time t = 1 h and t = 2 h. Valid for the time period load current I is equal to 337.5 A. The following equation shows the applied fracture.

$$\frac{R_{AC}(t = 2h)}{R_{AC}(t = 1h)} \tag{4.12}$$

For this to be possible, R_{AC} was calculated for the dynamic load case, using measured ambient and conductor temperature in the laboratory. The new scaling was then implemented into the estimation method. The new estimates are denoted as scaled for change in R_{AC} in the following results. The relevant time periods affected by this change is denoted by a upper right dash, such as t = 2'.

Chapter 5

Results

The observations and results from simulations and laboratory measurements are presented. These results are discussed in chapter 6. First the results of the two different procedures used as basis for dynamic load estimation are shown. Temperature response from the calculations according to the IEC, as described in section 4.1. As well as long-term measurement of temperature response at the conductor and sheath for the practical power cable in the laboratory setup, covered in section 4.2.

Further, the results from transient temperature response during dynamic loading are displayed. These are based on the estimation method that uses a scaling according to change in load current and the superposition principle to estimate the conductor temperature of the given XLPE cable. Results from using both calculations and measurement procedures as basis for estimation are included. Additional results that consider the temperature dependent resistance of the conductor in the scaling procedure are also covered. Moreover, the temperature responses are displayed graphically using plots. Observations are described using either text or tables.

5.1 Analytical calculation of conductor and sheath temperature response

This section displays the simulated temperature response of analytical calculations according to the IEC standards. Both conductor and sheath temperature response functions above ambient temperature has been calculated and simulated. The cable data used are identical to the practical cable in the laboratory setup, to resemble both cable and surrounding parameters. The ambient temperature was set to be 22°C, with the cable placed directly on the floor and air as surrounding medium. Simulations of calculated conductor and sheath temperature responses as well as ambient temperature are displayed in figure 5.1.

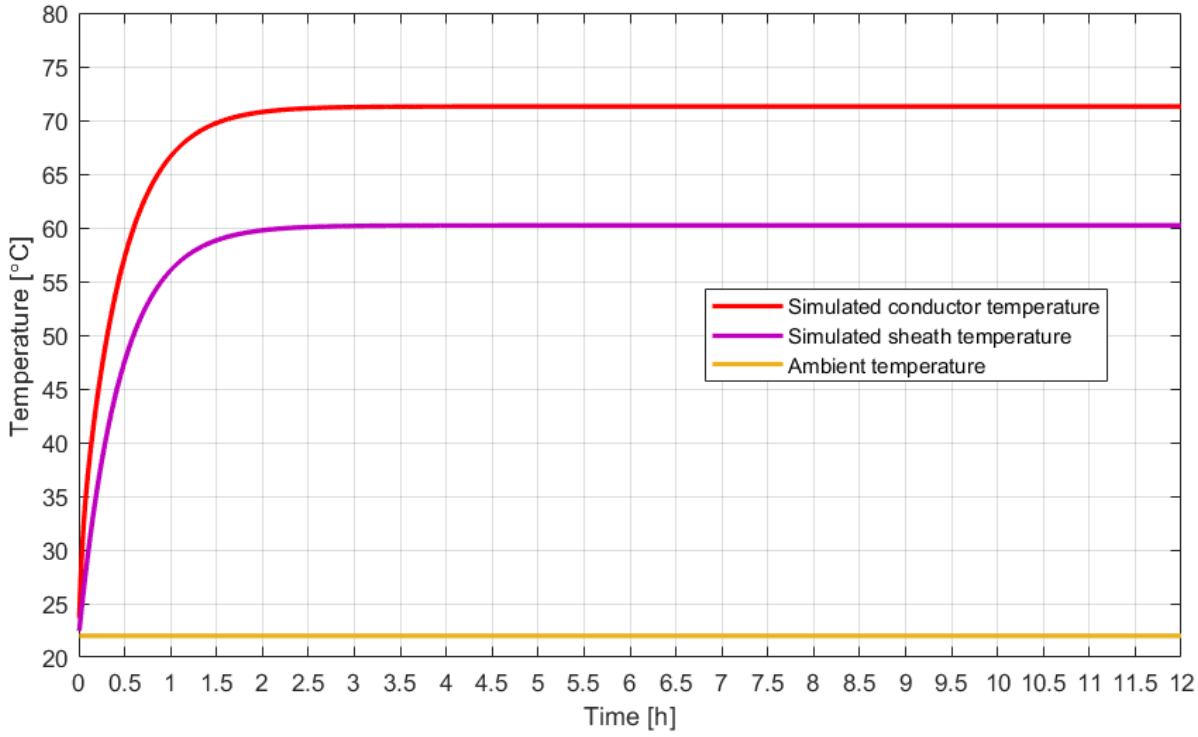

Figure 5.1: Simulated analytical calculation according to IEC standards of conductor (red line), beneath sheath (purple line) and ambient temperature responses (brown line).

The conductor temperature response displayed in figure 5.1 (red line) is the response used as basis for estimating the dynamic conductor temperature during dynamic loading. This is considered as $\theta_1(t)$ and is split into and equal amount of positive and negative parts that are scaled according to the estimation method. The scaled contributions that are applied the superposition principle are shown in appendix D. For the estimation not considering change in conductor resistance, R_{AC}, scaled contributions are shown in figure D.1. Contributions including change in R_{AC} are shown in figure D.2.

Simulation is imitating a load current of 225 A applied to the practical laboratory cable for a continuous period of 12 hours. The load current was chosen due to being the maximum current-carrying capacity of such a cable with given laying conditions. A period of 12 hours was used as this is considered sufficient time length for the cable to achieve steady-state temperature level. The cooling of the cable when the current is turned off after this time interval has not been included in the simulation. As the estimation method is based on scaling only a temperature response that achieves steady-state temperature, and this response can further be used to also estimate the cooling interval of the cable.

Table 5.1 displays observations from the simulated calculations in figure 5.1. This is further used in the discussion chapter when comparing the calculation basis with a long-term measurement. The steady-state temperature is calculated as the average temperature in the time interval t = 2.5 h to t = 12 h. Time to reach steady-state temperature is considered when the calculation first reaches the average temperature calculated in this time interval.

Table 5.1: Results obtained from simulating the analytical calculations of conductor and sheath temperature response functions.

Observation	**Conductor**	**Sheath**
Initial temperature before current was applied [°C]	23.1	22
Temperature after 30 minutes [°C]	57.1	47.6
Steady-state temperature [°C]	71.3	60.2
Time to reach steady-state [h]	3	3

Figure 5.2 shows the temperature difference between the conductor and sheath, $\Delta\theta_{sim}$, of the simulated responses. The temperature difference has an initial value of 1.1°C, and a maximum value of 11.1°C. The maximum value represents the difference in steady-state temperature between the conductor and the sheath. After nine minutes the temperature difference was 8°C.

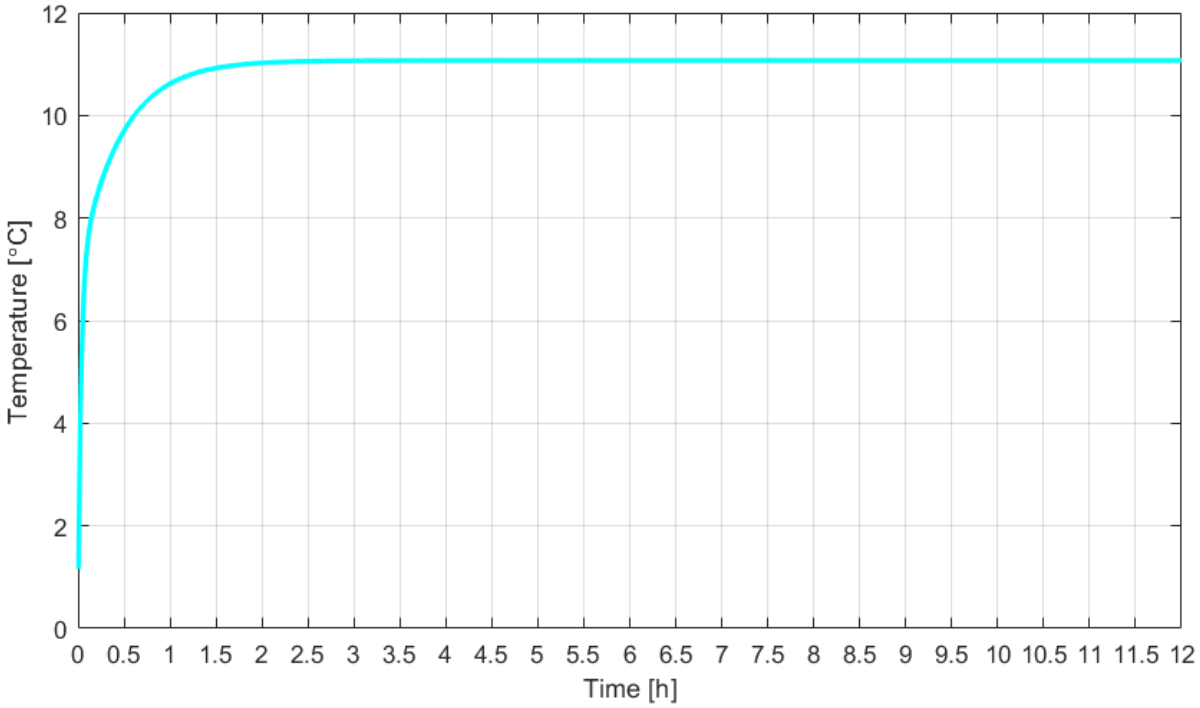

Figure 5.2: Simulated temperature difference between analytical calculations of conductor and sheath temperature responses, $\Delta\theta_{sim}$.

5.2 Long-term measurement of conductor, sheath and ambient temperature

This section holds the results from the second procedure used as basis for conductor temperature response estimation. Using the experimental laboratory setup with an XLPE power cable, long-term temperature response measurements has been established. The temperature has been measured at three different places, at the conductor, sheath and ambient temperature.

The XLPE cable was applied a current of 225 A for a period of 12 hours, equal to the analytical calculations. The applied load current was also measured for all experimental tests conducted. Figure 5.3 displays the current measurement used to establish the following temperature responses. The curve fluctuates, due to non-constant voltage in the grid as well as the temperature increase impact on the conductor resistance, which makes the current decrease until the temperature is stable.

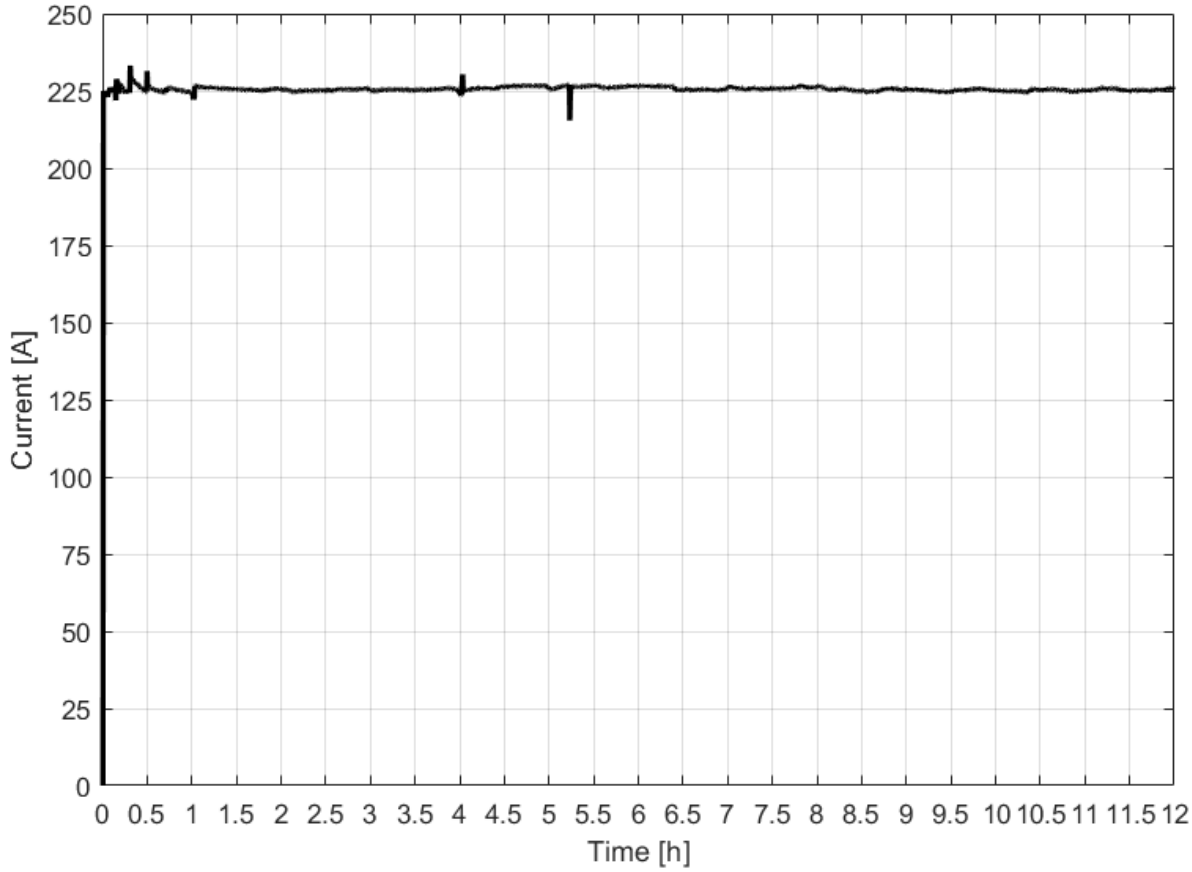

Figure 5.3: Measured applied current to the cable in the laboratory setup, a continuous current of 225 A was applied for a period of 12 hours.

Figure 5.4 displays the measured temperature at the conductor, sheath and ambient temperature of the cable surroundings. Table 5.2 contains observations from these measurements where steady-state temperature and time to reach steady-state is decided in the same way as for the analytical simulations. The average ambient temperature during this experiment was 23.67°C.

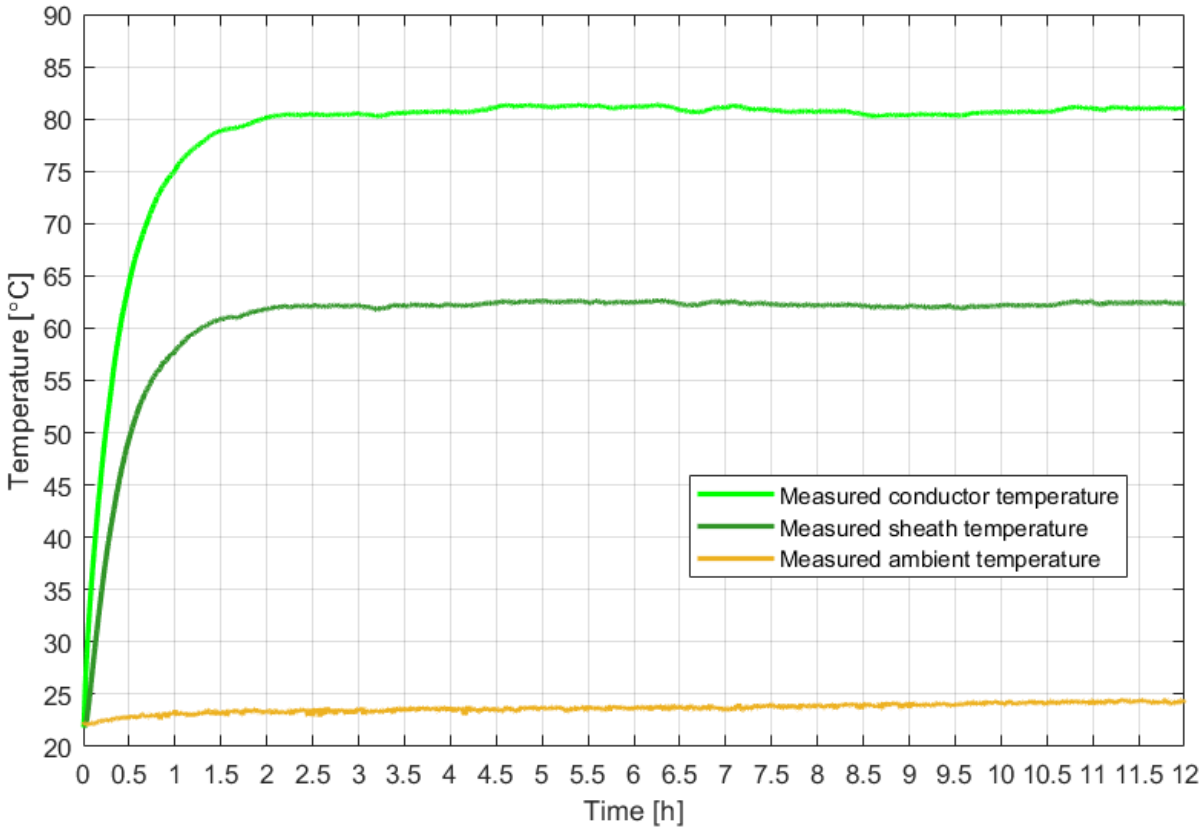

Figure 5.4: Measured conductor (light green line), sheath (dark green line) and ambient temperature (brown line) in the laboratory setup.

The measured conductor temperature of figure 5.4 is the temperature response that is applied the estimation method for the long-term temperature measurements. This response is split up into several individual contributions, that are then individually scaled to fit the change in current for a dynamic load case. Each contribution is then added together using the superposition principle to estimate the conductor temperature during dynamic loading. The scaled individual contributions are shown in appendix D. Figure D.3 and D.4 shows the scaled individual contributions without and with additional adjustments for change in R_{AC}, respectively.

Table 5.2: Results obtained from measuring the conductor and sheath temperature response functions.

Observation	**Conductor**	**Sheath**
Initial temperature before current was applied [°C]	21.9	21.9
Temperature after 30 minutes [°C]	64.3	49.3
Steady-state temperature [°C]	81.2	62.4
Time to reach steady-state [h]	3	3

Temperature difference between conductor and sheath, $\Delta\theta_{meas}$, are shown in figure 5.5. It has an initial value of 0. Between conductor and sheath, the maximum temperature difference is 18.8°C. After nine minutes the difference was measured to be 10.7°C.

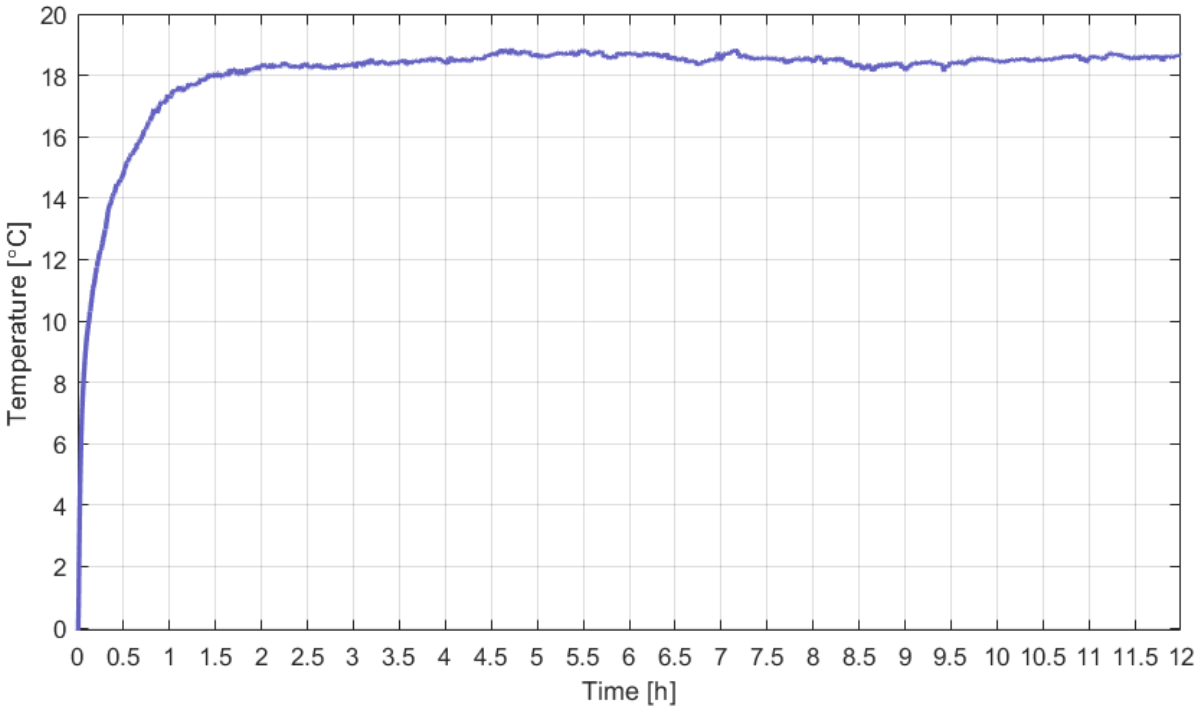

Figure 5.5: Measured temperature difference between conductor and sheath, $\Delta\theta_{meas}$.

5.3 Dynamic variable loading case - estimates

The dynamic variable loading case is presented. These sections includes both estimated and measured conductor temperature response according to the chosen dynamic current loading. The estimates have been done for both procedures of establishing temperature data at the conductor, and these are presented first. Further, the experimental measured temperature response during the same dynamic loading case is shown.

The change in load current and associated period are displayed in table 5.3. Each current value is a percentage increase or decrease of the maximum current-carrying capacity of the XLPE cable. Which also is the applied load current for both analytical and measured procedures used by the estimation method. The scaling is done accordingly to the presented method in section 3.4.2.

Table 5.3: Dynamic loading - size of load current and corresponding period for when the load current is applied.

Elapsed time from t = 0 [h]	1	2	3	4	5	5 - 8
Load current I [A]	225	337.5	112.5	281.25	225	0

5.3.1 Calculated conductor resistance, R_{AC}

During the simulations of the dynamic loading case, it was discovered a sizeable deviation between the estimated and measured conductor temperature. This discovery gave reason to include change in conductor resistance for currents larger than 300 A. As currents beyond this limit will generate high temperatures. The estimation was adjusted with a simplified scaling, covered in section 4.3.1, for the temperature dependent conductor resistance.

The calculation of the temperature dependent conductor resistance is displayed in figure 5.6. It shows the AC resistance of the conductor as a function of the measured temperature during dynamic loading. Resistance is calculated using equation (3.2) for the entire measurement period of the experiment, which was for 8 hours in total. Both increase and decrease in resistance are displayed, which is linear with change of temperature above ambient at the conductor.

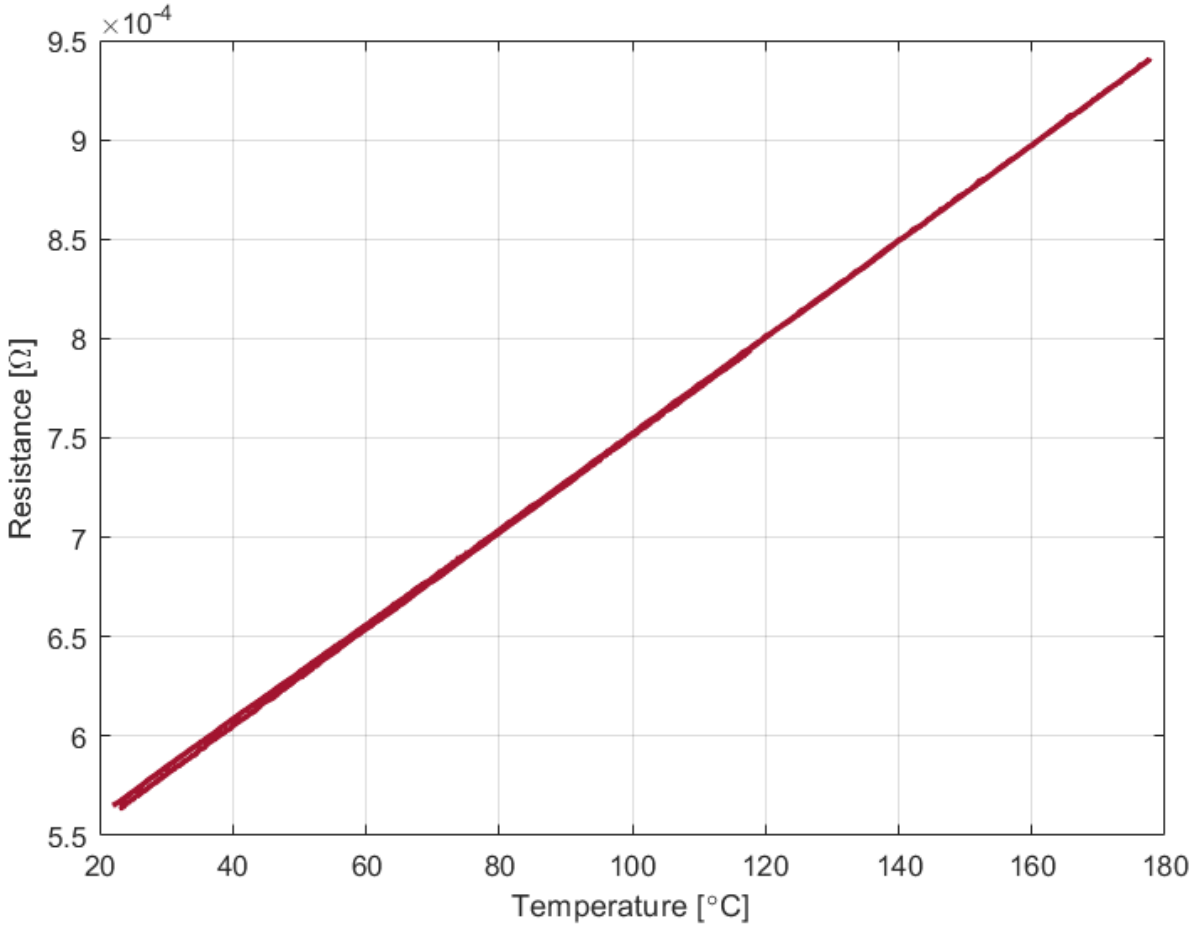

Figure 5.6: Calculated AC resistance of the conductor during dynamic variable loading.

5.3.2 Simulated estimation of conductor temperature using analytical calculations as basis

Following results are simulated estimation of the cable conductor temperature based on analytical calculations. Figure 5.7 displays the estimates with and without additional scaling for change in R_{AC}. The maximum emergency and operating temperature for XLPE cables are added in the plot. The red solid line is the estimated conductor temperature that only considers change in load current. The red dashed line further includes change in R_{AC} for the period between t = 1 h and t = 2 h.

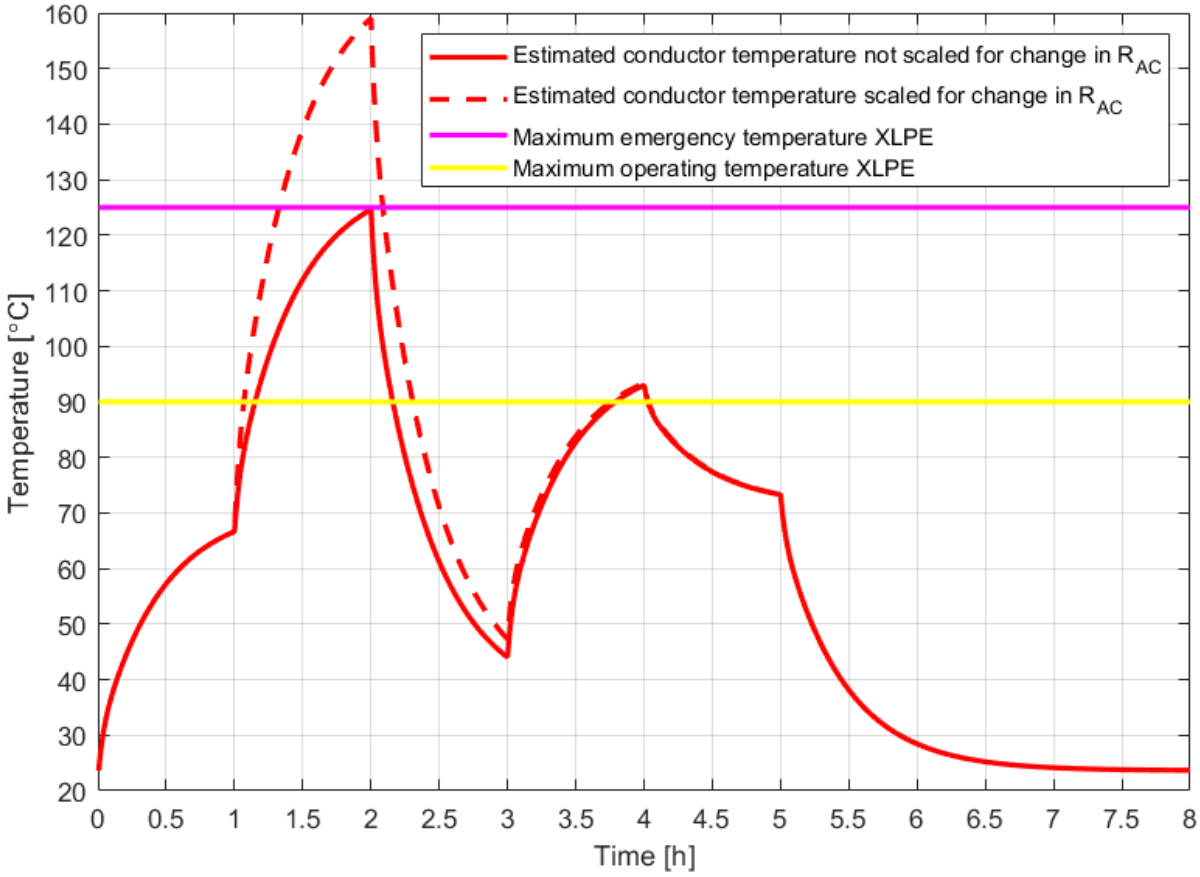

Figure 5.7: Estimated total temperature response at the conductor during dynamic loading, analytical calculations as basis.

Table 5.4 holds the estimated conductor temperature for the elapsed time when change in load current occurs and at the end of simulation. The dashed 2 and 3 (2' and 3'), are values corresponding to the red dashed line.

Table 5.4: Estimated conductor temperatures using analytical calculations as basis.

Elapsed time from t = 0 [h]	1	2	2'	3	3'	4	5	8
Conductor temperature [°C]	67	125	159	44	47	93	73	24

To analyze the rate of change in the estimated and measured temperature response, tangents for positions in the middle of each time interval was determined. In those points, the rate of change in temperature, $d\theta/dt$, for a period of one hour was calculated as the slope of the tangent. The temperature values are further used for comparison in the discussion chapter. Figure 5.8 demonstrate a tangent line for the temperature estimation at the point t = 1.5 h. Table 5.5 holds the different tangent slopes for both estimates based on analytical calculations shown in figure 5.7.

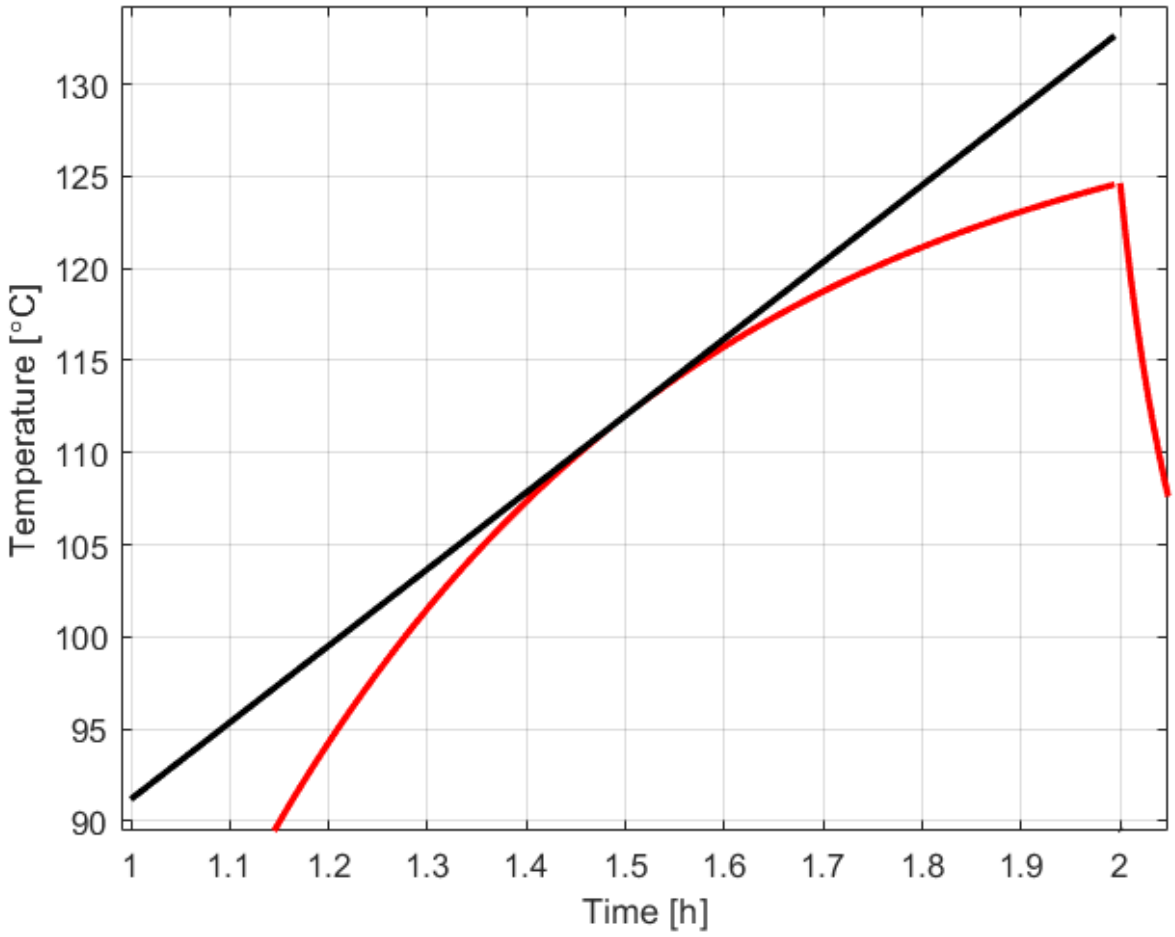

Figure 5.8: Tangent at the point t = 1.5 h, the slope of the tangent represents the rate of temperature change in that point.

Table 5.5: Calculated values of $d\theta/dt$ for the estimated conductor temperature using analytical calculations as basis.

Elapsed time from t = 0 [h]	0.5	1.5	1.5'	2.5	2.5'	3.5	4.5	5.5
$\frac{d\theta}{dt}$	31	41	66	- 56	- 78	31	- 14	- 32

5.3.3 Simulated estimation of conductor temperature using temperature measurement as basis

In the same way as in the previous section, results of the procedure that uses long-term established temperature measurements as basis are shown. These results are based on applying the estimation method on the results covered in section 5.2. Figure 5.9 displays the estimated conductor temperature response. Conductor temperature at elapsed time from t = 0 to t = 8 h are shown in table 5.6 and rate of temperature change at different points during the time intervals are found in table 5.7.

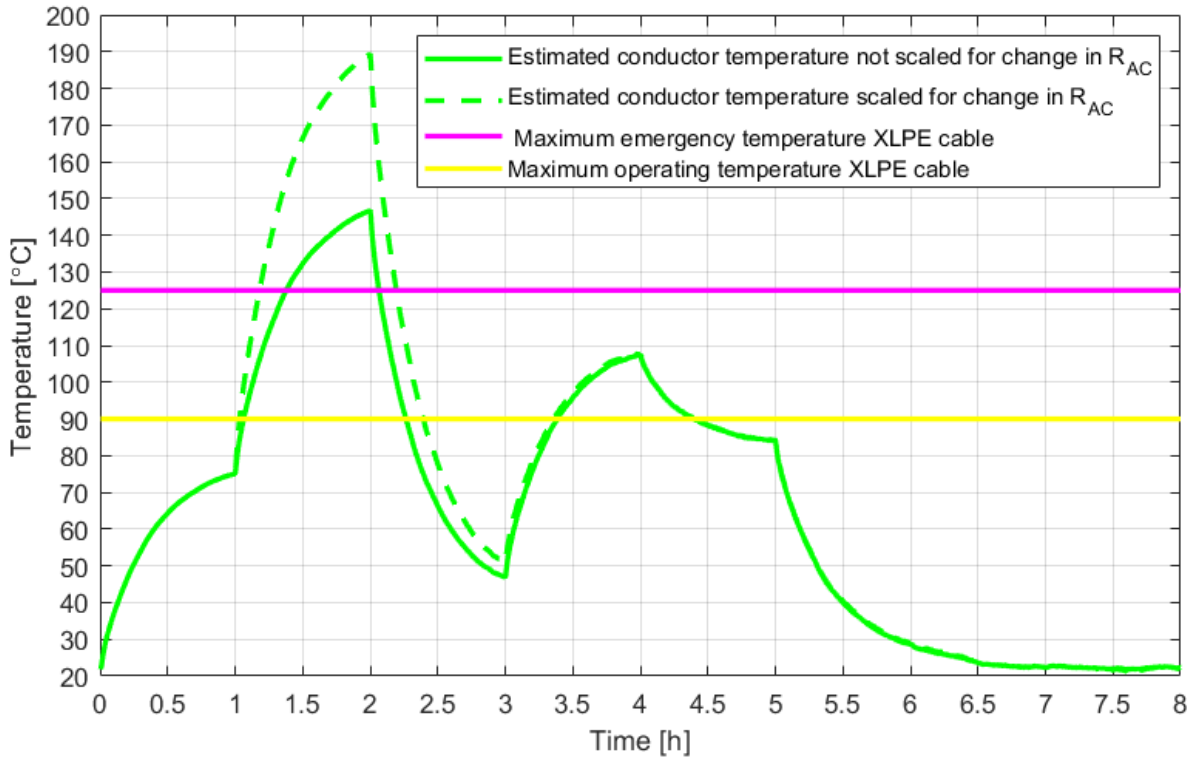

Figure 5.9: Estimated total temperature response at the conductor during dynamic loading with long-term temperature measurement as basis.

Table 5.6: Estimated conductor temperatures using long-term temperature measurement as basis.

Elapsed time from t = 0 [h]	1	2	2'	3	3'	4	5	8
Conductor temperature [°C]	75	147	189	47	51	107	84	22

Table 5.7: Calculated values of $d\theta/dt$ for the estimated conductor temperature using long-term temperature measurement as basis.

Elapsed time from t = 0 [h]	0.5	1.5	1.5'	2.5	2.5'	3.5	4.5	5.5
$\frac{d\theta}{dt}$	44	54	87	- 76	- 106	53	- 16	- 42

5.4 Dynamic variable loading case - experimental measured conductor temperature

In figure 5.10 the applied load current, measured conductor and ambient temperatures are shown. Load current was adjusted to be precisely as the simulated case. The experiment measured temperature and current in the laboratory setup for a total period of eight hours. The measured conductor temperatures at different time intervals are shown in table 5.8. After the test had been conducted, the rate of change in temperature for each hour was calculated, using same procedures as for the estimates, results are in table 5.9.

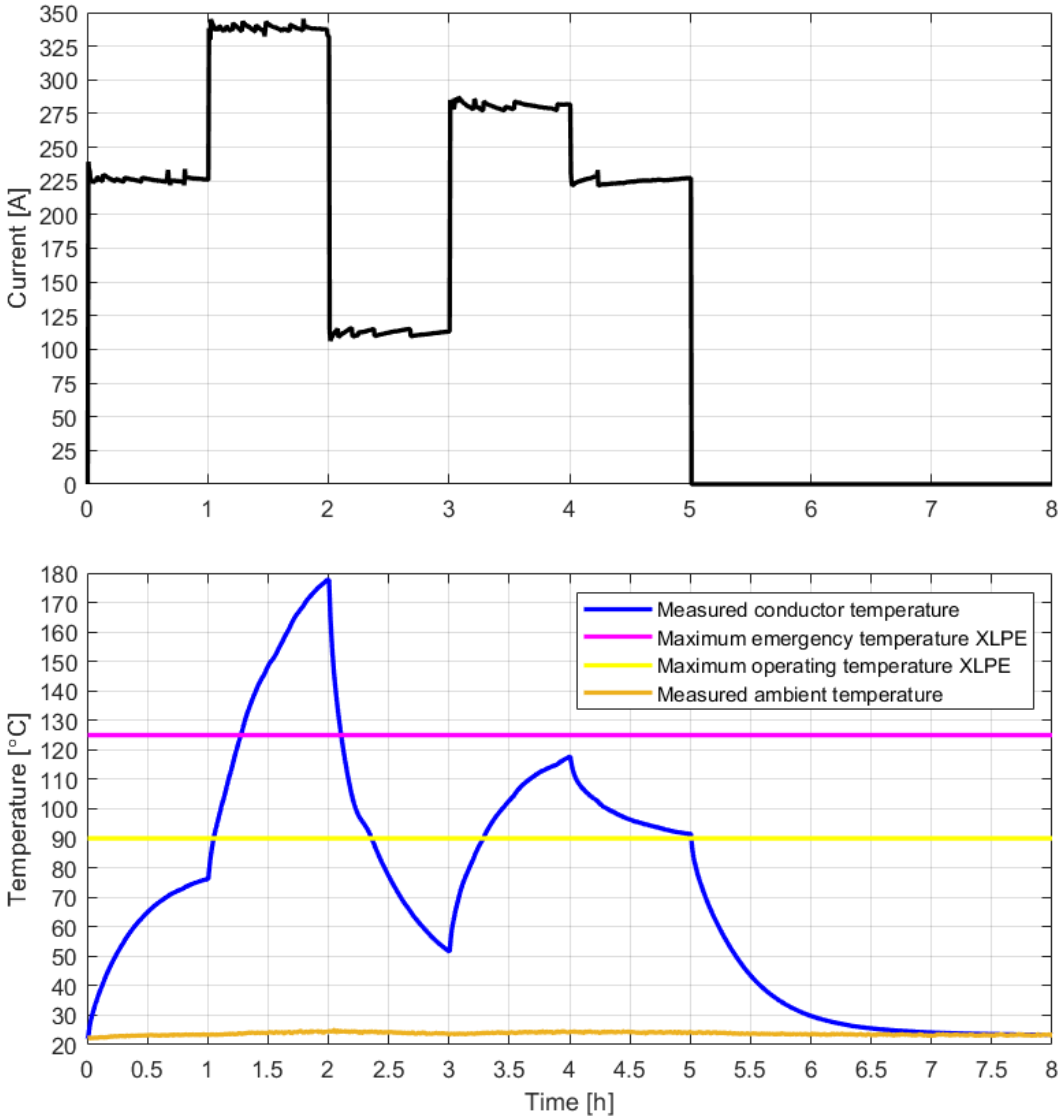

Figure 5.10: Measured current, upper figure (black line), conductor temperature lower figure (blue line) and ambient temperature lower figure (brown line) for dynamic loading case conducted in the laboratory setup.

Table 5.8: Measured conductor temperatures during dynamic loading using laboratory setup for testing.

Elapsed time from t = 0 [h]	1	2	3	4	5	8
Conductor temperature [°C]	76	178	52	118	91	23

Table 5.9: Calculated values of $d\theta/dt$ for the experimentally measurement of the dynamic loading case.

Elapsed time from t = 0 [h]	0.5	1.5	2.5	3.5	4.5	5.5
$\frac{d\theta}{dt}$	44	85	- 79	46	- 13	-48

5.4.1 Comparison of measured temperature and estimates based on analytical calculations

Here the estimates based on analytical calculations are compared to laboratory measured conductor temperature. The comparison are done graphically as shown in figure 5.11. For both estimates, average deviation between estimation and measurement has been calculated. The deviation was calculated as the average difference between two vectors containing the respective temperature data. The average deviation for both estimates compared to laboratory measurement are as follows:

- Average deviation of estimation using analytical calculations as basis, not scaled for change in R_{AC}: 13°C
- Average deviation of estimation using analytical calculations as basis, scaled for change in R_{AC}: 8.3°C

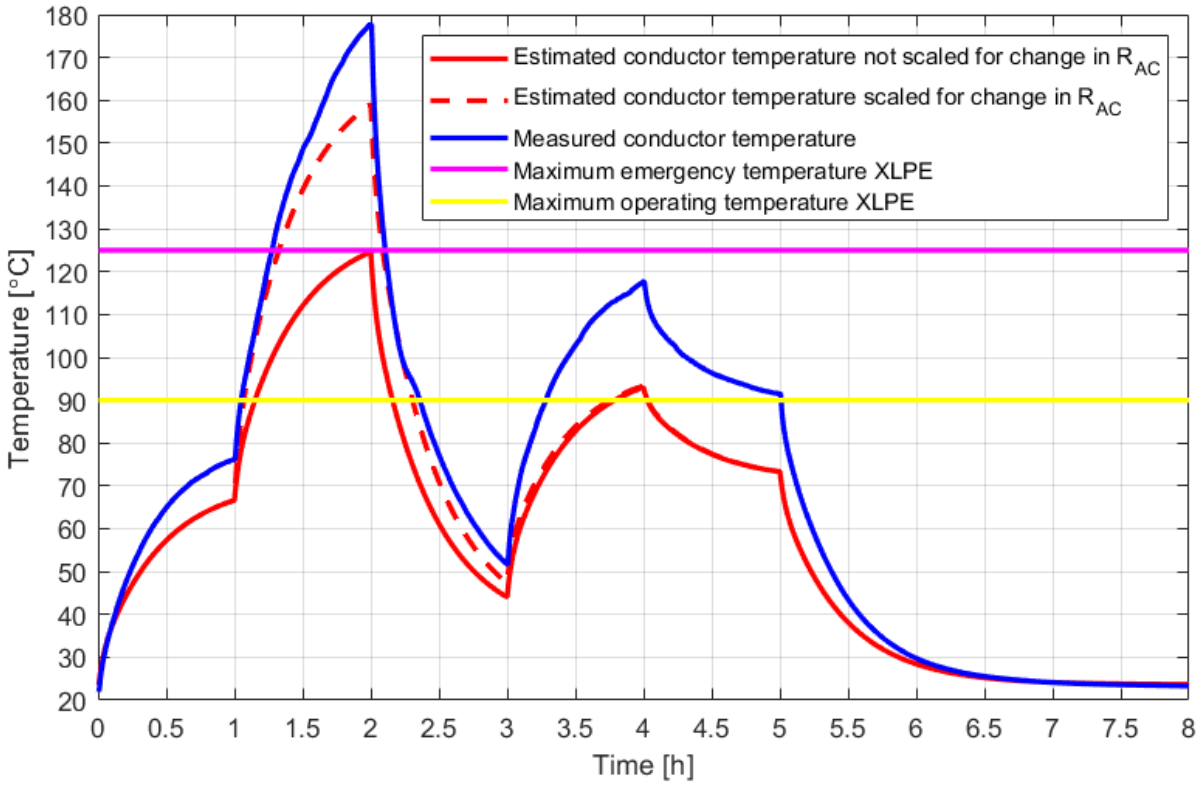

Figure 5.11: Measured conductor temperature during dynamic loading (blue line) compared to estimates based on analytical calculations as basis (solid and dashed red lines).

5.4.2 Comparison of measured temperature and estimates based on long-term measurement

Lastly, the estimates based on long-term temperature measurements are compared to experimentally measured conductor temperature. The comparison are shown in figure 5.12. The average deviation has been calculated in the same way as described in previous section. Average deviation for both estimates compared to the laboratory measurements are as follows:

- Average deviation of estimation using measured conductor temperature as basis, not scaled for change in R_{AC}: 6.1°C
- Average deviation of estimation using measured conductor temperature as basis, scaled for change in R_{AC}: 5.2°C

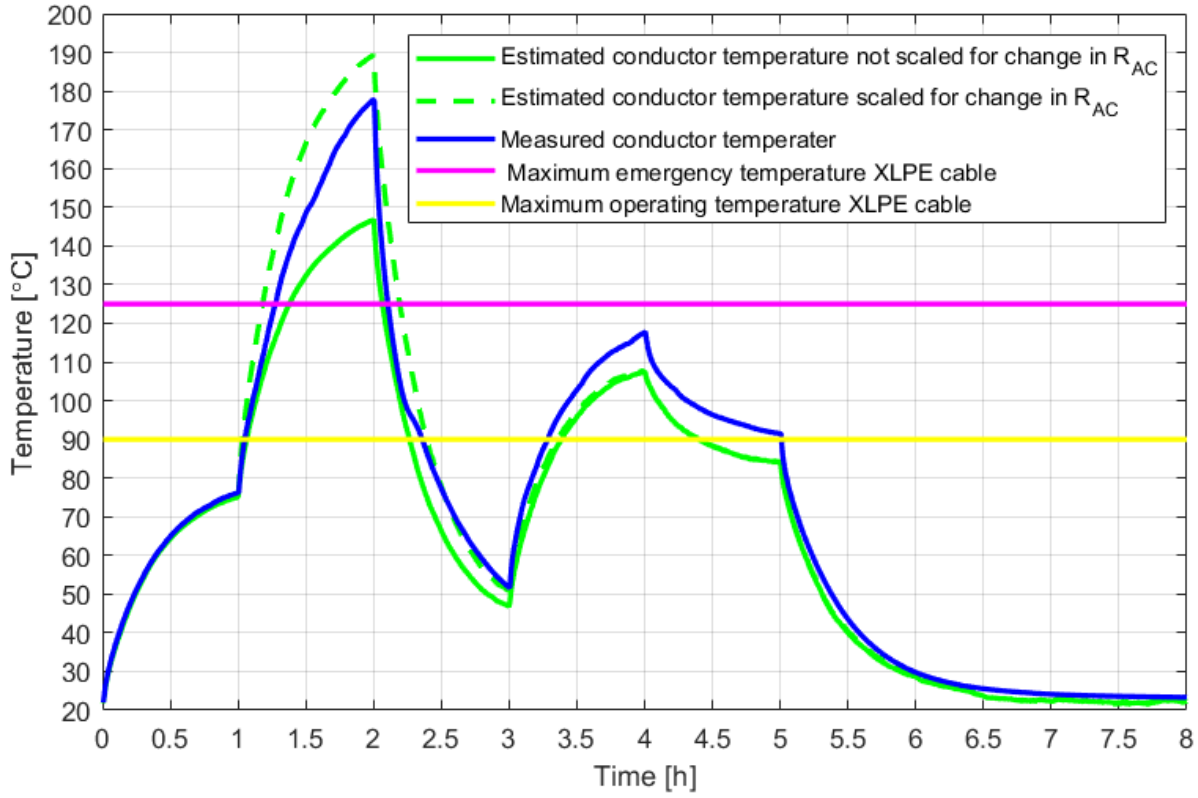

Figure 5.12: Measured conductor temperature during dynamic loading case (blue line) compared to estimates using long-term temperature measurements as basis (solid and dashed light green lines).

Chapter 6

Discussion

The objective of this thesis was to develop an estimation method that could be used to facilitate the dynamic current rating of power cables. This has been done with a method that uses established conductor temperature response for given load current and laying conditions. This response is then split into equal number of positive and negative sequences which are applied a scaling principle correlated to change in load current. These sequences, or contributions as they are referred to in this thesis, are then added up together using the superposition principle to estimate the total conductor temperature response during dynamic loading.

This chapter gives a more thorough discussion of the results presented in the previous chapter. Both procedures used as basis for establishing a known conductor temperature response are discussed using comparison of the calculated and measured temperature. Further, this chapter analyze the precision of the estimation method and the impact of implementing the temperature dependency of the conductor resistance, R_{AC}, into the method. Lastly, it examines the applicability and limits of the suggested method.

6.1 Comparison of analytical calculations and long-term measurement procedures as basis for estimation

This thesis researched two different procedures used as basis for estimating power cable conductor temperature during dynamic loading. One procedure used analytical calculations of conductor temperature based on international standards for a practical XLPE power cable. The other procedure used a long-term temperature measurement of the conductor temperature of the same cable in a constructed laboratory setup. The analytical calculations were modelled using parameter values identical to the practical power cable examined in the setup.

Conductor and sheath temperature for both procedures were obtained, having a rated current of 225 A applied to the power cable for a period of 12 hours. The analytical calculations were not simulated for a period of 12 hours, but it modelled the temperature response in the layers as if such a current was applied for the same period. The conductor temperature response was then further utilized in the estimation method and the estimates are later discussed. First, the difference between these two procedures as basis for the estimation are analyzed.

Figure 6.1 shows a graphical comparison of both calculated and measured temperature responses. The conductor and sheath temperature in both cases achieves steady-state at the same time, which is 3 hours after the single-step current of 225 A was applied. As the steady-state time was determined using the average temperature in the time interval between t = 2.5 to t = 12 hours, and further finding when the responses reach this temperature. It can be considered a simplified time estimate of when steady-state is achieved, the main point is that the time both procedures achieve steady-state coincides.

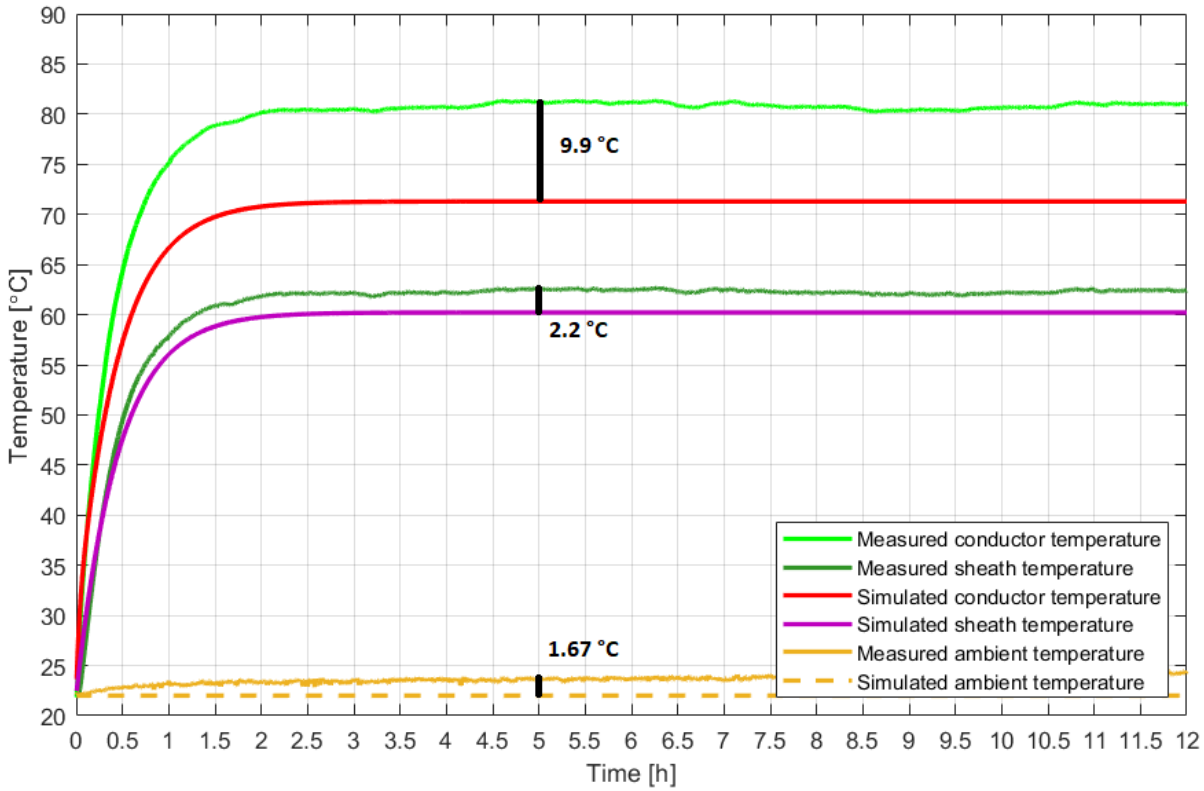

Figure 6.1: Comparison of the two procedures, conductor, sheath and ambient temperature for both calculated and measured temperature response.

For the conductor, the average steady-state temperature has a difference of 9.9°C between calculated and measured temperature. The difference is smaller for the sheath responses, which is 2.2°C. The responses follow each other closely until the calculated responses start deviating and approaching steady-state. This is more prominent in the conductor responses, which also have the largest deviation compared to sheath temperature.

The comparison shows that the analytical calculations give a realistic impression of the temperature response in both the conductor and sheath layer of the practical XLPE cable. The calculations based on IEC standards often contains simplifications, as covered in chapter 3, which will give some dissimilarities between calculated and measured temperature response. However, the deviations shown in figure 6.1 are considered as acceptable for both the conductor and sheath.

Further, the steady-state temperature is higher for the measured response compared to the response that is calculated. This will lead to larger differences in the estimated conductor temperature as the applied scaling principle will increase the deviation. Thus, making the estimates based on measured temperature to reach higher levels than the estimates based on calculated temperature.

An important observation is that none of the established procedures exceed the maximum operating temperature of XLPE cables, which is 90°C. As both of these are based on having maximum allowed load current of 225 A applied for a longer period of time, it would have been expected that the conductor temperature reached 90°C. The maximum current capacity is based on identical laying conditions that have been used in the laboratory setup and the calculations. This suggest that the rated current capacity of the practical power cable is too strict, and further results in grid operators not fully being able to exploit the potential.

Lastly, ambient temperature will have a great impact on conductor temperature. The ambient temperatures have a small average deviation of 1.67°C. It was set as constant 22°C in the analytical model and measured to an average of 23.67°C during the long-term measurements. This deviation would potentially have a small impact on the estimation, but as it is not of a remarkable size, it has not been considered in the estimates.

6.2 Simulated estimates using both procedures as basis

Both procedures were used to estimate the conductor temperature during a dynamic loading case, by applying the estimation method. The conductor temperature was estimated according to a case that had a change in load current occurring every hour, from t = 0 to t = 5 h. At t = 5 h the current was turned off and the cooling period was simulated until elapsed time at t = 8 h.

Figure 6.2 displays the comparisons of the estimates using the two different procedures as basis and not including change in conductor resistance for the period t = 2 h to t = 3 h. During the first hour, the maximum cable ampacity of I = 225 A was applied. This is the same current that was applied when establishing the procedures used as basis. The difference between the two estimates at t = 1 h is 8 °C, with estimate based on measurement having the highest temperature. At t = 1 h the current is increased by 50 % above maximum ampacity, which gives a load current I = 337.5 A. This was then applied for the consecutive hour.

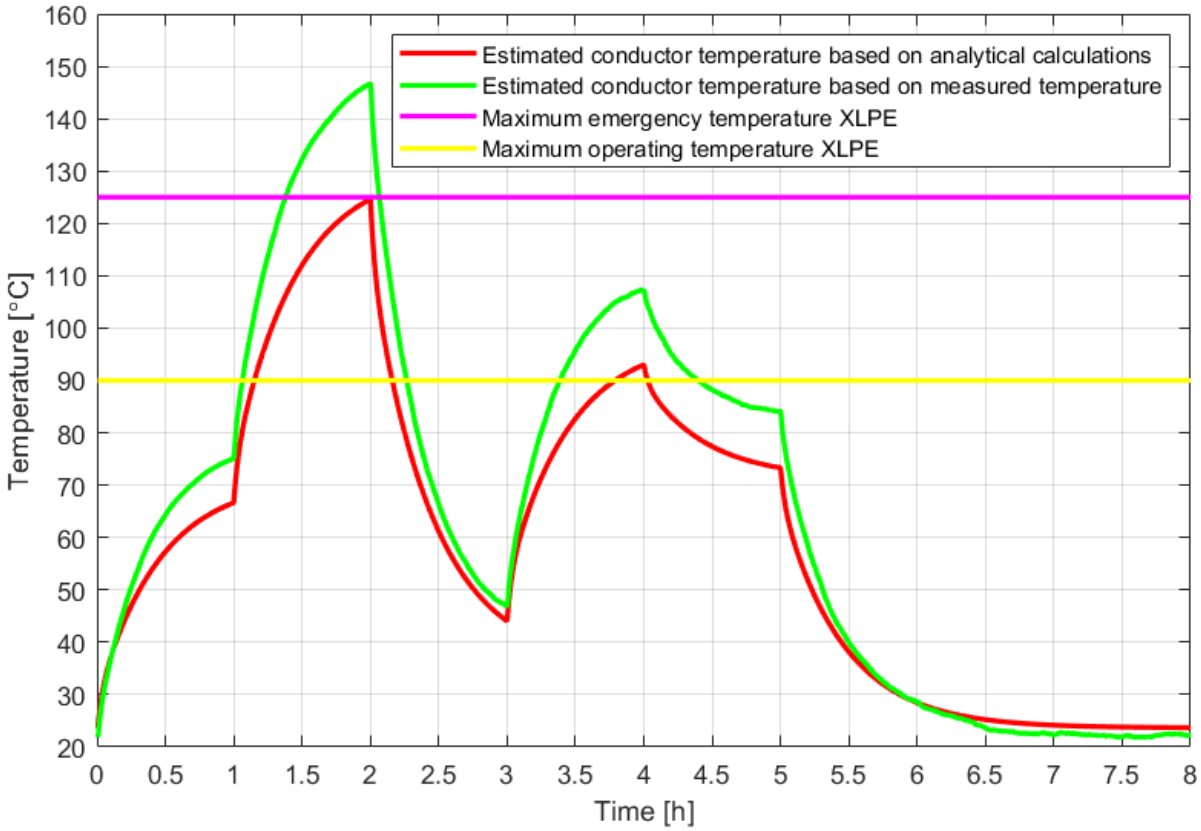

Figure 6.2: Comparison of estimated conductor temperature during dynamic loading. Both procedures as basis are displayed, not including change in conductor resistance.

During this period, t = 1 h to t = 2 h, estimate based on measured temperature, solid light green line, exceeds maximum operating temperature for XLPE cables at time t = 1.05 h. With this applied load current, it only takes three minutes until the cable is operated above safe measures, considering recent load history from the previous hour. At t = 1.4 h it exceeds the maximum emergency temperature, which means it only takes 21 additional minutes for the temperature to exceed maximum emergency temperature. The cable is not allowed to be operated more than one hour at this temperature and should not exceed emergency ratings at any point. At the end of this time interval, the conductor temperature is estimated to be 147°C, which is 22°C above the emergency limit.

Estimate based on analytical calculations, solid red line, exceeds maximum operating temperature at t = 1.16 h, seven minutes after the estimate based on measured response. It does also reach the maximum emergency temperature, however, this is at t = 2 h, thus it never exceeds this temperature level. There is a time gap of approximately 50 minutes between when the estimation exceeds maximum operating temperature until it reaches emergency temperature. As it estimates the cable to never exceed 125°C, the cable is considered to be operated within safe terms during this period.

At t = 2 h, the load current is reduced to 50 % of maximum ampacity for the XLPE cable, $I = 112.5$ A. Now both estimates have a rapid decrease in temperature due to one-third reduction in load current. The temperature response based on calculations have a slightly more rapid fall, reaching allowed operating temperature at t = 2.15 h. Response based on measurement reaches this temperature at t = 2.25, six minutes after, and drops to a temperature at t = 3 h of 47°C. Calculation based estimate is 44°C at t = 3h, 3°C less.

Furthermore, at t = 3h the current is again increased to simulate overloading. Load current is now equal to 281.25 A, a 25 % increase from maximum ampacity. Estimates based on measurement and calculations now exceed maximum operating temperature at time t = 3.39 h and t = 3.8 h respectively. This means that the estimate based on measured response indicates that the cable is operated above maximum operating temperature approximately 24.6 minutes longer than estimate based on calculations. At t = 4 h the temperature levels are at 107°C and 93°C, respectively for the measured and calculated response basis.

The last change in step-current is a reduction to maximum ampacity, $I = 225$ A. Respected estimates based on measurement and calculation reaches operational limit at t = 4.41 h and t = 4.03 h. At t = 5 h the estimates are at a temperature of 84°C and 73°C. At the end of the simulation, t = 8 h, the estimate based on calculated basis reaches 22°C, which is the ambient temperature set during the simulation. The estimate based on measured basis reaches 24°C which is close to the ambient temperature for the laboratory setup during the measurement.

Figure 6.3 displays the estimates when considering temperature dependency of the conductor resistance, R_{AC}. A noticeable observed difference for these estimates is that the estimates reach a higher temperature level for the period between t = 1 h and t = 2 h. As this is the only period with additional scaling for change in R_{AC}. The dashed green line represents the estimate based on measured temperature, the dashed red line is the estimate based on calculations. At t = 2 h, the temperature levels are 189°C and 159°C respectively for estimates based on measurement and calculations.

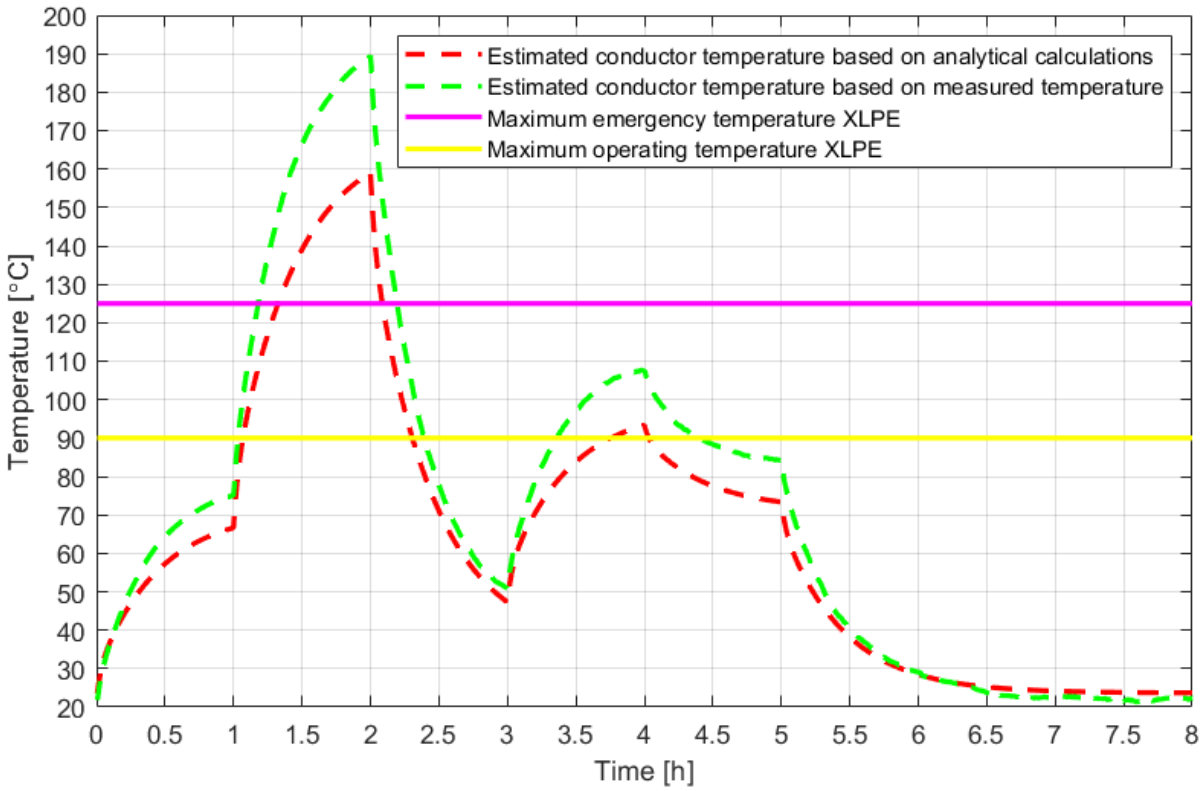

Figure 6.3: Comparison of estimated conductor temperature during dynamic loading. Both procedures as basis are displayed, including change in conductor resistance.

During the period with additional scaling, both estimates exceed maximum emergency and operating temperature faster compared to estimates not considering change in conductor resistance. Estimate based on measurement exceeds operational limit for XLPE at t = 1.02 h and emergency limit t = 1.18 h. Calculated procedure as basis exceeds operational limit at t = 1.08 h and emergency limit at t = 1.34 h. Then when load current is reduced to 112.5 A, at t = 2 h, estimate based on measurement reaches emergency limit at t = 2.19 h and operational limit t = 2.39 h. Calculated procedure reaches emergency limit at t = 2.08 h and operational limit t = 2.3 h.

Comparing the estimates based on measured temperature, by including change in R_{AC} it exceeds maximum operational temperature approximately two minutes faster, and maximum emergency temperature approximately four minutes faster. After a decrease in load current at t = 2 h, it uses eight minutes longer to reach emergency temperature and seven minutes longer to reach operational temperature compared to estimate not considering change in R_{AC}.

For the calculated procedure the time gaps are larger. As the estimate including change in R_{AC} now exceeds maximum operational temperature five minutes more rapidly and exceeds emergency limit, compared to not including change in R_{AC}. This during the period t = 1 h to t = 2 h. The estimate exceeds emergency temperature 40 minutes faster, and reaches a temperature level 34°C higher. Then at t = 3 h, when the load current decreases, it reaches operational temperature nine minutes later.

Lastly, for each estimate the rate of change in temperature was calculated using tangents at points in the middle of each time interval, and then finding the slope of each tangent. Comparing calculations for both estimates, the absolute value of the rate of change, $d\theta/dt$, is generally larger for the estimates based on measurement. It is also important to note the sign for each change of rate values are the same for both procedures.

6.3 Precision of the estimation method

The dynamic loading case that has been estimated using both procedures as basis, has also been experimentally measured with the laboratory setup. To be able to compare and verify the estimates with experimental measurement of the dynamic case. The measurement is shown in figure 5.10, see section 5.4. First the experimental measurement is analyzed, then compared to the previous discussed estimates.

During the first step of load current, $I = 225$ A, between t = 0 and t = 1 h, the measured conductor temperature reaches 76°C. After an increase in load current at t = 1 h, $I = 337.5$ A, the temperature reaches 178°C at t = 2 h. The following hour, during the period with $I = 112.5$ A, the temperature at the conductor drops to 52°C until t = 3 h. Then for another increase in load current for one hour, $I = 281.25$ A, temperature is measured to be 118°C at t = 4 h.

Last change in load current at t = 4 h, reduces current to initial maximum ampacity, $I = 225$ A. The conductor temperature is reduced to 91°C, measured at t = 5 h. After a cooling period of three hours from the current is turned off, the measured temperature is 23°C at t = 8 h. Time between when current is switched off until conductor reaches ambient temperature is 2.54 h.

During the experimental measurement of the loading case, the conductor temperature first exceeded maximum operational and emergency temperature during the time interval when $I = 337.5$ A is applied. The maximum operational temperature for XLPE is exceeded at t = 1.05 h and emergency temperature at t = 1.27 h. During the consecutive period, when load current is decreased, conductor temperature reaches emergency ratings again at t = 2.11 h and operational rating at t = 2.38 h.

Due to the changes in load current being an increase then a decrease, relative to the cable ampacity, the conductor temperature again exceeds and drops to the maximum operating temperature during another time interval. For the interval between t = 3 h and t = 5 h, the conductor exceeds operational limit at t = 3.27 h and reaches the same limit after the load current is switched off, at t = 5.01 h.

Figure 6.4 displays the comparison of estimates for both procedures, not including change in conductor resistance. Average deviation in temperature between estimates and measured loading case was calculated. The largest deviation was 13°C, this is between the estimate using analytical calculations as basis, not considering an additional scaling for change in conductor resistance, and measured conductor temperature during dynamic loading.

The solid red line in the figure which represents this estimate, have an extensive difference in temperature for the periods when the cable is overloaded. The difference in temperature between estimate and measurement at t = 2 h is 53°C. Also, the estimate gives an impression of the conductor not exceeding maximum emergency temperature during the first interval of overloading. Experimental measurement show that the conductor exceeds emergency limit at t = 1.27 h and is operated beyond this limit for 44 minutes.

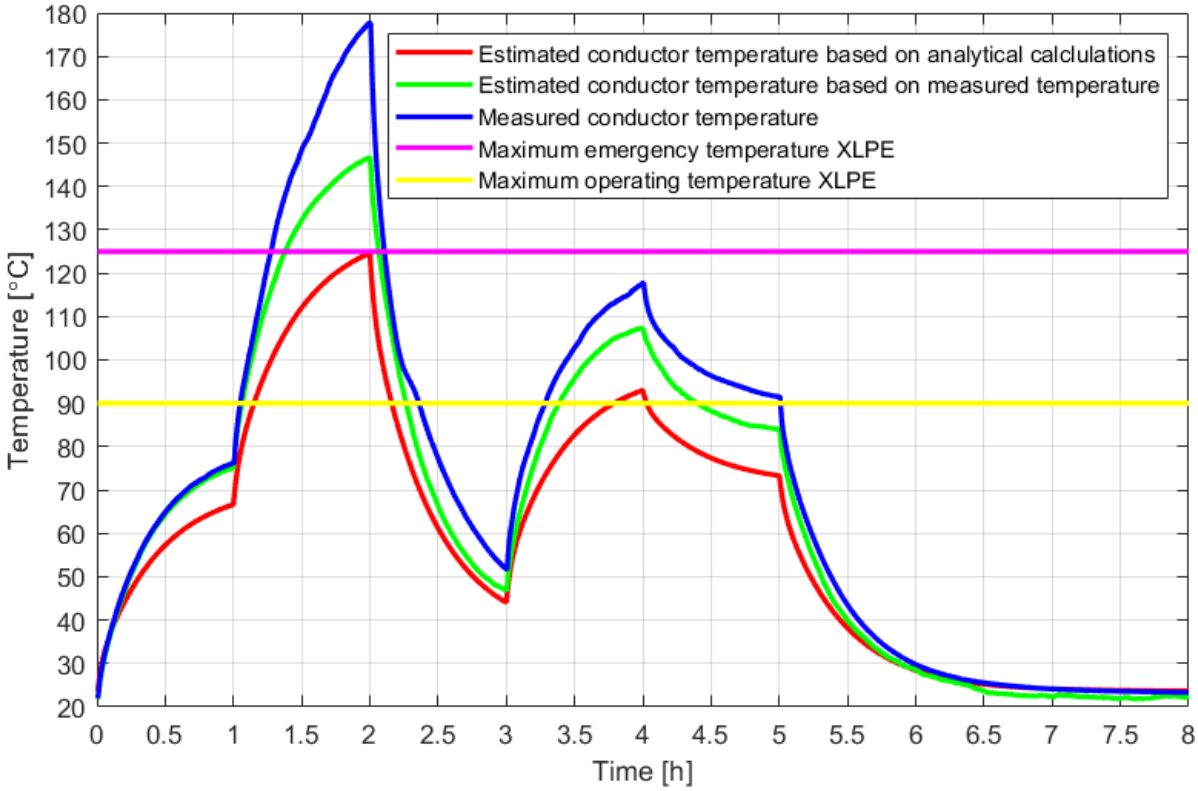

Figure 6.4: Comparison of measured and estimated conductor temperature during dynamic loading. Both procedures as basis are displayed, not including change in conductor resistance.

Estimate based on temperature measurement, solid light green line in figure 6.4, has an average temperature deviation of 6.1°C compared to the measured temperature during dynamic loading. The long-term measurement used as basis for this estimate have been conducted on the same laboratory setup as when measuring the temperature during dynamic loading. This means the same thermocouple that measures temperature at the conductor is used in both cases.

This estimate also has a large temperature difference during the first overloading interval, at t = 2 h the temperature difference between estimate and measurement is 31°C. Even though the estimate gives a realistic impression of when the conductor temperature exceeds both operating and emergency temperature ratings, temperature levels that the conductor reaches is not estimated sufficiently, at least during overloading.

Furthermore, the estimates not including change in conductor resistance gives a proper impression of the sign in front the rate of change in temperature during each time interval. Table 6.1 shows a comparison of calculated $d\theta/dt$ for the measured dynamic load case and the estimates. Once more, the largest deviation is found during the first time interval with overloading, at elapsed time t = 1.5 h. These differences are 44°C per hour for estimate based on calculations and 31°C per hour for estimate based on measurements. Generally, the estimate based on measurement gives a more realistic impression of $d\theta/dt$, compared to the other procedure.

Table 6.1: Comparison of calculated $d\theta/dt$ for the dynamic loading case measurement and estimates. Both procedures used as basis, not including change in R_{AC}.

Elapsed time from t = 0 [h]	0.5	1.5	2.5	3.5	4.5	5.5
$\frac{d\theta}{dt}$**, measured dynamic loading case**	44	85	- 79	46	- 13	- 48
$\frac{d\theta}{dt}$**, estimate based on analytical calculations**	31	41	- 56	31	- 14	- 32
$\frac{d\theta}{dt}$**, estimate based on measured temperature**	44	54	- 76	53	- 16	- 42

6.3.1 Impact of change in conductor resistance, R_{AC}

The scaling principle applied to the individual contributions was initially constructed to only consider change in load current. Excluding the change in the conductor resistance, R_{AC}, which is temperature dependent. Equation for ohmic losses, (3.1), includes change in R_{AC}. During the process of comparing estimates to measured temperature for the dynamic load case, the large deviation during overloading was considered due to not including R_{AC}. Thus, making the applied initial scaling principle insufficient. Therefore, for the period between t = 1 h and t = 2 h, an additional simplified scaling was added to the individual contribution. This additional scaling is described in section 4.3.1.

Figure 6.5 shows the new estimates including change in R_{AC}, compared to measured conductor temperature during dynamic loading. The red dashed line represents estimate based on calculations and the light green dashed line represents estimate based on measured temperature. For the estimate with calculations as basis, the average deviation decreased from 13°C to 8.3°C, a total decrease of 4.7°C.

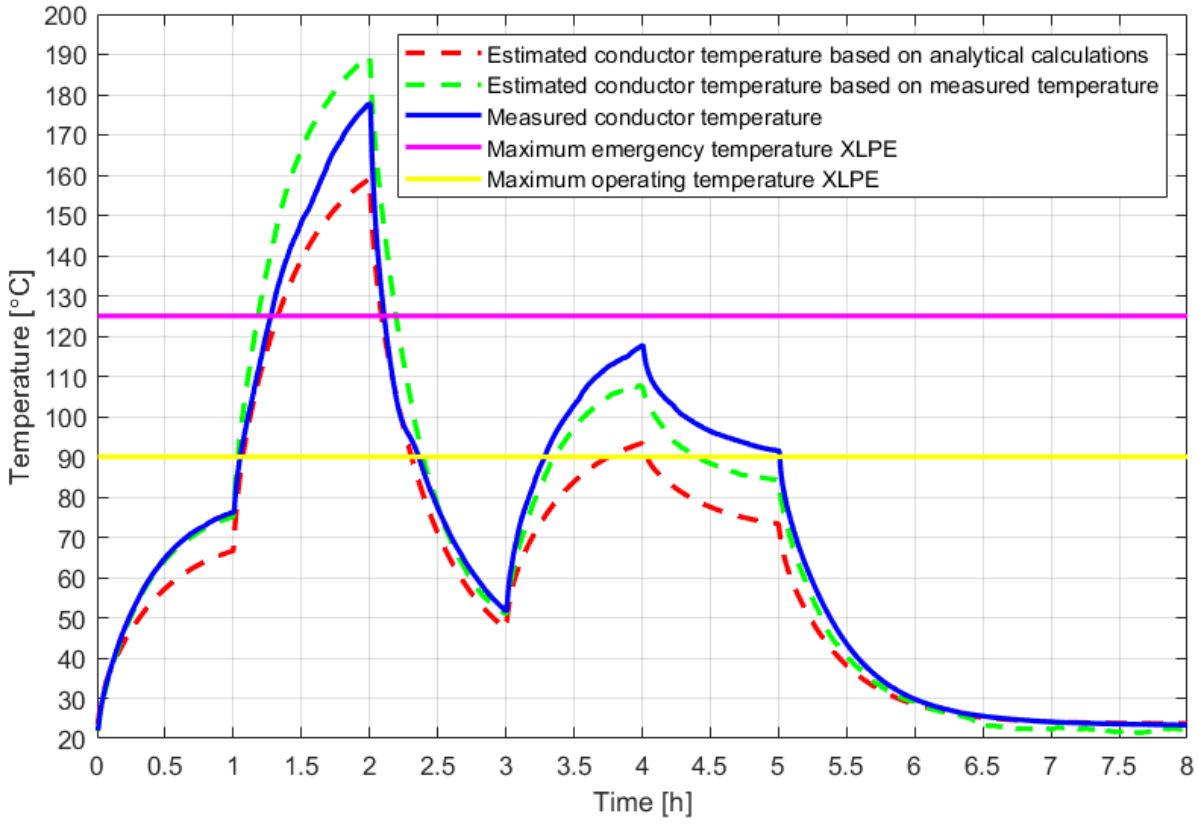

Figure 6.5: Comparison of measured and estimated conductor temperature during dynamic loading. Both procedures as basis are displayed, including change in conductor resistance.

During this time interval, the estimate based on calculations now gives a more thorough representation of when the conductor temperature exceeds the maximum operating and emergency ratings during an increase in load current. As well as reaching these ratings again when the current is decreased. The deviation between temperatures at t = 2 h is reduced to 19°C. An improvement of 34°C by using an additional simplified scaling for change in R_{AC}.

Estimate based on measurement did already give a proper estimate regarding the operating and emergency temperature limits for XLPE cables. The improvement in average deviation compared to measured conductor temperature during dynamic loading is 0.9°C, which makes the average deviation now 5.2°C. The largest impact on this estimate during the time interval additional scaling has been added, is that the temperature at t = 2 h is now increased from 147°C to 189°C. This is 11°C higher than the measured temperature at the same time, and 42°C higher than the initial estimate.

The estimate during this time interval is then giving a larger estimate of conductor temperature compared to measurement. This could be considered as a safety margin for the presented method and be used to further ensure that the conductor temperature during overloading is estimated to be operated within safe measures at all times. As the estimate will always be higher than the measured conductor temperature. However, this estimate could also lead to poor utilization of the power cable if temperature is estimated too high and operated below temperature ratings.

Further, the additional scaling also affected the rate of change in temperature. Both for time interval between one and two hours and the consecutive time interval between two and three hours. Table 6.2 shows a comparison of the rate of change in temperature and how the calculated result changes for the time interval when additional scaling is added. The points that include the change in R_{AC} are denoted with a upper right dash, such as 1.5' and 2.5'.

The rate of increase in temperature at point t = 1.5' h is now improved compared to estimates not including change in R_{AC}. The estimate based on measurements still provide an optimal estimate compared to the estimate using calculated basis, at least during overloading. During the decrease in temperature at point t = 2.5' h, the estimate based on calculations is more realistic compared to measurement procedure. The estimate based on measurements has a too steep rate of change in temperature during this time interval.

Table 6.2: Comparison of calculated $d\theta/dt$ for the dynamic loading case measurement and estimates. Both procedures used as basis, including change in R_{AC}.

Elapsed time from t = 0 [h]	1.5	1.5'	2.5	2.5'
$\frac{d\theta}{dt}$**, measured dynamic loading case**	85		- 79	
$\frac{d\theta}{dt}$**, estimate based on analytical calculations**	41	66	- 56	- 78
$\frac{d\theta}{dt}$**, estimate based on measured temperature**	54	87	- 76	- 106

6.4 Applicability of the estimation method

In addition to examining the precision of the presented method, the possible limitations and applicability are further discussed. Creating these simulated estimates differs in complexity. Calculations of transient conductor temperature according to IEC standards could be tedious. Then using these calculations further as a basis for temperature response during dynamic loading increases the probability of deviations in the estimate. Compared to mounting a thermocouple on the conductor of a power cable in the laboratory, which is considered uncomplicated.

In a practical power cable, it could be difficult to mount a physical temperature measurement device at the conductor. This could cause harm to the cable insulation as well as other layers. Which could make calculations more feasible, considering applicability. However, most practical cables are mounted with DTS systems, which could establish a sufficient long-term conductor temperature during known load and laying conditions as a basis for a dynamic estimation.

One of the main advantages of the presented estimation method is the possibility to apply the superposition principle. The principle is applied on individual contributions representing change in temperature during dynamic loading. This simplifies the method considerably, as each contribution can then be scaled individually and then added together. However, for each change in load current, two additional contributions need to be considered in the total temperature response. This could complicate the method if a large number of changes occur in the load current within a short period of time.

The estimates were carried out for a planned dynamic loading case. Subsequently, the simulation model should not have considered a dynamic load case that could result in the practical laboratory XLPE cable being damaged. As the period was within one hour for the overloading cases, it was considered to be a safe operation for this purpose. A further advancement to the model could be to limit currents that estimate the cable temperature to exceed maximum emergency ratings for longer than one hour.

Also, the step changes in load current case deviates considerably from rated ampacity, where a practical case might have smaller changes in current. However, larger changes in load current lead to greater variations in current dependent losses, which then emphasize the great precision level of the estimation method. As it is tested for larger and more rapid variations in temperature.

One of the objectives for developing this method was to contribute to power cables evolving from static to dynamic current ratings. As old static rating methods are considered too conservative and creates a possible grid reserve that is not exploited well enough. And state of the art technology and algorithms are not being used for its purpose by grid operators according to surveys. The simplicity of this method displays potential to facilitate dynamic rating of power cables.

As the estimated temperature response at the cable conductor has a small average deviation compared to the experimentally verified dynamic loading case. The method is able to predict when the cable is operated above its limits. This could then facilitate the dynamic current rating for cables, due to its ability of predicting conductor temperature in advance to overloading situations.

For dynamic loading the recent load history is an important factor to include. Due to the estimates not giving a adequate approximation of the conductor temperature levels if the load history is neglected. For the load history to not have any impact, the cable needs to be cooled until it reaches ambient temperature. It is not often cables have zero load current applied, which makes load history a factor to consider at all times. As this method applies the superposition principle on individual contributions corresponding to changes in load current, recent load history is included.

Chapter 7

Conclusion

A new method for estimating the transient temperature response of a power cable conductor was developed and verified using experimental laboratory measurements. Two different procedures have been used as basis for the estimates and have further been compared to a measured dynamic loading case. The first procedure being analytical calculations based on IEC standards, second procedure a long-term measurement of the conductor temperature in a practical laboratory setup.

For the studied dynamic loading case, the estimate based on analytical calculations, not including change in conductor resistance, is considered to be insufficient. With an average deviation of 13°C when not considering change in resistance and 8.3°C if conductor resistance is included. The large average deviation combined with risk of endangering the power cable during overloading with conductor resistance excluded is inadequate. The estimate is improved with an additional scaling for change in conductor resistance, however, it is not as optimal as when using the other procedure as basis.

Using measured temperature as basis gives the smallest deviation between estimates and measured conductor temperature during dynamic loading. With an average deviation of 6.1°C not considering change in conductor resistance and 5.2°C if conductor resistance is included. This estimate also has the best prediction of temperature levels during overloading as well as the points when temperature exceeds limitations for XLPE insulated cables.

The method displays great ability for estimating the dynamic current rating of power cables, by giving a decent imitation of the conductor temperature during dynamic loading. The simplicity of considering ohmic losses linear with temperature changes and applying the superposition principle to scaled individual contributions shows great potential when enhancing thermal considerations of power cables from static to dynamic ratings.

Chapter 8

Further work

Suggestions for further scientific research based on this thesis are listed below.

- Use numerical methods to establish a basis to be applied the estimation method for comparison to analytical calculations and measurement procedures.
- Combine the presented scaling principle with a more exact consideration of the temperature dependency in the conductor resistance.
- Further develop the estimation method to handle more rapid change in dynamic load current, without increasing its complexity due to several more individual contributions being added together.
- Utilize the temperature difference between conductor and sheath at steady-state. Applying the scaling principle to further estimate possible steady-state temperature of the conductor and sheath for a given load current.
- Use real temperature data and measured dynamic changes in load current to estimate the total transient temperature response in a practical grid implemented power cable.
- Implement current limitations in the method. For currents that could lead to conductor temperature exceeding emergency and operating limits for longer periods.
- Use bases that are established within shorter periods than 12 hours.
- Include seasonal effects on ambient temperature in the estimation method. That will further impact the conductor temperature during dynamic loading.

Bibliography

[1] ENERGINET, FINGRID, Statnett and SVENSKA KRAFTNÄT. *NORDIC GRID DEVELOPMENT PERSPECTIVE 2021*. 2021. URL: https://www.statnett.no/globalassets/for-aktorer-i-kraftsystemet/planer-og-analyser/nordic-grid-development-perspective-2021.pdf (Accessed: 30/06/2022).

[2] A. Safdarian, M. Z. Degefa, M. Fotuhi-Firuzabad and M. Lehtonen. *Benefits of Real-Time Monitoring to Distribution Systems: Dynamic Thermal Rating*. In: IEEE Transactions on Smart Grid (Volume: 6 , Issue: 4), pp. 2023-2031, 2015. DOI: 10.1109/TSG.2015.2393366.

[3] R. Huang, J. A. Pilgrim, P. L. Lewin and D. Payne. *Dynamic Cable Ratings for Smarter Grids*. In: IEEE PES ISGT Europe, 2013. DOI: 10.1109/ISGTEurope.2013.6695230.

[4] D. A. Douglass and A.-A. Edris. *Real-time monitoring and dynamic thermal rating of power transmission circuits*. In: IEEE Transactions on Power Delivery (Volume: 11, Issue: 3), pp. 1407-1418, 1996. DOI: 10.1109/61.517499.

[5] R. S. Olsen, J. Holboll and U. S. Gudmundsdóttir. *Dynamic Temperature Estimation and Real Time Emergency Rating of Transmission Cables*. In: IEEE Power Energy Society General Meeting, 2012. DOI: 10.1109/PESGM.2012.6345324.

[6] C. Fu, W. Si, L. Zhu, Y. Liang and H. Li. *Rapid Transfer Matrix-Based Calculation of Steady-State Temperature Rises in Cable Ducts Containing Groups of Three Phase Cable*. In: IEEE Power and Energy Technology Systems Journal (Volume: 6, Issue 4), pp. 208-213, 2019. DOI: 10.1109/JPETS.2019.2933677.

[7] S. A. Kaldheim. *Transient Temperature Response of Low Voltage Electrical Installation in Thermally Insulated Wall*. NTNU, Department of Electrical Power Engineering, 2022.

[8] R. Adapa and D. A. Douglass. *Dynamic thermal ratings: monitors and calculation methods*. In: IEEE Power Engineering Society Inaugral Conference and Exposition in Africa, 2005. DOI: 10.1109/PESAFR.2005.1611807.

[9] C. J. Wallnerström, P. Westerlund and P. Hilber. *Using power system temperature sensors for more uses than originally intended - Exemplified by investigating dynamic rating possibilities*. In: Conference: NORDAC 2014 At: Stockholm, 2014. DOI: 10.13140/2.1.1563.0723.

[10] Y. Zhang et al. *Conductor Temperature Monitoring of High-Voltage Cables Based on Electromagnetic-Thermal Coupling Temperature Analysis*. In: Energies 15(2):525, 2022. DOI: 10.3390/en15020525.

[11] S. Cherukupalli and G. J. Anders. *Distributed Fiber Optic Sensing and Dynamic Rating of Power Cables*. First edition. John Wiley & Sons, Inc., 2020.

[12] C. M. Lai and J. Teh. *Comprehensive review of the dynamic thermal rating system for sustainable electrical power systems*. In: Energy Reports 8, pp. 3263–3288, 2022. DOI: 10.1016/j.egyr.2022.02.085.

[13] Y. Shen, H. Niu, Y. You, X. Zhuang and T. Xu. *Promoting Cable Ampacity by Filing Low Thermal Resistivity Medium in Ducts*. In: IEEE PES Asia-Pacific Power and Energy Engineering Conference (APPEEC), 2013. DOI: 10.1109/APPEEC.2013.6837287.

[14] H. Brakelmann and G. Anders. *Ampacity Reduction Factors for Cables Crossing Thermally Unfavorable Regions*. In: IEEE Transactions on Power Delivery (Volume: 16, Issue: 4), pp. 444-448, 2001. DOI: 10.1109/61.956718.

[15] Q. Su, H.-J. Li and K. C. Tan. *Hotspot location and mitigation for underground power cables*. In: IET Proceedings - Generation Transmission and Distribution 152(6): pp. 934 - 938, 2005. DOI: 10.1049/ip-gtd:20050093.

[16] Y. Sun, X. Li, C. Ren, H. Xu and A. Han. *Distributed Fiber Optic Sensing and Data Processing of Axial Loaded Precast Piles*. In: IEEE Access 8, 2020. DOI: 10.1109/ACCESS.2020.3023626.

[17] B. Hennuy et al. Cigre WG B1.45. *Thermal monitoring of cable circuits and grid operators*. In: Cigre B1 Insulated cables, reference 756, 2019.

[18] D. Aegerter and S. Meier. *Model-based predictive control for use in RTTR temperature sensing systems of high voltage cables*. In: 10th International Conference on Insulated Power Cables, 2019.

[19] G. J. Anders. *Rating of Electric Power Cables Ampacity Computations for Transmission, Distribution and Industrial Applications*. First edition. McGraw-Hill Professional, 1997.

[20] N. Duraisamy and A. Ukil. *Cable Ampacity Calculation and Analysis for Power Flow Optimization*. In: Asian Conference on Energy, Power and Transportation Electrification (ACEPT), 2016. DOI: 10.1109/ACEPT.2016.7811535.

[21] E. Ildstad. *TET4195 High Voltage Equipment - Cable compendium*. NTNU, 2019.

[22] Z. Hou et al. *Application of Transformer Heat Circuit Model in Power Substation Area*. In: IOP Conference Series Earth and Environmental Science 804(3):032050, 2021. DOI: 10.1088/1755-1315/804/3/032050.

[23] G. J. Anders. *Rating of Electric Power Cables In Unfavorable Thermal Environment*. First edition. John Wiley & Sons, 2005.

[24] IEC 60287-2-1:2015. *Calculation of the current rating - Part 2-1: Thermal resistance - Calculation of thermal resistance*. Second edition. Norwegian electrotechnical publication, 2015.

[25] A. Segaghat and F. de León. *Thermal Analysis of Power Cables in Free Air: Evaluation and Improvement of the IEC Standard Ampacity Calculations*. In: IEEE Transactions on Power Delivery (Volume: 29, Issue: 5), pp. 2306-2314, 2014. DOI: 10.1109/TPWRD.2013.2296912.

[26] F. C. Van Wormer. *An Improved Approximate Technique for Calculating Cable Temperature Transients*. In: Transactions of The American Institute of Electrical Engineers. Part III: Power Apparatus and Systems (Volume: 74, Issue: 3), pp. 277-281, 1955. DOI: 10.1109/AIEEPAS.1955.4499079.

[27] P. Wang et al. *Dynamic thermal analysis for underground cables under continuously fluctuant load considering time-varying van wormer coefficient*. In: Electric Power Systems Research 199:107395, 2021. DOI: 10.1016/j.epsr.2021.107395.

[28] IEC 60853-2:1989. *Calculation of the cyclic and emergency current rating of cables. Part 2: Cyclic rating factor for cables greater than 18/30(36) kV and emergency ratings for cables of all voltages*. First edition. Norwegian electrotechnical publication, 1989.

[29] S. S. M. Ghoneim, M. Ahmed and N. A. Sabiha. *Transient Thermal Performance of Power Cable Ascertained Using Finite Element Analysis*. In: Processes 9(3):438, 2021. DOI: 10.3390/pr9030438.

[30] R. Stout. *Part One: Linear Superposition Speeds Thermal Modeling*. 2007. URL: https://www.electronicdesign.com/technologies/thermal-management/article/21189351/part-one-linear-superposition-speeds-thermal-modeling (Accessed: 05/05/2022).

[31] MATLAB. *R2020b Update 6 (9.9.0.1718557)*. Natick, Massachusetts, United States: The MathWorks Inc., 2021.

[32] Nexans. *TSLF 24kV 1x50A*. URL: https://www.nexans.no/no/products/Utility-and-Power-cables/24---36-kV-Distribution-Cable/TSLF-24-36kV/TSLF-24---32762/product~ID540395461~.html (Accessed: 22/03/2022).

Appendix

A Difference in conductor temperature measurement position 1 and position 2 in the laboratory setup setup

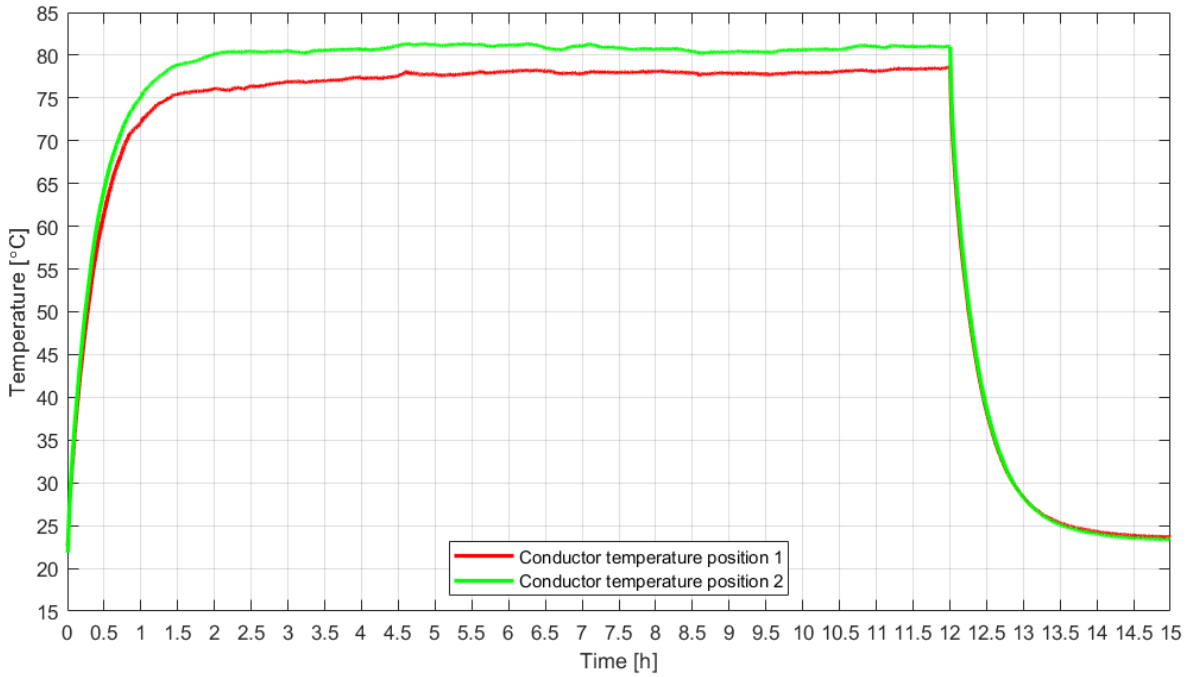

Figure A.1: Comparison of measured conductor temperature at both positions of the laboratory setup. Position 2 (light green line) is the measurement further used as basis in the estimation method. Position 1 (red line) has not been used.

B Constructed MATLAB code used for analytical calculations of conductor and sheath temperature responses

```
% MATLAB script for analytical calculations of conductor and sheath
% temperature response functions, according to IEC standards
% Cable data from Nexans datasheet for TSLF 24kV 1x50A
% Cross-section area of cable conductor
A = 50*10^-6; %
% Conductor diameter [m]
d_con = 8*10^-3;
% Diameter insulation [m]
d_ins = 19.3*10^-3;
% Nominal outer diameter of cable [m]
d_cable = 27*10^-3;
% Nominal insulation thickness [m]
ins_thickness = 5.5*10^-3;
% Average sheath thickness [m]
sheath_thickness = 2.1*10^-3;
% Making background of plots white
set(0,'defaultfigurecolor',[1 1 1])

% Thermal resistivity values
% Specific resistivity for aluminium @ 20 degree Celsius
rho_20_con = 2.8264*10^-8;
% Thermal resistivity XLPE [K*m/W)]
rho_xlpe = 3.5;
%Thermal resistivity, PE Lead Sheath [K*m/W]
rho_lead_sheath = 3.5;
% Temperature coefficient for aluminium (Al)
alpha_alu = 0.0043;
% Conductor resistance @ 20 degrees Celsius
res_20 = rho_20_con / A;


% Current and time
% Name of excel document to read
excel_data = 'matlabscriptinputhoved1.xlsx';
% Number of seconds between intervals, if minutes / hours remember
% to change label value!
time_const = 20/3600;
```

```
time = readmatrix(excel_data, 'Range', 'A4:A2163').*time_const;

% Current used for establishing steady-state temperature
% response of the cable
current = zeros(size(time));

for i=1:size(time)
    if time(i) <= 12
        current(i) = 225;
    else
        current(i) = 0;
    end
end


% Temperature vectors
amb_temp = zeros(size(time));
con_temp = zeros(size(time));
sheath_temp = zeros(size(time));

for j=1:size(time)
    amb_temp(j) = 22; % Ambient temperature
    % Starting values in conductor temperature vector
     con_temp(j) = amb_temp(j);
    % Starting values in sheath temperature vector
     sheath_temp(j) = amb_temp(j);
     +j;
end



% Specific heat capacity, volumetric
% Specific heat capacity of conductor, Al [J/(m^3*K)]
c_con = 2.422 * 10^6;
% Thermal capacity XLPE [J/(m^3*K)]
thermal_capacity_xlpe = 2.4*10^6;
% Thermal capacity XLPE [J/(m^3*K)]
thermal_capacity_lead_sheath = 2.4*10^6;
% Thermal capcity metallic screen, [J/(m^3*K)]
thermal_capacity_pe_screen = 3.45*10^6;


% Ambient temperature
theta_amb = 22;
```

```
% Van Wormer coefficients calculation
p = 1/(2*log(d_ins/d_con)) - 1/((d_ins/d_con)^2-1);
p_dash = 1/(2*log(d_cable/d_ins)) - 1/((d_cable/d_ins)^2-1);

% Cable parameters for black surface cable on ground with
% air as surrounding medium
Z = 1.69;
E = 0.63;
G = 0.25;

% Calculating thermal resistance of different cable parts
% Thermal resistance of the insulation
T_1 = rho_xlpe/(2*pi) * log(1+2*ins_thickness/d_con);
% Thermal resistance of sheath
T_3 = rho_lead_sheath/(2*pi) * log(1 +
2*sheath_thickness/(d_cable-sheath_thickness));
% Thermal resistance of the cable installation
T_internal = T_1 + T_3;

% External thermal resistance of Cables in air - simple configurations
% Heat transfer coefficient (W/m^2K^(5/4)), includes convection,
% radiation, conduction and mutual heating
h = Z / (d_cable)^G + E;
% Parameter to use when iterating for delta_s
K = (pi*d_cable*h*T_internal)/(1);

delta_s = 0;
delta_s_start = 2;
delta_s_threshold = 0.001;
delta_s_diff = abs(delta_s_start - delta_s);
i = 0;

while(delta_s_diff > delta_s_threshold)
  delta_s = ((90-0)/ (1+K*delta_s_start^(1/4)))^(1/4);
  delta_s_diff = abs(delta_s_start-delta_s);
  delta_s_start = delta_s;
  i = i + 1;
end


T_4_ext = 1 / (pi*d_cable*h*delta_s);
```

```
% Calculation of heat generated, W_c
% Vector to hold the AC resistance values
R_ac = zeros(size(time));
% Vector to hold the heat generated values
W_c = zeros(size(time));


for n=1:size(time)
    R_ac(n) = res_20;
    W_c(n) = current(n)^2.*R_ac(n);
    +n;
end



% Thermal capacitance calculations
% Thermal capacitance of conductor
Q_con = A*c_con;
% Thermal capacitance of XLPE insulation
Q_ins = pi/4 *(d_ins^2-d_con^2)*thermal_capacity_xlpe;
% Thermal capacitance of PE screen
Q_screen = pi/4 *((d_cable-2*sheath_thickness)^2-d_ins^2)...
*thermal_capacity_pe_screen;
% Thermal capacitance of sheath
Q_sheath = pi/4 * (d_cable^2-(d_cable-2*sheath_thickness)^2)...
    *thermal_capacity_lead_sheath;

%2 loop-network parameters calculations
T_A = T_1;
T_B = 1/2 * T_1 + ((1+0)*(T_3+T_4_ext));
Q_A = Q_con + p*Q_ins;
Q_B = (1-p)*Q_ins + Q_screen + p_dash*Q_sheath;

M_0 = 1/2*(Q_A*T_A + Q_B*T_B + Q_A*T_B);
N_0 = Q_A*T_A * Q_B*T_B;

a = (M_0 + sqrt(M_0^2-N_0)) / N_0;
b = (M_0 - sqrt(M_0^2-N_0)) / N_0;

% Conductor
T_11 = 1/(a-b) * (1/Q_A -b*(T_A + T_B));
T_12 = T_A + T_B - T_11;
```

```
% Sheath
T_21 = 1/ (Q_A*Q_B*T_A*(a-b));
T_22 = 1/ (Q_A*Q_B*T_A) * 1 / (a*b-b^2);


for q=1:size(time)


    con_temp(q) = con_temp(q)+ W_c(q)*(T_11*(1-exp...
        (-a*time(q)*3600)) + T_12*(1-exp(-b*time(q)*3600)));

    sheath_temp(q) = sheath_temp(q) + W_c(q)*(T_21*(1-exp...
        (-a*time(q)*3600)) + T_22*(1-exp(-b*time(q)*3600)));

    R_ac(q) = res_20*(1+alpha_alu*(con_temp(q)-amb_temp(q)));

    W_c(q) = current(q)^2*R_ac(q);
    +q;
end

figure
plot(time, con_temp, 'LineWidth', 2, 'color', 'r')
set(gca, 'ytick', 0:5:100);
set(gca, 'xtick', 0:0.5:12);
grid on
xlabel('Time [h]')
ylabel('Temperature [{\circ}C]')
hold on
plot(time, sheath_temp,'LineWidth', 2, 'color', [0.75, 0, 0.75])
hold on
plot(time, ones(size(time))*22, 'LineWidth', 2, 'color', ...
    '[0.9290 0.6940 0.1250]')
legend({'Simulated conductor temperature',...
    'Simulated sheath temperature', 'Ambient temperature' }...
    ,'Location','best')

delta_tetha_con_sheath = con_temp - sheath_temp;


figure
plot(time, delta_tetha_con_sheath, 'LineWidth', 2, 'color', 'c')
set(gca, 'ytick', 0:2:24);
set(gca, 'xtick', 0:0.5:12);
grid on
xlabel('Time [h]')
ylabel('Temperature [{\circ}C]')
```

C Constructed MATLAB code for simulating the dynamic loading case using long-term temperature measurement as basis

```
% MATLAB script for estimating conductor temperature
% during variable loading.
% Using the procedure of established temperature
% measurement as basis.

% Data from established long-term temperature measurement
excel_data = 'matlabscriptinputhoved1current_on.xlsx';

% Data from measured dynamic loading case
excel_data_2 = 'matlabscriptinputhoved2.xlsx';

% Making figure backgrounds white
set(0,'defaultfigurecolor',[1 1 1])

% Number of seconds between intervals,
% if minutes / hours remember to change label value!
time_const = 20/3600;

% Time measurement.
time = readmatrix(excel_data, 'Range', 'A4:A1443').*time_const;

% Measured ambient temperature of the surroundings.
amb_temp = readmatrix(excel_data, 'Range', 'U4:U1443');

% Long-term measured conductor temperature.
measured_conductor_temp = readmatrix(excel_data, 'Range',...
    'M4:M1443');


% Measured conductor temperature dynamic load case.
measured_conductor_temp_dynamic = readmatrix(excel_data_2,...
    'Range', 'M4:M1443');

% Measured current during dynamic load case.
current = readmatrix(excel_data_2, 'Range', 'C4:C1443');


%%Conductor resistivity calculation and plot
% AC resistance calculation of using measured
% temperature of conductor.
```

```
% Cross-section area of cable conductor.
A = 50*10^-6;
% Conductor resistance that will vary.
res_con_meas_pos2 = zeros(size(measured_conductor_temp_dynamic));
% Specific resistivity for aluminium @ 20 degrees Celsius.
rho_20 = 2.8264*10^-8;
% Temperature coefficient for aluminium (Al).
alpha_alu = 0.0043;
% Conductor resistance @ 20 degrees Celsius.
res_20 = rho_20 / A;

% AC resistance calculation.
for i = 1:size(time)
    res_con_meas_pos2(i) = res_20*(1 + alpha_alu*...
        (measured_conductor_temp_dynamic(i)...
        - amb_temp(i)));
end

% Figure for plotting AC conductor resistance.
figure
plot(measured_conductor_temp_dynamic, res_con_meas_pos2,...
    'LineWidth', 2, 'color', '[0.6350 0.0780 0.1840]')
grid on
xlabel('Temperature [{\circ}C]')
ylabel('Resistance [{\Omega}]')

% Setting all individual contributions to have
% same base.
con_temp_displacement = measured_conductor_temp(1);

measured_conductor_temp = measured_conductor_temp...
    - measured_conductor_temp(1);
conductor_current_off = measured_conductor_temp.*(-1)...
    + measured_conductor_temp(1);

% Creating a vector to hold the adding of
% scaled individual contributions.
temp_curve = zeros(size(measured_conductor_temp));

%Scaling individual contributions to fit
% changes in load current.
% Contributions for when current is on.
con_temp_scale_on_150 = measured_conductor_temp.*(2.25);
con_temp_scale_on_50 = measured_conductor_temp.*(0.25);
con_temp_scale_on_125 = measured_conductor_temp.*(1.5625);
```

```
% Contributions for when current is off.
con_temp_scale_off_150 = con_temp_scale_on_150.*(-1);
con_temp_scale_off_50 = con_temp_scale_on_50.*(-1);
con_temp_scale_off_125 = con_temp_scale_on_125.*(-1);

% Using the superposition principle to add contributions
% together.
for i = 1:size(time)
    if time(i) < 1
        temp_curve(i) = measured_conductor_temp(i);

    elseif time(i) >= 1 && time(i) < 2
        temp_curve(i) = measured_conductor_temp(i)...
            + conductor_current_off(i-179)...
            + con_temp_scale_on_150(i-179);

    elseif time(i)>=2 && time(i) < 3
         temp_curve(i) = measured_conductor_temp(i)...
             + conductor_current_off(i-179)...
             + con_temp_scale_on_150(i-179)...
             + con_temp_scale_off_150(i-359)...
             + con_temp_scale_on_50(i-359);

    elseif time(i)>=3 && time(i) < 4
         temp_curve(i) = measured_conductor_temp(i)...
             + conductor_current_off(i-179)...
             + con_temp_scale_on_150(i-179)...
             + con_temp_scale_off_150(i-359)...
             + con_temp_scale_on_50(i-359)...
             + con_temp_scale_off_50(i-539)...
             + con_temp_scale_on_125(i-539);

    elseif time(i)>=4 && time(i) < 5
        temp_curve(i) = measured_conductor_temp(i)...
            + conductor_current_off(i-179)...
            + con_temp_scale_on_150(i-179)...
            + con_temp_scale_off_150(i-359)...
            + con_temp_scale_on_50(i-359)...
            + con_temp_scale_off_50(i-539)...
            + con_temp_scale_on_125(i-539)...
            + con_temp_scale_off_125(i-719)...
            + measured_conductor_temp(i-719);
```

```
    elseif time(i) >= 5
        temp_curve(i) = measured_conductor_temp(i)...
            + conductor_current_off(i-179)...
            + con_temp_scale_on_150(i-179)...
            + con_temp_scale_off_150(i-359)...
            + con_temp_scale_on_50(i-359)...
            + con_temp_scale_off_50(i-539)...
            + con_temp_scale_on_125(i-539)...
            + con_temp_scale_off_125(i-719)...
            + measured_conductor_temp(i-719)...
            + conductor_current_off(i-899);

    end
 +i;
end


% Adding the displacement back to the estimate
% to have ambient temperature as starting point.
temp_curve = temp_curve + con_temp_displacement;


figure
plot(time,temp_curve, 'LineWidth', 2, 'color', 'g')
set(gca, 'ytick', 0:10:200);
set(gca, 'xtick', 0:0.5:8);
grid on
xlabel('Time [h]')
ylabel('Temperature [{\circ}C]')
hold on

% Adding additional scaling for including the
% change in conductor resistance
% for the time interval t = 1 h to t = 2 h.

con_temp_scale_on_150 = measured_conductor_temp.*(2.25)...
    .*res_con_meas_pos2(359)/res_con_meas_pos2(179);
con_temp_scale_on_50 = measured_conductor_temp.*(0.25);
con_temp_scale_on_125 = measured_conductor_temp.*(1.5625);

con_temp_scale_off_150 = con_temp_scale_on_150.*(-1);
con_temp_scale_off_50 = con_temp_scale_on_50.*(-1);
con_temp_scale_off_125 = con_temp_scale_on_125.*(-1);
```

```
for i = 1:size(time)
    if time(i) < 1
        temp_curve(i) = measured_conductor_temp(i);

    elseif time(i) >= 1 && time(i) < 2
        temp_curve(i) = measured_conductor_temp(i)...
            + conductor_current_off(i-179)...
            + con_temp_scale_on_150(i-179);

    elseif time(i)>=2 && time(i) < 3
         temp_curve(i) = measured_conductor_temp(i)...
             + conductor_current_off(i-179)...
             + con_temp_scale_on_150(i-179)...
             + con_temp_scale_off_150(i-359)...
             + con_temp_scale_on_50(i-359);

    elseif time(i)>=3 && time(i) < 4
         temp_curve(i) = measured_conductor_temp(i)...
             + conductor_current_off(i-179)...
             + con_temp_scale_on_150(i-179)...
             + con_temp_scale_off_150(i-359)...
             + con_temp_scale_on_50(i-359)...
             + con_temp_scale_off_50(i-539)...
             + con_temp_scale_on_125(i-539);

    elseif time(i)>=4 && time(i) < 5
        temp_curve(i) = measured_conductor_temp(i)...
            + conductor_current_off(i-179)...
            + con_temp_scale_on_150(i-179)...
            + con_temp_scale_off_150(i-359)...
            + con_temp_scale_on_50(i-359)...
            + con_temp_scale_off_50(i-539)...
            + con_temp_scale_on_125(i-539)...
            + con_temp_scale_off_125(i-719)...
            + measured_conductor_temp(i-719);
```

```
    elseif time(i) >= 5
        temp_curve(i) = measured_conductor_temp(i)...
            + conductor_current_off(i-179)...
            + con_temp_scale_on_150(i-179)...
            + con_temp_scale_off_150(i-359)...
            + con_temp_scale_on_50(i-359)...
            + con_temp_scale_off_50(i-539)...
            + con_temp_scale_on_125(i-539)...
            + con_temp_scale_off_125(i-719)...
            + measured_conductor_temp(i-719)...
            + conductor_current_off(i-899);

    end
 +i;
end


plot(time,temp_curve+con_temp_displacement, 'LineWidth', 2,...
    'color', 'g','LineStyle','--')
hold on
plot(time, measured_conductor_temp_dynamic,  'LineWidth', 2,...
    'color', 'b','LineStyle','-')
hold on
plot(time, ones(size(time))*125, 'LineWidth', 2, 'color', 'm')
hold on
plot(time, ones(size(time))*90, 'LineWidth', 2, 'color', 'y')
legend(...
    {'Estimated conductor temperature not scaled for change in R_{AC}'...
    ,'Estimated conductor temperature scaled for change in R_{AC}'...
    ,'Measured conductor temperature',...
    ' Maximum emergency temperature XLPE cable',...
    'Maximum operating temperature XLPE cable',...
    'Location','northeast'})
```

D Scaled individual contributions that is applied the superposition principle

D.1 Individual contributions analytical simulations, not including change in R_{AC}

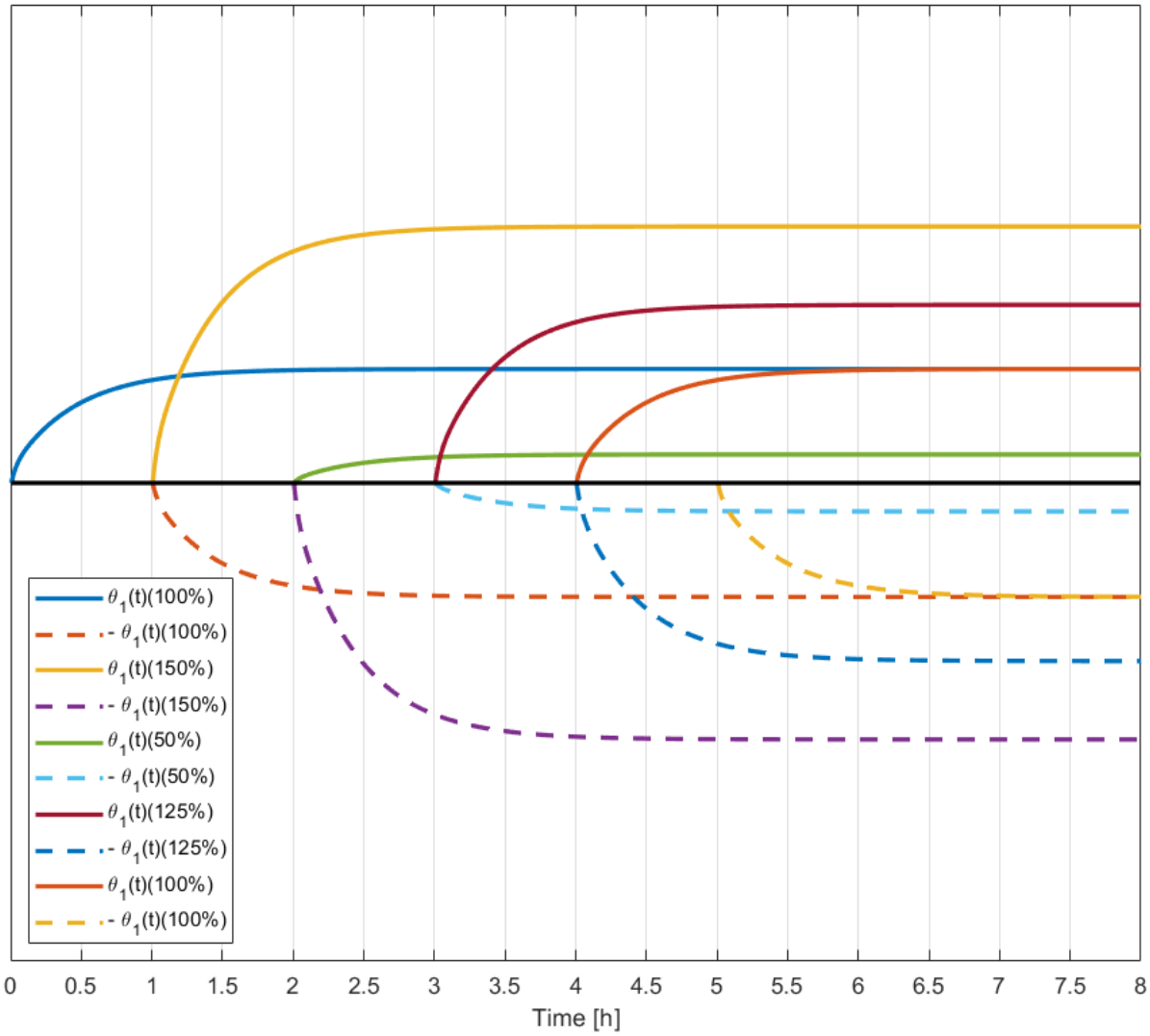

Figure D.1: Individual contributions of scaled analytical calculations used as basis for estimating conductor temperature. Not including scaling for R_{AC}.

D.2 Individual contributions analytical simulations, including change in R_{AC}

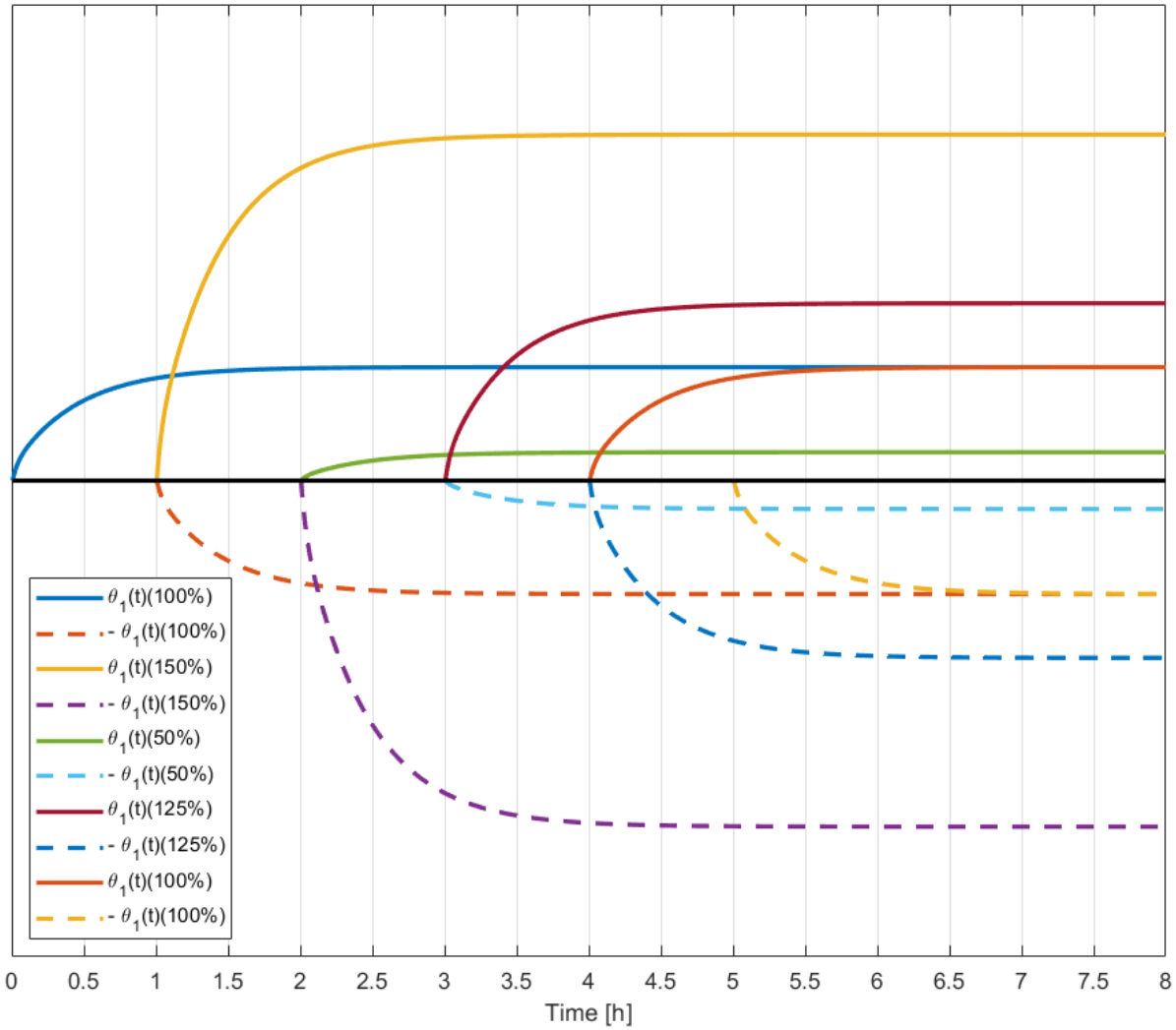

Figure D.2: Individual contributions of scaled analytical calculations used as basis for estimating conductor temperature. Including additional scaling for R_{AC} on $\theta_1(t)(150\%)$.

D.3 Individual contributions long-term temperature response measurements, not including change in R_{AC}

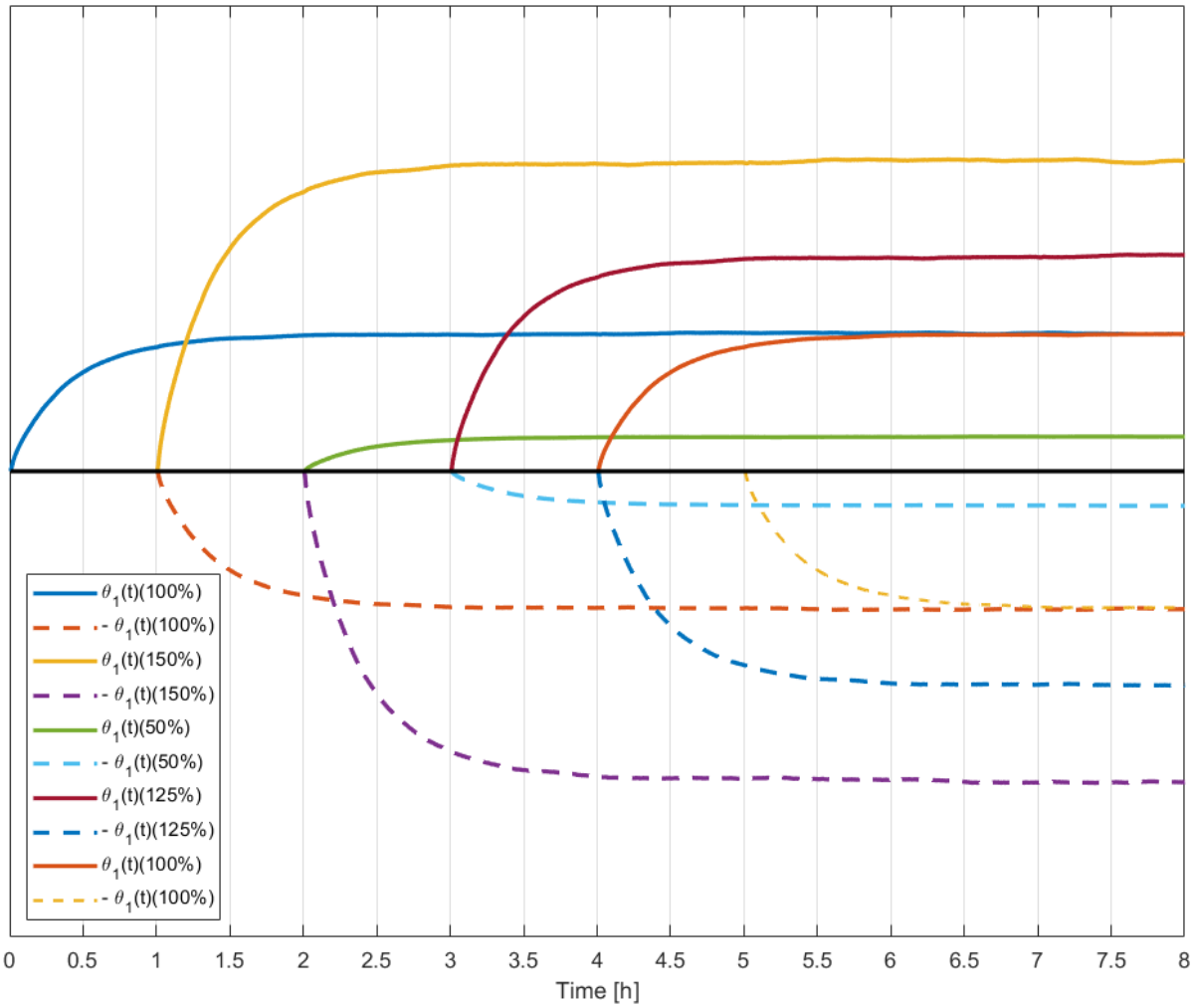

Figure D.3: Individual contributions of scaled long-term temperature measurement as basis used for estimating conductor temperature. Not including scaling for R_{AC}.

D.4 Individual contributions for long-term temperature response measurement as basis, including change in R_{AC}

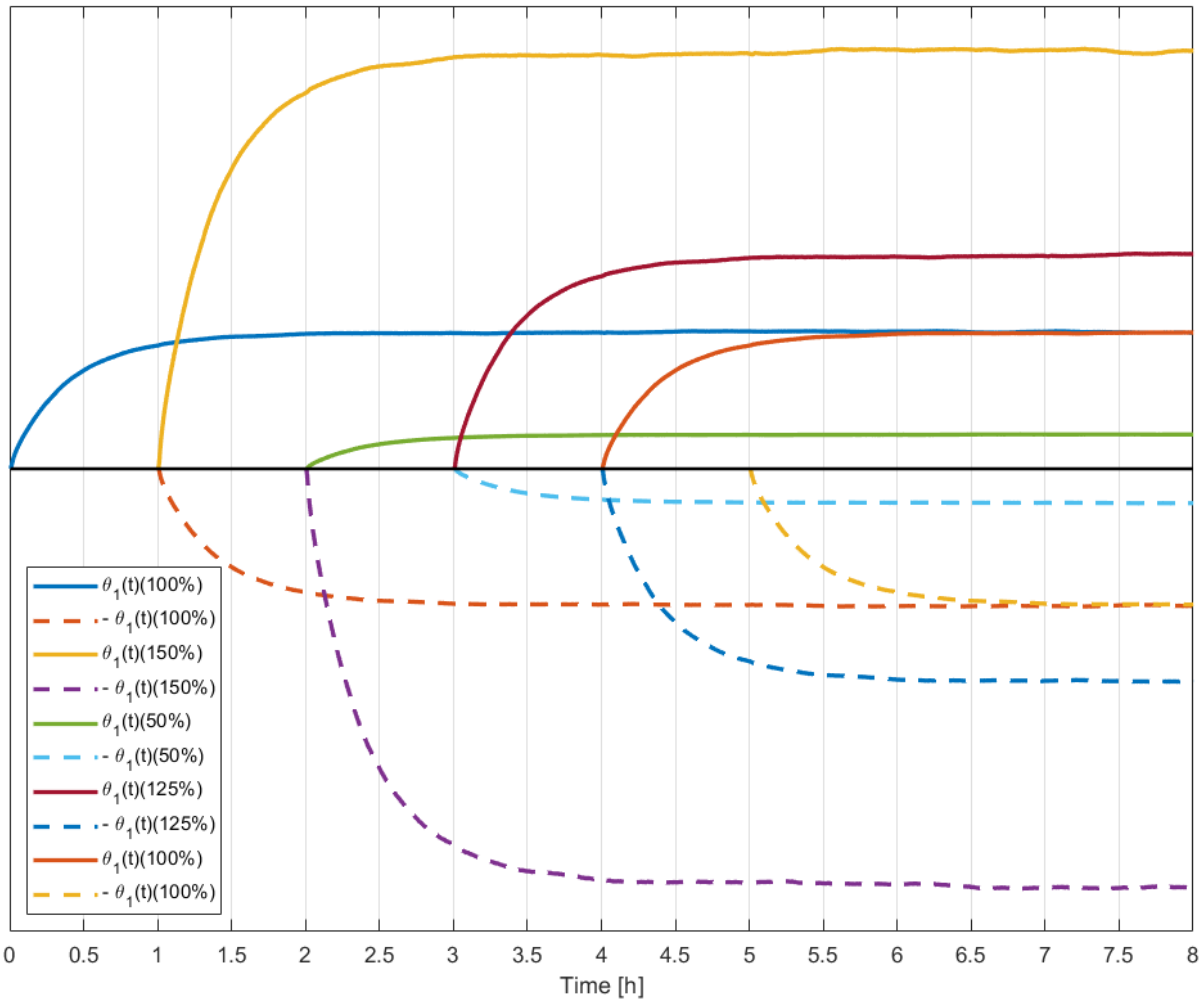

Figure D.4: Individual contributions of scaled long-term temperature measurement used for estimating conductor temperature. Including additional scaling for R_{AC} on $\theta_1(t)(150\%)$.

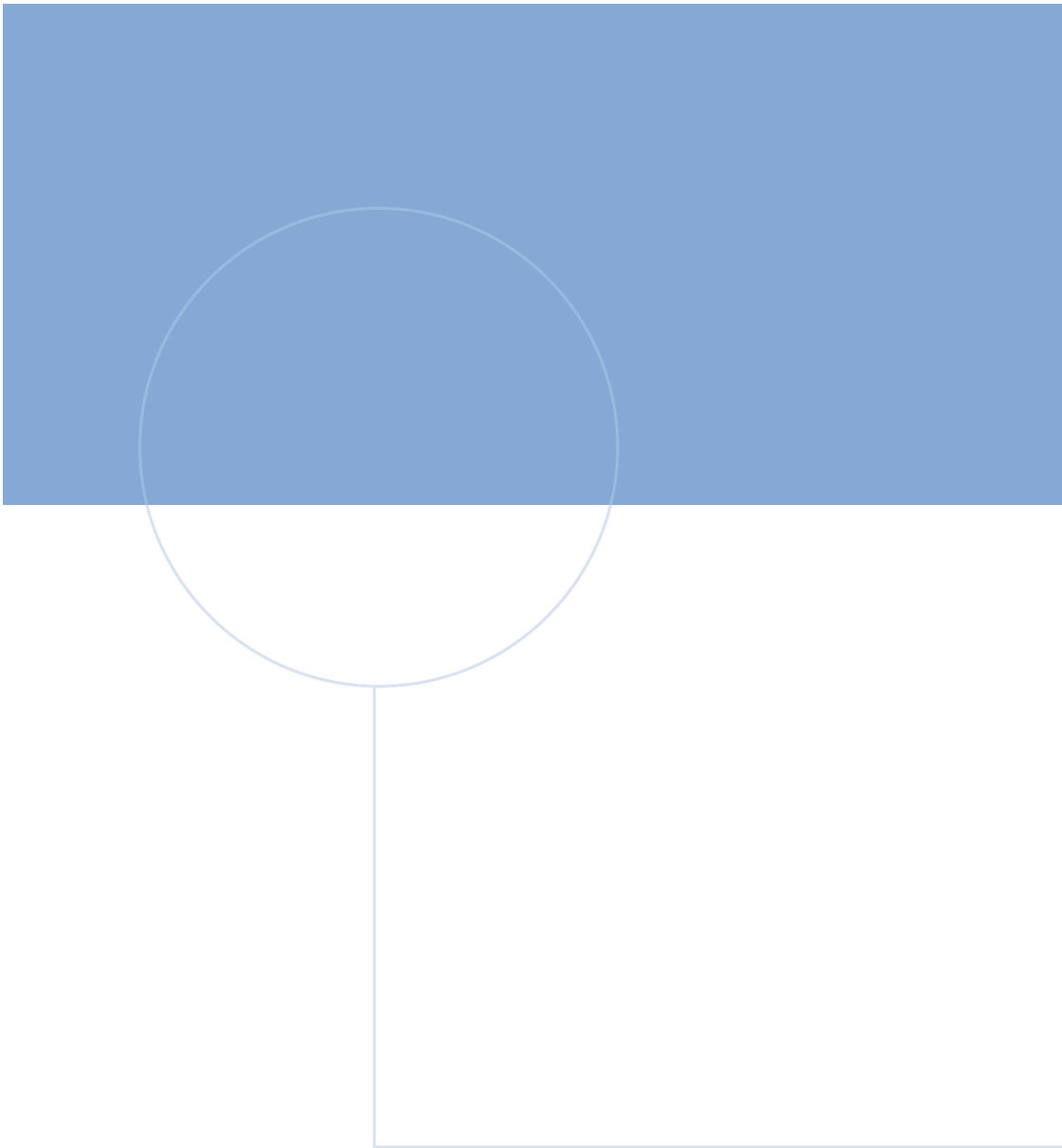

NTNU

Norwegian University of
Science and Technology